Oregon State University | College of Forestry

Swiss Needle Cast Cooperative

2019 ANNUAL REPORT

Members of the Swiss Needle Cast Cooperative

Cascade Timber Consulting

Greenwood Resources, Inc. Lewis & Clark Tree Farms, LLC

Oregon Department of Forestry

Starker Forests

Stimson Lumber

USDA Forest Service

Weyerhaeuser Corporation

Swiss Needle Cast Cooperative Staff

Dave Shaw – Director and Associate Professor of Forest Health

Gabriela Ritóková – Assistant Director

Edited by Gabriela Ritóková and David Shaw
Cover photo by Tom Brandt on Flickr

Table of Contents

SNCC Income Sources and Expenditures: 2019

Income

Membership dues	70,000
Oregon State Legislature	95,000
Carry-over	141,054
Total 2019 Income	**$306,054**

Expenditures

Salaries and wages	168,851
Travel	8,079
Operating expenses	14,022
Contracts	10,890
Materials and Supplies	5,324
Indirect Costs (@17.5%)	36,254
Total 2019 Expenditures	**$243,420**

Balance	**$62,634**

SNCC Background and Organization

A major challenge to intensive management of Douglas fir in Oregon and Washington is the current Swiss needle cast (SNC) epidemic. Efforts to understand the epidemiology, symptoms, and growth losses from SNC have highlighted gaps in our knowledge of basic Douglas-fir physiology, growth, and silviculture. The original mission of the Swiss Needle Cast Cooperative (SNCC), formed in 1997, was broadened in 2004 to include research aiming to ensure that Douglas-fir remains a productive component of the Coast Range forests. The SNCC is located in the Department of Forest Engineering, Resources and Management within the College of Forestry at Oregon State University. The Membership is comprised of private, state, and federal organizations. Private membership dues are set at a fixed rate. An annual report, project reports, and newsletters are distributed to members each year. Our objective is to carry out projects in cooperation with members on their land holdings.

SNCC Mission

To conduct research on enhancing Douglas-fir productivity and forest health in the presence of Swiss needle cast and other diseases in coastal forests of Oregon and Washington.

SNCC Objectives

(1) Understand the epidemiology of Swiss needle cast and the basic biology of the causal fungus, *Nothophaeocryptopus gaeumannii*.

(2) Design silvicultural treatments and regimes to maximize Douglas-fir productivity and ameliorate disease problems in the Coast Range of Oregon and Washington.

(3) Understand the growth, structure, and morphology of Douglas-fir trees and stands as a foundation for enhancing productivity and detecting and combating various diseases of Douglas-fir in the Coast Range of Oregon and Washington.

Note from the Director

2019 was a year of progress: 4 major papers on Swiss needle cast were published by researchers at OSU and SNCC. In addition, our colleagues in Canada have described a new lineage of *Nothophaeocryptopus gaeumannii,* which appears to occur only in the drier eastern regions of the Northern Rockies in the US and Canada (contribution in 2019 Annual Report). These lineages indicate the long time and close association of *N. gaeumannii* with Douglas-fir. A paper by Kevin Bladon et al. is the first publication to demonstrate that a foliage fungus can impact watershed scale hydrology! Sky Lan and colleagues have shown that young Douglas-fir trees are generally more severely infected than nearby mature trees. The reason remains elusive, but it appears that pseudothecia emerge in 3-5-year needles in mature trees, while consistently emerging in 2-year-old needles on young trees. This is not due to nitrogen or differences in leaf wetness. Currently we are working on the idea that temperature is a key factor controlling timing of pseudothecia emergence.

Gabi Ritóková is currently leading efforts to resample our SNCC Research and Monitoring Plot Network, which is five years old now. It takes three years to remeasure the plots, and we are in the second year in 2020. The plots will be retired after 10 years of monitoring, ending in 2026. The first paper to emerge from this plot network by Sky Lan involved an investigation of foliage nutrition and SNC disease severity. As expected, nitrogen was associated with higher disease severity. Patrick Bennett and Jeff Stone published an article concerning the distribution and environmental linkages to the two western Oregon and Washington lineages. They found clear differences with one lineage restricted to the near coast and another distributed much more widely. Both lineages are now found in New Zealand. Patrick and Jeff now believe there are no discernable differences in pathogenicity between these lineages.

As we move into 2020, we are focused on re-measurement of the Research and Monitoring Plot Network within 35 miles of the coast, but Gabi also maintains a monitoring plot network along the west slope of the Cascades at low elevations that is monitored annually. Although needle retention can be low (< 3 years), disease severity tends to be low to moderate, and rarely high. Gabi has been deploying weather stations near monitoring locations and has hopes of measuring spore dispersal near these weather stations to more closely link local climate to disease patterns.

We hope you find the work in this annual report useful. Thank you all very much for supporting the SNCC. We believe the SNCC is a global model for research and management of forest disease, and will continue to contribute to science into the foreseeable future.

Sincerely,

David C. Shaw

Five-year remeasurement of the SNCC research and monitoring plots

Year Two of the first remeasurement of the SNCC Research and Monitoring Plot Network

Gabriela Ritóková

SNCC, Forest Engineering, Resource, and Management, Oregon State University,

Figure 1. SNCC RPN.

The establishment of the new Swiss needle cast cooperative (SNCC) research and monitoring plot network (RPN) was initiated in 2013, and over a three-year period 106 plots (fig 1) were installed in 10-25 year old Douglas-fir plantations from the California-Oregon border to southwest Washington. The first five-year period of plot re-measurement is currently taking place and thus far has provided information about disease severity, growth loss and its geographic distribution on 66 plots (pink and blue symbols in fig 1) throughout the Coast Range. Yellow symbols denote the remaining plots to be measured n the fall 2020 and sampled in the spring 2021. Analyses of the two years of remeasurement data are discussed in this annual report on page 9 (Mainwaring et al. SNCC AR 2019).

In the early spring of 2019 we installed two weather stations on Stimson Lumber property in the Tillamook region and in late September installed a third station on the Lewis and Clark Tree Farm (L&C Timberlands, Greenwood Resources) near Seaside (weather stations are denoted by blue symbols in fig 1). In each location, all-in-one weather station, ATMOS 41 (fig 2a, b), was placed on a topped tree for maximum solar radiation exposure. It integrates twelve sensors to monitor the following environmental conditions: solar radiation, precipitation, vapor pressure, relative humidity, air temperature, barometric pressure, horizontal wind speed and direction, maximum wind gust, lightning strike and distance, and tilt.

The compact size of the weather station allowed for a somewhat uncomplicated installation at the top of each tree and minimized clutter on the tree, an important feature for weight minimization due to the young age of the trees. In addition to the multi-parameter ATMOS 41, three leaf wetness sensors, PHYTOS 31 (fig 3a, b), were placed in mid crown to measure onset and duration of wetness, as well as levels of water condensing on the surface of a simulated leaf. Environmental data are transmitted to and stored in a ZL 6 data logger (fig 4a, b), afterwhich they can be either downloaded via a USB or with an internet connection (Zentra Cloud), and transmitted for near real-time data viewing. All equipment was purchased from METER Group, Inc. USA, in Pullman, WA.

This information will help to determine which seasonal or site factors affect SNC severity within the study area. In the spring of 2020 we will install spore traps in these three locations to determine the link between spore load, disease impact (foliage retention and pseudothecial occlusion), and predict disease severity.

Figure 2 a, b. ATMOS 41, multi-parameter sensor.

Figure 3 a, b. PHYTOS 31, leaf wetness sensors.

Figure 4 a, b. ZL 6, data logger.

Effect of SNC on growth of infected trees

Doug Mainwaring[1], Doug Maguire[1], Gabriela Ritóková[2], Dave Shaw[2]
Center for Intensive Planted-Forest Silviculture[1], Swiss Needle Cast Cooperative[2],
Oregon State University

Abstract

Approximately two-thirds of the permanent plots in the Swiss Needle Cast Cooperative's Research Plot Network (RPN) have now been remeasured after five years of growth. Cubic volume growth of surviving trees on plots with severe Swiss needle cast (SNC) (foliage retention=1.15 yrs) was compared to volume growth of plots with the highest foliage retention (3.8 years), suggesting relative growth losses of up to 36.6% for 2013-2019, and average loss of 14.9% (mean retention of 2.52 years). These losses are lower than those estimated during the 1998-2008 growth periods covered by the SNC Growth Impact Study.

Introduction

The RPN was initiated in 2013 to address two major objectives: 1) to monitor Swiss needle cast (SNC) symptoms and tree growth in 10-25-yr-old Douglas-fir plantations throughout the Oregon Coast Range and southwest Washington; and 2) to provide an improved estimate of growth losses associated with a given initial level of SNC. Volume growth losses were estimated to average 23% for the target population in 1996, with losses reaching 50% in the most severely impacted stands. Four subsequent remeasurements through 2008 confirmed these estimates (Maguire et al. 2011).

The objectives of this report are: 1) to quantify the most recent 5-yr growth responses relative to initial SNC severity; and 2) to compare these 5-yr growth responses to those estimated from 1998-2008.

Methods

Study sites

Establishment of the RPN began in the Fall of 2013, and ultimately included 106 plots installed over three years. These plots were established in 10-25 year old Douglas-fir plantations (>80% BA in Douglas-fir) that had not been treated in the last five years, and were distributed from the Oregon-California border to SW Washington, and from the coastline to 35 miles inland. These plots and their measurement protocols are identical to the original Growth Impact Plots (Maguire et al. 2011).

Plots were square (0.08 ha) and installed in a representative location within each sampled stand. All Douglas-fir trees with a dbh > 3 cm were tagged (other species with dbh > 5 cm) and measured for dbh to the nearest 0.1 cm. A subsample of 40 undamaged Douglas-fir were measured for height and height to crown base to the nearest 0.01 m, including the 10 largest by dbh and the four smallest by dbh, with the others evenly distributed across the diameter

distribution. Breast height age of the stand was determined by increment core for the largest trees by dbh, and applied to the eight largest undamaged trees (by dbh) to determine site index (Bruce 1981).

In the spring following establishment, foliage retention (nearest 0.1 year) was estimated from laterals within the middle crown third of five dominant trees on the plot. In young stands with highly visible crowns, this could usually be done visually from the ground; for older stands, estimation required climbing.   Sixty-six of the 106 plots have now been remeasured following five years of growth (fig. 1).   Data summaries of the plot network can be found in a previous SNC annual report (Ritóková et al. 2017).

Site index

In previous stand-level analyses of cubic volume growth, site index has been included in the predictive equation (Maguire et al. 2001, Maguire et al. 2002a, Maguire et al. 2004, Maguire et al. 2008, Maguire et al. 2011), despite complications from its usage. Height increment is known to be negatively affected by SNC (Maguire et al. 2002b, Hann et al. 2014), and thus any estimate of site index using height-age pairs (equation [1]) not accounting for this effect will be underestimated, with a subsequent underestimation of the potential volume PAI. To attempt to correct for this, the ORGANON height modifier equation (equation [2]) was used to correct the measured heights used to estimate SI, under the assumption that the foliage retention estimated for the plot at the start of the growth period had been constant for the entire life of the current stand. This method is considered justifiable due to the fact that these young stands have probably been growing under the influence of SNC since establishment.

Figure 1. Map of the 66 measured sites.

[1] $SI = f(height, age)$

[2] $Htmod_{SNC} = (1-exp(b_0+b_1 \cdot Folret^3))$

[3] $SI_{Adj}=f((height/(Htmod_{SNC}), age)$

Statistical analysis

Cubic volume PAI was determined by applying the Bruce and Demars (1974) volume equation to the tree measurements at the beginning and end of the growth period, calculating the difference between the two and dividing by the length of the growth period. A simple stand-
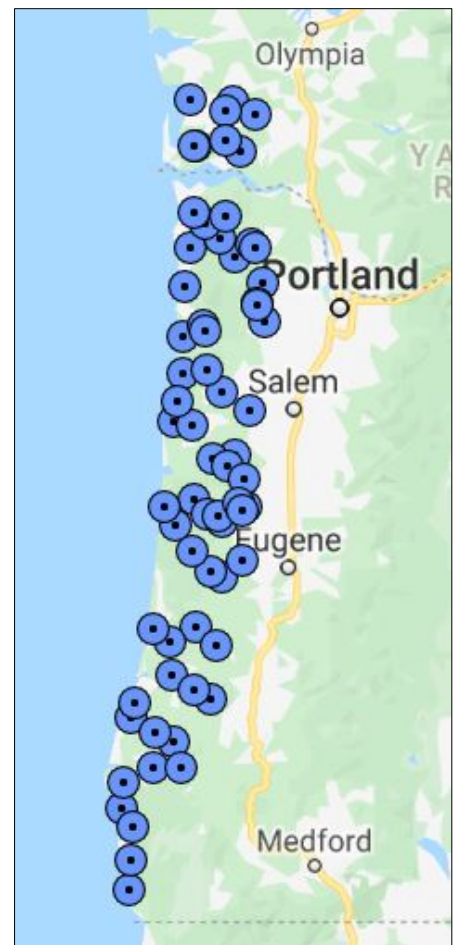
level growth model was fitted to the data from the 66 RNP plots, using initial foliage retention (with or without pseudothecial occlusion) as the index of SNC severity:

[4] $\ln[PAI] = b_0 + b_1X_1 + b_2X_2 + \ldots + b_kX_k + b_{k+1}FOLRET + b_{k+2}(\%\_Pseudothecial\ occlusion)$

where:

    PAI=plot-level periodic annual increment for cubic volume of surviving Douglas-fir
    X_i=plot-level predictor variables
    FOLRET is initial foliage retention
    %_Pseudothecial occlusion is just what it says

Results and Discussion

The final base equation describing cubic volume PAI included terms accounting for stocking (initial Douglas-fir basal area, initial basal area in other conifers, initial basal area in hardwoods), productivity (adjusted site index, equation [3]), and foliage retention.

[5a] $\ln[VPAI] = a_0 + a_1\ln(BA_{df}) + a_2\ln(BA_{oc}) + a_3\ln(BA_{hard}) + a_4\ln(SI_{adj}) + a_5\ln(FR)$

Parameter	Estimate	SE
a_0	2.24448	0.89623
a_1	0.37694	0.05782
a_2	-0.01649	0.00552
a_3	-0.01131	0.00658
a_4	0.9511	0.24122
a_5	0.38072	0.08764
	R^2=0.663	MSE = 0.03438

Table 1: Parameter estimates, equation [5a]

where:

    VPAI = Cubic volume periodic annual increment (m^3/ha)
    BA_{df} = Douglas-fir basal area (m^2/ha)
    BA_{oc} = Basal area in other conifers(m^2/ha)
    BA_{hard} = Basal area in hardwoods (m^2/ha)
    SI_{adj} = Adjusted site index (m, 50 yrs)
    FR= Douglas-fir foliage retention (yrs)

Cubic volume PAI was found to increase with increasing Douglas-fir basal area, decreasing basal area in other species (conifers and hardwoods), increasing adjusted site index, and increasing foliage retention (table 1). With a dataset maximum foliage retention of 3.8 years and a minimum of 1.15 yrs, the relationship between cubic volume PAI and foliage retention implies a maximum cubic volume growth loss of ~36.6% and an average growth loss of 14.9% (dataset average foliage retention = 2.52 years) (fig. 2). Use of the adjusted site index is quite influential. When using the unadjusted site index, growth losses are estimated to be about one-third lower (fig. 2).

Because % pseudothecial occlusion varies widely with foliage retention (fig. 3), inclusion of % pseudothecial occlusion (b_6) within the model was thought to be of value (equation [5b]).

[5b] $\ln[VPAI] = b_0 + b_1\ln(BA_{df}) + b_2\ln(BA_{oc}) + b_3\ln(BA_{hard}) + b_4\ln(SI_{adj}) + b_5\ln(FR) + b_6\%PO$
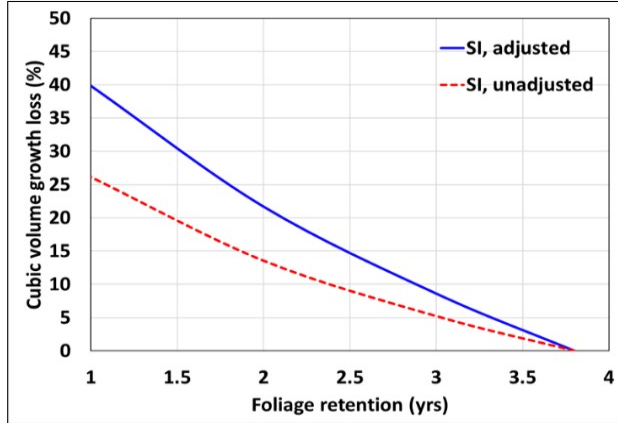
Figure 2. Cubic volume growth loss implied by relationship between foliage retention and cubic volume (equation [5a]).
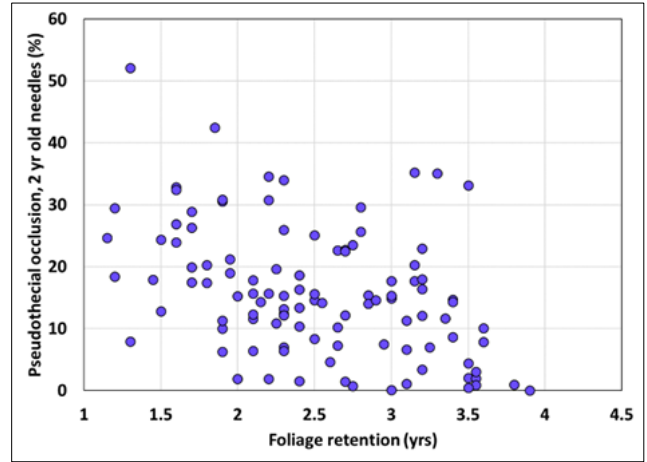
Figure 3. Relationship between foliage retention and % pseudothecial occlusion on 2-year old needles.

When included, both foliage retention and % pseudothecial occlusion were significant (p=0.0029 and p=0.0173, respectively) (fig. 4). Previous growth performance reports have discussed the varying performance of stands with similar levels of foliage retention, and in recognition of that fact the SNC Stand Assessment Tool *http://sncc.forestry.oregonstate.edu/stand-growth-assessment-tool* was created to determine how well a stand was growing relative to expectations. The significance of the two indices of SNC included in equation [5b] suggest that in addition to estimating foliage retention, inspecting the underside of needles in the spring may also help assess the current status of stands.
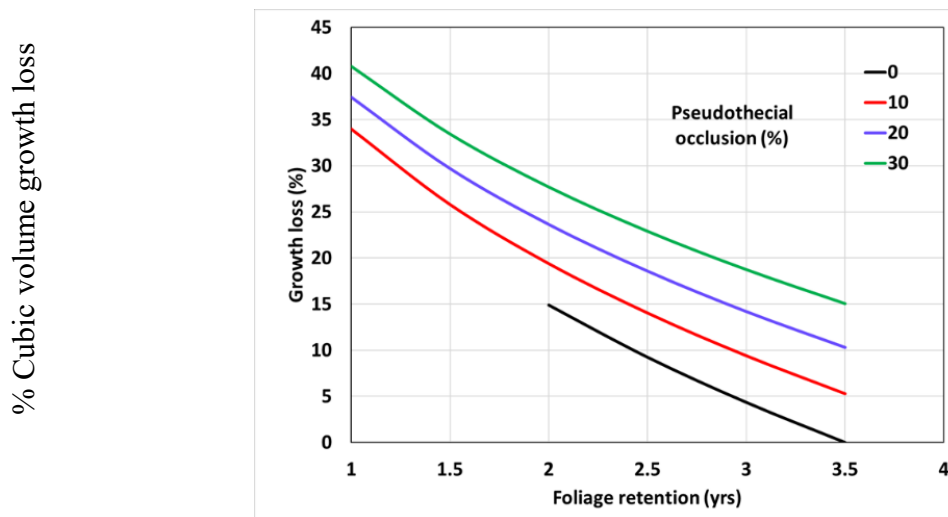
Figure 4. Cubic volume growth loss implied by relationship between foliage retention, % pseudothecial occlusion and cubic volume (equation [5b]).

12

The estimate of maximum growth loss from equation [5a] is significantly lower than those estimated for the 1998-2008 period (fig. 5) despite similar ranges in foliage retention. Because SNC has been a problem in coastal forests since the 1990s, managers have had opportunities to harvest both merchantable and pre-merchantable stands that were exhibiting limited growth or growth potential. With fewer such stands in the population of interest, the poorest performing stands are less likely to be represented in the sample, which may explain the lower estimate of maximum growth loss for the RPN than the GIS.
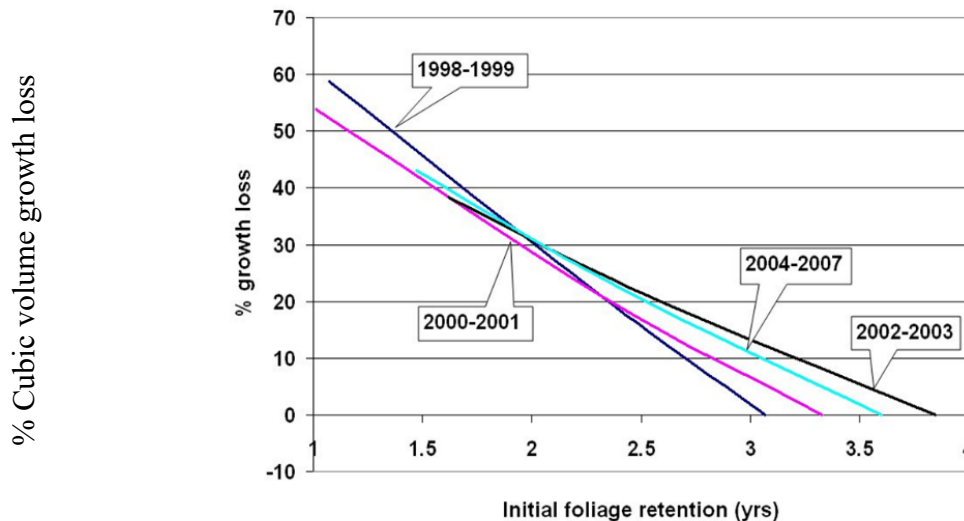
Figure 5. Cubic volume growth loss versus foliage retention estimated for four separate growth periods of the SNC Growth Impact Plots (1998-2008).

A previous review of Douglas-fir genetic tolerance to SNC recommended the use of tolerant Douglas-fir stock in moderately infected areas (Jayawickrama et al. 2012) and planting non-susceptible species such as western hemlock in areas where disease conditions are worst.   If managers act on this advice, the most poorly performing stands may not suffer from as high a growth loss, but the resulting estimates of growth loss would also not accurately reflect the potential maximum growth loss suffered by stands if Douglas-fir were to be regenerated in those coastal areas that had previously suffered from the highest disease levels.   In other words, the maximum growth loss might be expected to change over time depending upon where managers choose to establish Douglas-fir plantations.

Literature Cited

Bruce, D., 1981. Consistent height-growth and growth-rate estimates for remeasured plots. For. Sci. 27:711-725.

Bruce, D. and DeMars, D.J., 1974. Volume equations for second-growth Douglas-fir. Res. Note PNW-239. Portland, OR: USDA, Forest Service. *Pacific Northwest Forest and Range Experiment Station*, 5.

Hann, D.W., Maguire, D.A., Mainwaring, D.B., and Zhao, J. 2014. Effect of Swiss Needle Cast Infection upon Diameter and Height Increment of Douglas-fir Trees. Center for Intensive Planted-forest Silviculture, Internal report. 17 pp.

Jayawickrama, K.J., Shaw, D. and Terrance, Z.Y. 2012. Genetic selection in coastal Douglas-fir for tolerance to Swiss needle cast disease. In: Sniezko, Richard A.; Yanchuk, Alvin D.; Kliejunas, John T.; Palmieri, Katharine M.; Alexander, Janice M.; Frankel, Susan J., tech. coords. Proceedings of the fourth international workshop on the genetics of host-parasite interactions in forestry: Disease and insect resistance in forest trees. Gen. Tech. Rep. PSW-GTR-240. Albany, CA: Pacific Southwest Research Station, Forest Service, US Department of Agriculture. pp. 256-261 (Vol. 240, pp. 256-261).

Maguire, D., and Kanaskie, A. 2001. Growth Impact Study: Growth trends in the first 2-yr period following establishment of Phase III permanent plots and pre-commercial thinning controls. P. 14-17 in Swiss Needle Cast Cooperative annual report, Filip, G. (ed.). College of Forestry, Oregon State Univ., Corvallis, OR.

Maguire, D., Kanaskie, A., and Mainwaring, D. 2004. Growth Impact Study: Growth trends during the third 2-yr period following establishment of permanent plots. P. 24-27 in Swiss Needle Cast Cooperative annual report, Mainwaring, D. (ed.). College of Forestry, Oregon State Univ., Corvallis, OR.

Maguire, D.A., Mainwaring, D.B. and Kanaskie, A., 2011. Ten-year growth and mortality in young Douglas-fir stands experiencing a range in Swiss needle cast severity. Can. J. For. Res. 41:2064-2076.

Maguire, D., Kanaskie, A., Mainwaring, D., Johnson, R., and Johnson, G. 2002a. Growth Impact Study: Growth trends during the second 2-yr period following establishment of permanent plots. P. 28-32 in Swiss Needle Cast Cooperative annual report, Filip, G. (ed.). College of Forestry, Oregon State Univ., Corvallis, OR.

Maguire, D.A., Kanaskie, A., Voelker, W., Johnson, R. and Johnson, G., 2002b. Growth of young Douglas-fir plantations across a gradient in Swiss needle cast severity. West. J, Appl. For. 17:86-95.

Mainwaring, D., Maguire, D., and Kanaskie, A. 2008. Growth Impact Study: Growth trends during the third 2-yr period following establishment of permanent plots. P. 13-17 in Swiss Needle Cast Cooperative annual report, Shaw, D., and Woolley, T. (eds.). College of Forestry, Oregon State Univ., Corvallis, OR.

Ritóková, G., Shaw, D., Maguire, D., Mainwaring, D., Browning, J., Gourley, M., Filip, G., Kanaskie, A., and Marshall, B. 2017. Swiss Needle Cast Cooperative Research and Monitoring Plot Network in Coastal Oregon, Southwestern Washington, and Oregon Cascade Foothills. P. 7-13 in Swiss Needle Cast Cooperative annual report, Shaw, D., and Ritóková, G. (eds.). College of Forestry, Oregon State Univ., Corvallis, OR.

Swiss Needle Cast in British Columbia:

Disease and Growth Monitoring, Climate Data and Genomic Analyses

Stefan Zeglen[1], Nicolas Feau[2], and Harry Kope[3]

[1]British Columbia Ministry of Forests, Lands and Natural Resource Operations and Rural Development, West Coast Region, Nanaimo, BC

[2]Department of Forestry and Conservation Sciences, University of British Columbia

[3]British Columbia Ministry of Forests, Lands and Natural Resource Operations and Rural Development, Resource Practices Branch, Victoria, BC

A monitoring network for Swiss needle cast (SNC; causal agent *Nothophaeocryptopus gaeumannii*) on coastal Douglas-fir in British Columbia (BC), was started in 2017 and completed in 2019. There are now 43 0.08 ha plots spread across three biogeoclimatic subzones on Vancouver Island and the Lower Mainland (Figure 1). Fourteen plots have weather stations installed, measuring microsite data on air temperature, relative humidity, solar irradiance and leaf wetness. Soil samples were collected to determine nutrient availability or uptake. These and other site variables may be correlated with SNC occurrence and be used to determine the risk of SNC for certain site types.

During the three years of plot installation, foliar retention was measured on plot trees along with their physical attributes. Now that plot installation is complete, the five-year remeasurements are scheduled to begin in late 2021. It is envisaged that this network will help track defoliation of Douglas-fir by the disease and capture tree response (growth impacts) over the next decade.

A genomic analysis of the pathogen in foliar samples from the coast as well as the interior of BC was conducted by the University of British Columbia. The results to date show there are two distinct lineages of the SNC fungus on the coast, **Lineage 1c** and **2** (from BC to Oregon – and **Lineage 1c** is also found in New Zealand and Europe). Another lineage, **Lineage 1i,** is found in the interior of BC (Figure 2).
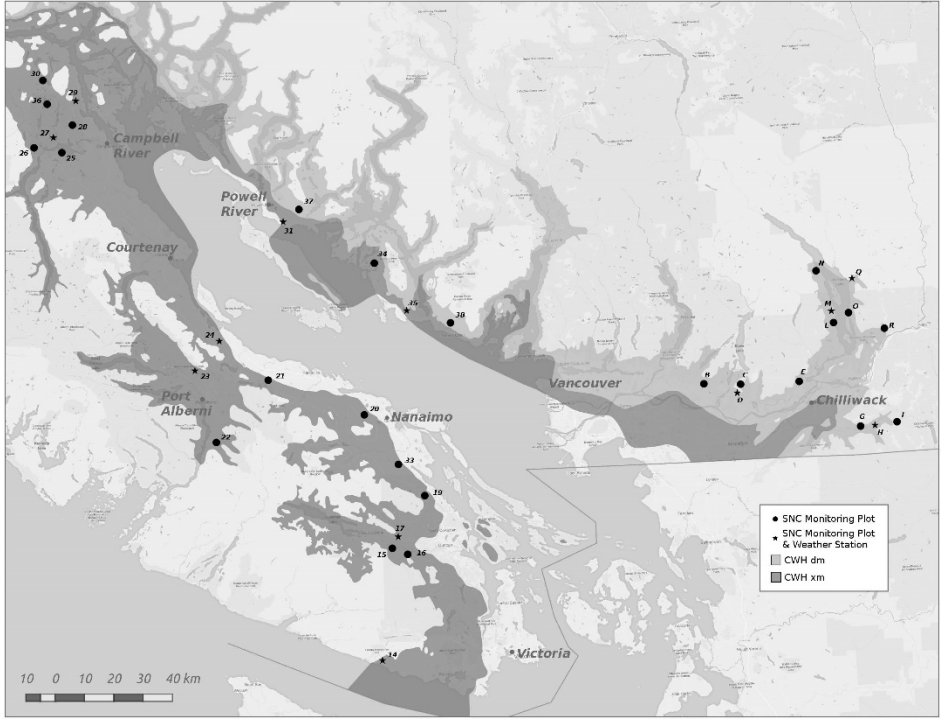
Figure 1. The location of 43 SNC monitoring sites including those with
weather stations on Vancouver Island and south coastal British Columbia.
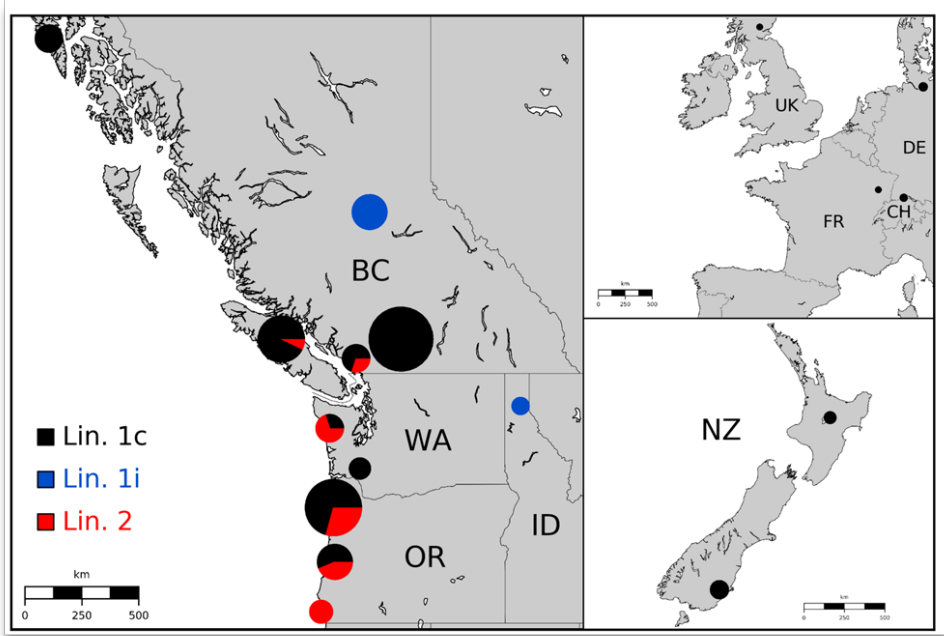
Figure 2. The co-existence of three lineages of SNC in British Columbia.

Swiss needle cast transect plots in the Oregon Cascade foothills

Gabriela Ritóková, Dave Shaw

SNCC, Forest Engineering, Resource, and Management, Oregon State University

Background

Forty-seven disease monitoring transects were established in the Oregon Cascades foothills in 2017. The sites are located in young Douglas-fir plantations between the ages of 10 and 25 years on SNCC member lands: Weyerhaeuser, Cascade Timber Consulting (CTC), Oregon Department of Forestry (ODF), and a private landowner, Melcher Logging and Timber Harvesting Inc. (fig. 1). In 2019, a third continuous annual survey was made to evaluate Swiss needle cast (SNC) conditions.

A subset of the original stands was monitored in 2019 due to the difficulties of observing foliage retention in the larger (and older) trees. The initial study proposal and field methodology did not involve tree climbing, a lack of which limits foliage sampling opportunities in older trees. As a result, during the resampling period in May and June 2019, 41 transect were evaluated for foliage retention and 12 were evaluated for pseudothecial occlusion. Sampling methodology was described in detail on page 45 in the 2018 SNCC annual report.

During summer 2019 two weather stations (blue symbols in fig. 1) were installed on a CTC and Melcher property. Details are provided in the SNCC RPN report on page 6 in this annual document.

Figure 1. Transect plot locations in the Oregon Cascade foothills.

2019 Results

Although the pathogen was present in some sites classified as healthy, disease symptoms were minimal. This was observed especially in 2018, when disease severity was more intense and second year needles had a greater number of occluded stomates than in 2017 and 2019 (fig. 2). Nevertheless, foliage retention was higher and foliage color observed was healthier, darker green. In comparison with 2017, the foliage retention of sampled stands in 2018 was a slightly greater. Foliage retention values in 2018 and 2019 were similar (fig. 3).
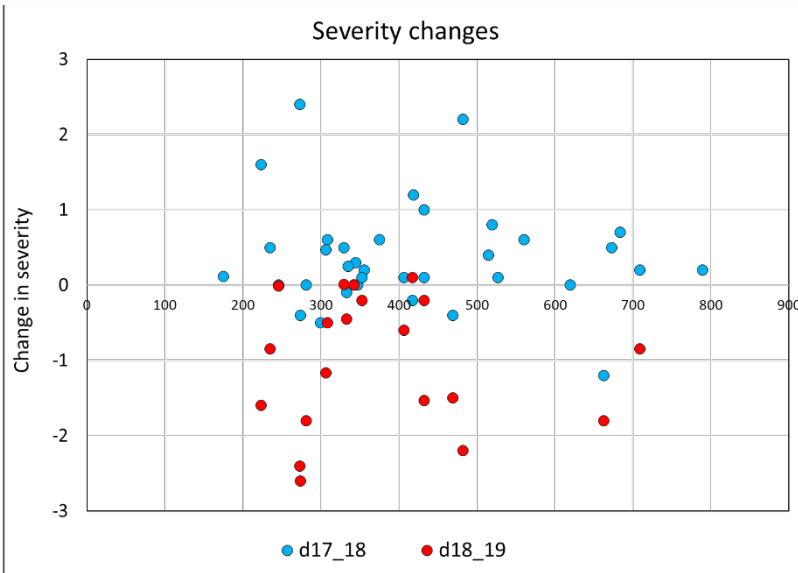
Figure 2. Plot-level severity changes by elevation and year.
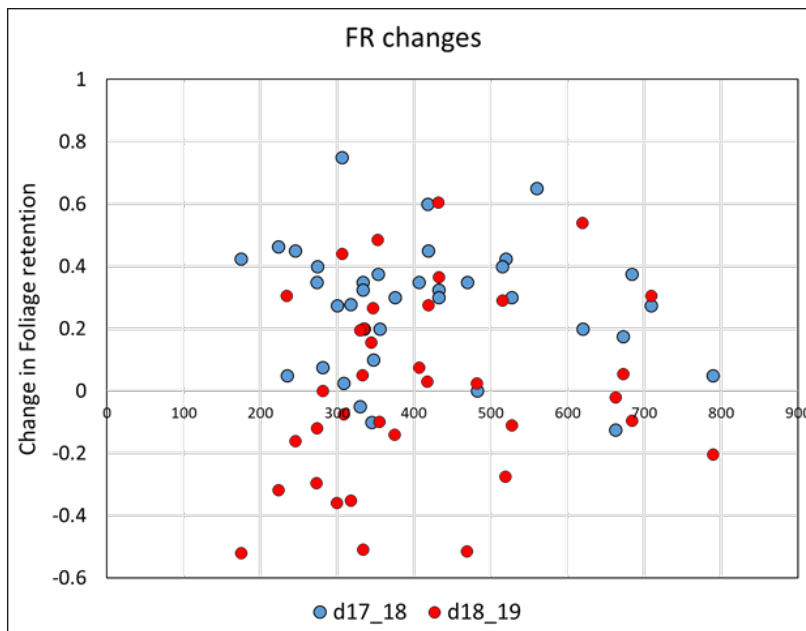
Figure 3. Plot-level foliage retention changes by elevation and year.

The relationship between foliage retention and disease severity on twelve of the sites monitored during all three years is shown in figure 4, indicating a relatively linear relationship between the two variables in 2019.
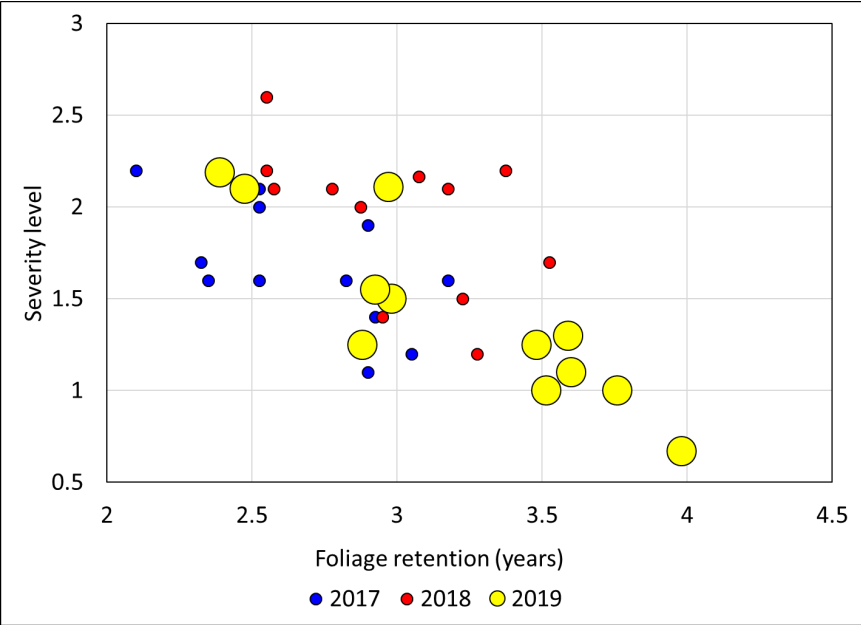
Figure 4. Twelve transects were sampled all three years. Graph shows the relationship between foliage retention and disease severity by year.

Swiss needle cast in mature forests: Needle age and canopy distribution of *Nothophaeocryptopus gaeumannii*

Yung-Hsiang (Sky) Lan

Forest Engineering, Resources, and Management, Oregon State University

Epidemiology of *Nothophaeocryptopus gaeumannii* is generally well known in plantation trees, but the dynamics of Swiss needle cast (SNC) in older trees is poorly understood. In the previous study, Lan et al. 2019 compared SNC severity, disease incidence, needle retention, and foliar nitrogen in tree crowns of mature and old-growth forests and nearby young forests at three locations in the Oregon Coast Range and four locations in the western Cascade Mountains of Oregon. In 2016 and 2017 three old trees and three young trees were sampled (total of 21 mature trees and 21 young trees across seven sites) at Cascade Head, Klickitat Mountain, Woods Creek, Moose Mountain, Falls Creek, Soapgrass Mountain and Toad Creek. We found that pseudothecial incidence was highest on two-year-old needles in young trees, and on three-, four- and five- year old needles in mature trees with the exception of Cascade Head.

In this study, we used the same dataset to assess pseudothecial density across two-six-year old needles from upper, middle, and lower canopy positions of mature trees. We excluded data from Soapgrass Mountain and Toad Creek because of the low SNC incidence.

In mature Douglas-fir, pseudothecial density varied year to year depending on needle age and canopy position. Canopy position was important for three-, and four-year-old needles, showing that pseudothecial density in upper and middle crown is higher than in lower crown.

This study confirms that *N. gaeumannii* pseudothecial density is greatest in three-, and four-year old needles of mature trees. Therefore, the one- and two- year old needles are healthier in mature trees. Also, pseudothecial density on all needles of mature trees was less than two-year old needles in young plantation trees. Pseudothecial density is directly related to biomass of the fungus in the needle, therefore it appears that mature trees have less fungus in the needles. This combination of healthier young needles, higher needle retention, and later needle age of peak pseudothecial density may explain why mature trees are less impacted by SNC.

Figure 1. Mature forest canopy at Falls Creek, Oregon

Reference

Lan, Y-H, Shaw, D., Beedlow, P, Lee, H.E., Waschmann, R. 2019. Severity of Swiss needle cast in young and mature Douglas-fir forests in western Oregon, USA. *Forest Ecology and Management* 442: 79-95.

Assessing variation in Douglas-fir foliar endophyte community as a function of neighborhood tree species diversity

Austin Himes

FES, College of Forestry, OSU and Greenwood Resources Inc.

Background

In the summer of 2017, an exploratory study to investigate the impacts of tree species diversity and composition on ecosystem functions and services was implemented in Coastal Pacific Northwest industrial forest plantations. The design included orthogonal representation of all mixture combinations of Douglas-fir (DF), red alder (RA), and western hemlock (WH) in roughly equal proportions following a simplex-centroid model. Each of the seven possible mixtures (DF, RA, WH, DFRA, DFWH, RAWH, DFRAWH) was represented in six 10 m radius circular plots for a total of 42 plots. Each plot contained 22-29 trees with DBH > 10cm in stands planted between 1978 and 1982.

Diameter at breast height (DBH), stem defects, and crown classes (Kraft) of all trees in the plot > 10 cm DBH were measured. Trees were labeled sequentially from the center of the plot out starting uphill and working clockwise. Total height, height to live crown, and stem diameter at 25-35% of the total tree height for the three trees of each target species closest to the center of the plot were also recorded. Two 5mm cores were taken at 1.4m on the uphill side of the stem and at 90 degrees from one tree of each target species, and the tree number and distance to trees that have canopy touching or overlapping the cored tree were recorded. Understory species and cover were surveyed in four 1m square sampling frames at located with top right corners (facing uphill) at 2m and 6m from the center of the plot in both directions along a transect running uphill/downhill.

Plant species diversity has been suggested to reduce risk of plant disease through the dilution effect (Keesing et al., 2010), or through increased abundance of organisms that are antagonistic to pathogens (Latz et al., 2012). Most of the plots in this study are within the "blast zone" of Swiss needle cast (SNC), which is the most impactful disease in the region affecting Douglas-fir. It would be meaningful to managers in the region to know if SNC risk can be reduced by managing a higher diversity of tree species. Furthermore, mechanisms underlying any patterns of disease prevalence as a function of tree species diversity would be important for furthering basic understanding of ecosystem processes. For instances, increasing tree species diversity may positively corelate with foliar endophyte diversity which could increase abundance of organisms that are antagonistic or faciliatory to *Nothophaeocryptopus gaeumannii*, the fungus that causes SNC.

Research Questions

1. Does tree species diversity and/or composition effect severity and occurrence of swiss needle cast disease?

2. Does tree species diversity and/or composition effect foliar endophyte composition and diversity?

3. If Swiss needle cast disease is impacted by tree species diversity and/or composition, is it mediated by foliar endophyte community functional composition?

Methods

Three to five Douglas-fir trees will be felled, needle retention will be determined using standard methods, and foliage collected for qPCR analysis to determine endophyte species richness, diversity, and functional composition. The presence and quantity of *N. gaeumannii* will be determined. A response surface model using a constraint simplex space containing only Douglas-fir mixtures will be adapted from the simplex centroid surface as illustrated in Figure 1. A simpler factorial analysis approach could be used with DF, DFRA, DFWH, DFWHRA as factors. The analytical model should include parameters to account for spatial distribution since there is known correlation between swiss needle cast and proximity to the coast. Other factors may also need to be added to the model and will be determined by the respective experts on swiss needle cast and foliar endophytes.
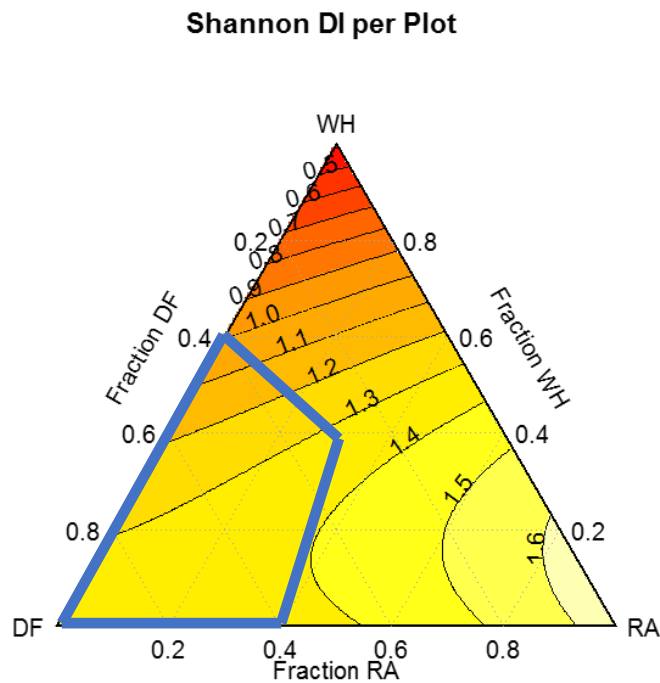
Figure 1. Complete response surface of understory biodiversity with approximated DF constrained space outlined in blue.

Scope of Work

Two of the original DF plots were harvested recently, leaving 22 plots with some component of DF (see Table 1). Geographic distribution of plots is shown in figure 2. The three DF with height, height to live crown, and upper stem diameter measurements will be priorities for destructive sampling. If three to five trees are sample per plot, it will be a total of 66-110 trees. Austin Himes will provide access to the plots and tree felling (assuming no alternative feller is found). Dave Shaw's group will provide the field crew for data and sample collection. Posy Busby's group will provide the molecular analysis. I believe there is potential for manuscript on Douglas-fir foliar endophyte composition and diversity as a function of tree species diversity that would be led by Posy's group. These may be a second manuscript or white paper specific to SNC that could be led by Dave's group. Integration of endophyte diversity and composition and disease risk would potentially be integrated into an assessment of trade-offs between different ecosystem functions as a function of tree species composition and diversity lead by Austin.

Table 2. Plot details. Species proportions based on estimated plot level above ground biomass of each species.

Plot #	Lat	Long	Species Treatment	Estimated Site Index	Prop. WH	Prop. DF	Prop. RA
2	45.5765	123.9114	DF	NA	0	1	0
6	45.87193	123.6983	DFRA	152	0.028932	0.703441	0.267627
7	45.87221	123.6984	WHDFRA	152	0.41906	0.398593	0.182348
8	45.95382	123.7185	DFRA	150	0	0.686194	0.313806
10	45.93701	123.7566	WHDFRA	120	0.531974	0.27715	0.190876
11	45.93679	123.7557	WHDF	120	0.63337	0.366631	0
13	45.93544	123.9237	WHDFRA	132	0.358816	0.261966	0.379218
19	46.01863	123.6229	WHDFRA	139	0.331959	0.324537	0.343504
20	46.01361	123.6206	WHDF	139	0.424776	0.575224	0
24	46.00858	123.6787	DF	126	0	0.977629	0.022371
28	46.00901	123.6788	DFRA	126	0.051746	0.656923	0.291331
29	45.96991	123.7639	WHDF	125	0.491144	0.496491	0.012365
30	45.96903	123.7611	DF	125	0.046213	0.941798	0.011989
31	46.29818	123.6044	DFRA	NA	0.012593	0.768001	0.219406
32	46.01036	123.689	DF	107	0	1	0
36	46.27893	123.8163	WHDF	NA	0.5376	0.4624	0
37	46.38264	123.6607	DF	NA	0.109378	0.890622	0
39	46.00997	123.745	WHDFRA	117	0.197275	0.473079	0.329646
40	46.00964	123.7449	WHDF	117	0.380838	0.619162	0
41	46.0234	123.7535	WHDF	116	0.578482	0.421518	0
42	45.95798	123.7079	WHDFRA	143	0.411599	0.428073	0.160328
43	45.56604	123.9141	DFRA	NA	0	0.671921	0.328079
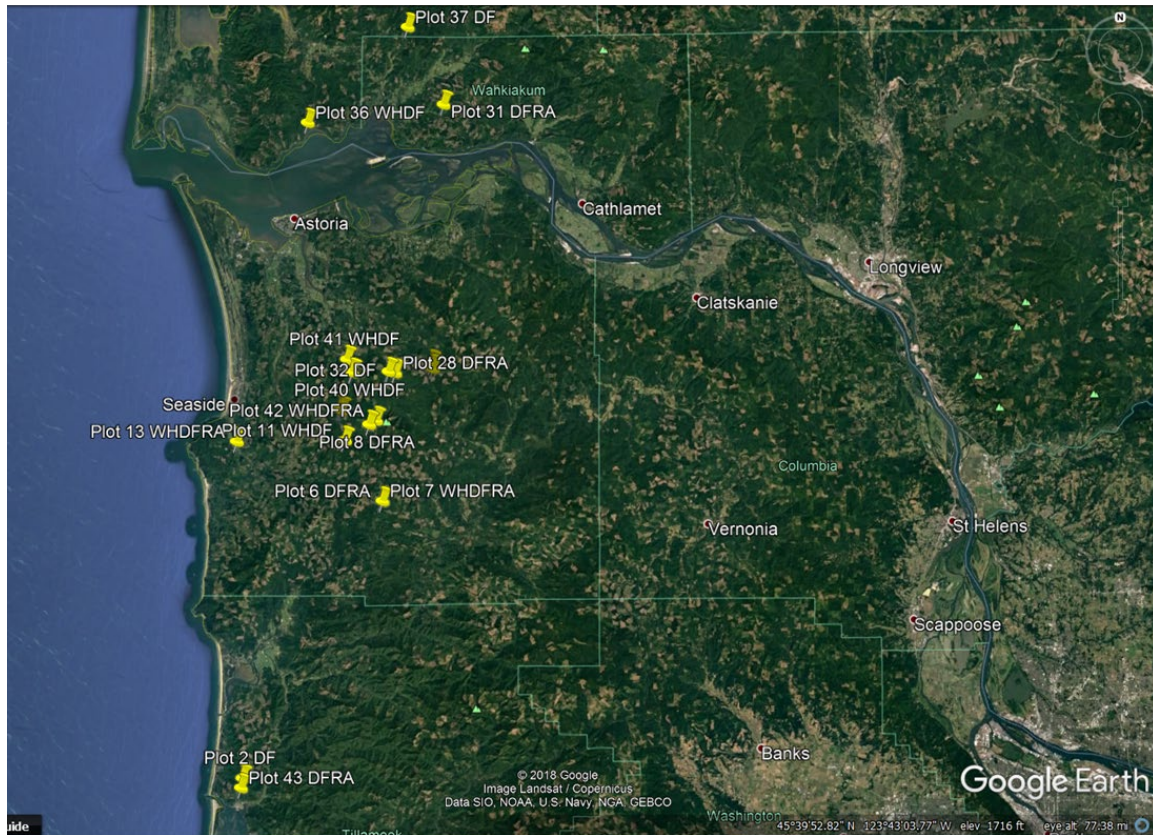
Figure 2. Geographic distribution of plots.

Timeline

The foliage sample collections were completed in June 2018.

References

Keesing, F., Belden, L. K., Daszak, P., Dobson, A., Harvell, C. D., Holt, R. D., ... & Myers, S. S. (2010). Impacts of biodiversity on the emergence and transmission of infectious diseases. Nature, 468(7324), 647.

Latz, E., Eisenhauer, N., Rall, B. C., Allan, E., Roscher, C., Scheu, S., & Jousset, A. (2012). Plant diversity improves protection against soil-borne pathogens by fostering antagonistic bacterial communities. Journal of Ecology, 100(3), 597-604.

Metabarcoding fungi in Douglas-fir needles:

the community around *Nothophaeocryptopus gaeumannii*

Kyle A. Gervers*, Posy E. Busby*
Department of Botany and Plant Pathology, Oregon State University*

Introduction

Surveys for *Nothophaeocryptopus gaeumannii* have traditionally been performed by directly observing stomatal occlusion by pseudothecia, employing microscopy, and by culturing discharged ascospores. Other endophytic fungi of coastal Douglas-fir needles have been observed using similar approaches, though each suffers from deficiencies; fruiting bodies are superficial, microscopy is not high-throughput, and culturing places metabolic constraints on the fungi that one can observe. While each of these techniques has provided the research community with invaluable insight and directions for future research, the availability and affordability of high-throughput sequencing protocols allows for the rapid characterization of needle endophyte communities. It has been experimentally demonstrated that common endophytic fungi have the capacity to influence foliar disease severity in their hosts (Busby, Peay and Newcombe, 2016), in addition to modulating host resistance to abiotic stresses (Giauque and Hawkes, 2013; Rodriguez *et al.*, 2008). For these reasons, we have initiated projects which employ ITS metabarcoding to describe variation needle endophyte community composition in relation to changes in canopy position and host density in a stand. We hypothesized that the upper canopies of old-growth Douglas-fir would be compositionally distinct from the lower canopy as the former experiences "micro-continental" conditions which might limit colonization by certain fungi (McCune, 1993). Additionally, we expected that plots containing greater tree diversity would have different needle endophyte compositions, with perhaps lower relative abundance of *N. gaeumannii*.

Methods

All projects begin with needles that were surface sterilized in solutions of ethanol and bleach to remove debris and epiphytes from needle surfaces. Samples were stored at -80° C prior to freeze-drying. After freeze-drying, DNA was extracted from five needles randomly selected from each sampled tree. We then used fungal-specific primers (Taylor *et al.*, 2016) and polymerase chain reaction (PCR) to amplify the ITS2 region of all fungi in the sample. The amplified fungal barcodes were then sequenced on the Illumina MiSeq platform (2x300, v3 chemistry). MiSeq sequence reads then underwent processing and quality checks before we unique reads were called. Each unique sequence was then cross-referenced with a database of fungal barcode sequences, allowing us to assign a taxonomic identity to each unique sequence. Within each sample, we then tally up the number of reads for each unique sequence; total reads correspond to abundance within the sample. Finally, we will use multivariate analysis of variance to estimate the amount of variation in the community that can be explained by project-specific variables

Foliar endophyte communities of Douglas-fir canopies at the H.J. Andrews

Six old-growth/late-succession trees rigged for climbing at the H.J. Andrews Experimental Research Forest (fig 1) were sampled (by Dan Thomas; University of Oregon) in early summer 2017. Accessible branches (starting from the lowest portion of the canopy, ending at the top) were sampled in each tree and the height of each sample collection was noted. Needles from a branch were separated into 4 age classes (I, II, III, IV; each age class approximates tissue age in years). 265 needle samples (each comprised of several needles) were surface sterilized for 1 minute in 70% ethanol, 4 minutes in 5% sodium hypochlorite, 1 minute again in 70% ethanol, followed by a sterile distilled water rinse before being frozen at -80 degrees Celsius. Another two OG/LS trees were similarly sampled in winter 2017-2018 (by Adam Sibley and Mark Schulze).

Douglas-fir foliar endophyte communities functions of neighborhood tree species diversity

Twenty-two plots in the northwest of Oregon were sampled by Dave Shaw's research group, in a manner designed by Austin Himes (page 22, 2019 SNCC Annual Report). These plots contained varying mixtures of coastal Douglas-fir (*Pseudotsuga menziesii* var. *menziesii*;
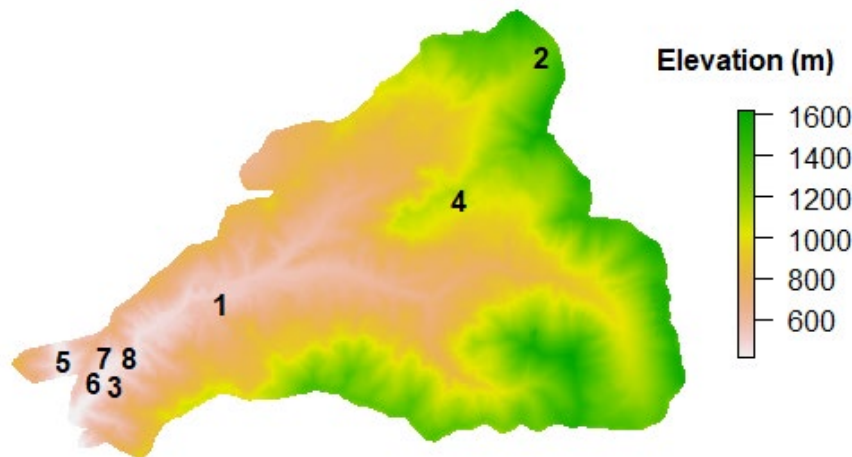
Figure 1. Location of trees across the H.J. Andrews Experimental Forest (Oregon, USA). Trees 2 and 4 were observed to have reduced relative abundance of *N. gaeumannii*.

DF), red alder (*Alnus rubra*; RA), and western hemlock (*Tsuga heterophylla*; WH) planted between 1978 and 1982. DF plots contained only Douglas-fir, RADF plots contained around two-thirds to half red alder (the remaining proportion Douglas-fir), WHDF plots contained around two-thirds to half western hemlock (the remaining proportion Douglas-fir), and WHRADF plots contained all three species in varying proportions. We removed three-year-old needles from a single twig segment for each of 62 trees (up to three trees per plot) and washed them in successive solutions of 95% ethanol, 0.5% sodium hypochlorite, and 70% ethanol to remove debris and epiphytes from needle surfaces. Samples were stored at -80° C prior to freeze-drying and DNA extraction.

Results

Foliar endophyte communities of Douglas-fir canopies at the H.J. Andrews

294 unique fungal sequences (i.e. putatively unique organisms) were identified across all eight trees. Trees had different communities relative to each other; within trees, some needle communities covaried more strongly with needle age class, while some covaried strongly with relative position within the canopy. For trees in which relative canopy position was a relevant factor, *N. gaeumannii* increased in relative abundance in the upper canopy (Figure 2). Those trees for which age was more relevant had relatively more *R. parkeri* in young needles (age class II-III) and more *N. gaeumannii* older needles (age class III-IV). Two high elevation trees (trees 2 and 4 on the map; Figure 1) were found to have reduced relative abundance of *N. gaeumannii*.

Douglas-fir foliar endophyte communities and neighborhood tree species diversity
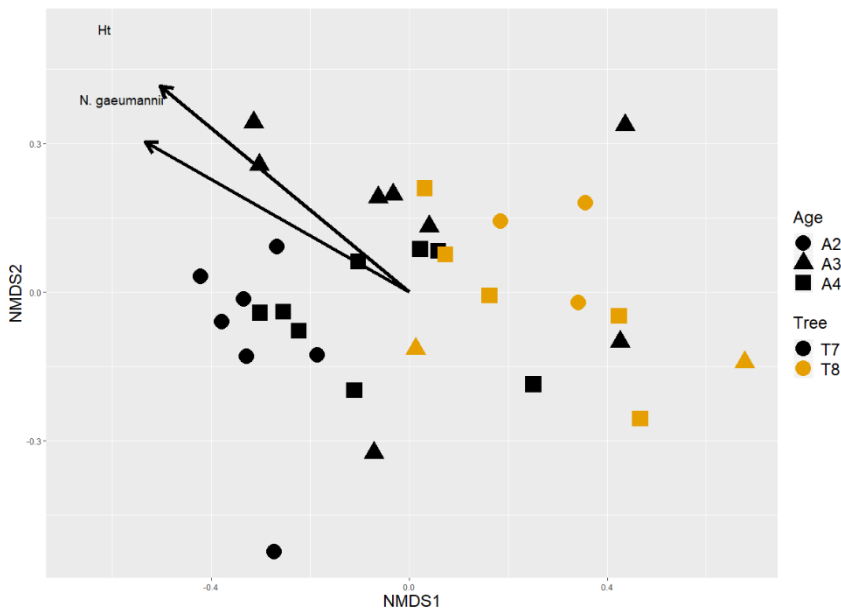
Figure 2. Ordination of samples from vertically composed trees in the H.J. Andrews canopy survey. Points represent samples taken from a single tree; samples closer to each other have more similar communities. Vectors ($p < 0.05$, $r^2 > 0.5$) show compositional correlations with variables (Ht = tree height, N. gaeumannii = Hellinger-transformed abundance). Vectors are nearly parallel, indicating covariation.

Altogether, 61 unique fungal sequences were identified across all 62 trees (fig 3). *N. gaeumannii* had the highest relative abundance in nearly every sample, followed by *R. parkeri*. The composition of the endophytic fungal community did not significantly covary with tree diversity treatments, foliar retention, or even plot of origin (fig 4).

Discussion

Communities from both surveys are likely under-sampled, but this seems especially true
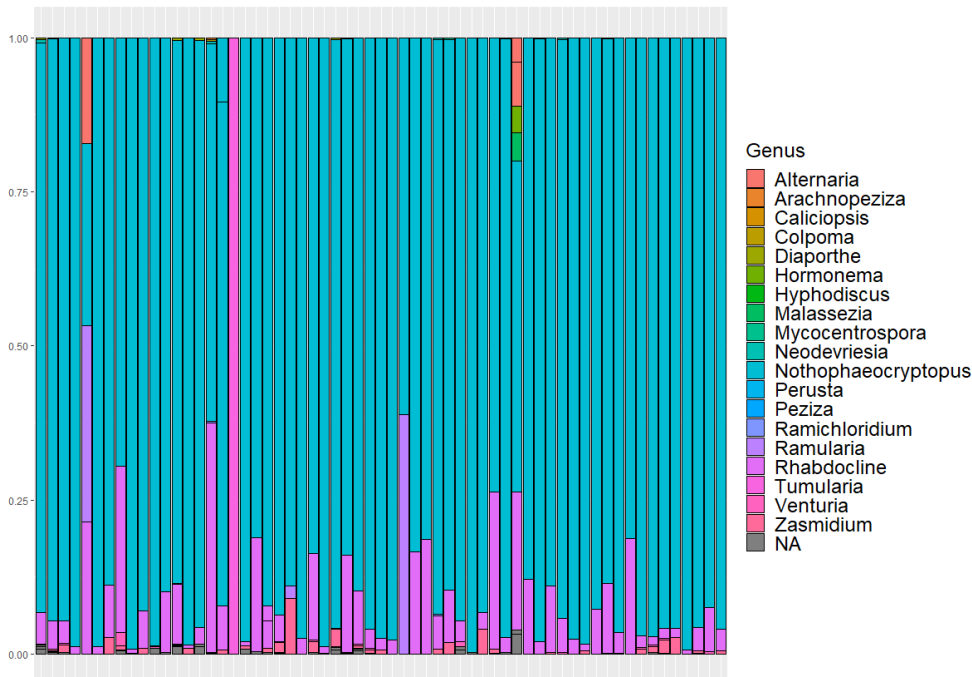
Figure 3. Relative abundance of fungal genera observed in the study of neighborhood tree species diversity effect on needle endophyte communities. Each stack of bars is a single sample. Note the dominance of *Nothophaeocryptopus* across samples.

for the species diversity study. To this point, all of the samples from all 62 trees in the tree species diversity study possess only slightly more unique fungal sequences than the well-sampled canopy of a single old-growth tree at the Andrews (61 vs 38). Accepting this, it is still possible that we have a genuine snapshot of the needle endophyte community, given that most plots are located very near the Tillamook SNC epidemic zone (fig 5). Regarding the lack of treatment effect or within-plot similarity, it is possible that plot heterogeneity is sufficiently high that community assembly appears stochastic.
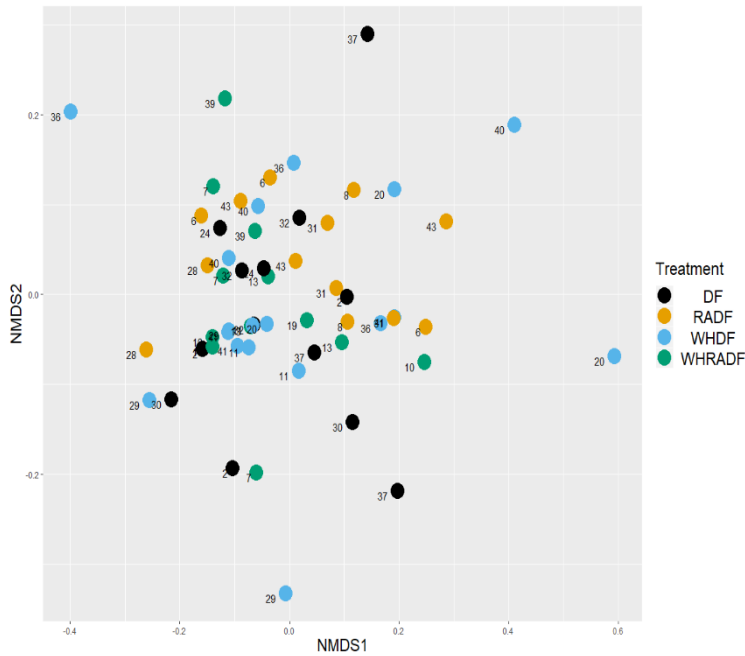
Figure 4. Ordination of all samples in the study of neighborhood tree species diversity. Points represent samples taken from a single tree; samples closer to each other have more similar communities. Numbers to the bottom left of each point indicate plot ID. Note: samples from the same plot are often very distant from one another, and samples that received the same treatment do cluster with each other.

Figure 5. Geographic distribution of plots used in the study of neighborhood tree species diversity effect on needle endophyte communities.

Canopy patterns are inconsistent across the eight trees studied at the Andrews, but it is expected that variation in microclimate at the stand level is responsible. Trees in this study are rigged with light intensity, air temperature, and leaf wetness sensors, recording at sub-hourly

intervals over a period of several years. These data are in hand and will be examined soon in preparation of a manuscript. However, for trees in which canopy position is observed to influence community composition, we did find positive covariation of *N. gaeumannii* with increasing height in the canopy, while trees at high elevations were found to have reduced relative abundance of *N. gauemannii*. Similar results have been observed when pseudothecial incidence is used to track *N. gaeumannii* (Lan *et al.*, 2019), but it should be noted that canopy foliage did not exhibit any symptoms of SNC. Drawing the link between metabarcoding and traditional detection methods should be a goal for future studies.

Future metabarcoding efforts are planned which will leverage nearly 3000 samples taken from six of the Douglas-fir Seed Source Movement Trial common gardens run by the U.S. Forest Service in Oregon and Washington. 30 populations, grown in replicate, have been sampled from each site. These needles have been processed and are currently awaiting DNA extraction and sequencing. The large sample size, combined with replication, should alleviate issues of undersampling.

References

Busby, P. E., Peay, K. G. and Newcombe, G. (2016) 'Common foliar fungi of Populus trichocarpa modify Melampsora rust disease severity', *New Phytologist*, 209(4), pp. 1681–1692. doi: 10.1111/nph.13742.

Giauque, H. and Hawkes, C. V. (2013) 'Climate affects symbiotic fungal endophyte diversity and performance', *American Journal of Botany*, 100(7), pp. 1435–1444. doi: 10.3732/ajb.1200568.

Lan, Y.-H. *et al.* (2019) 'Severity of Swiss needle cast in young and mature Douglas-fir forests in western Oregon, USA', *Forest Ecology and Management*. Elsevier, 442(October 2018), pp. 79–95. doi: 10.1016/j.foreco.2019.03.063.

McCune, B. (1993) 'Gradients in Epiphyte Biomass in Three Pseudotsuga-Tsuga Forests of Different Ages in Western Oregon and Washington, *The Bryologist*, 96(3), pp. 405–411.

Rodriguez, R. J. *et al.* (2008) 'Stress tolerance in plants via habitat-adapted symbiosis', *ISME Journal*, 2(4), pp. 404–416. doi: 10.1038/ismej.2007.106.

Taylor, D. L. *et al.* (2016) 'Accurate Estimation of Fungal Diversity and Abundance through Improved Lineage-Specific Primers Optimized for Illumina Amplicon Sequencing', 82(24), pp. 1–11. doi: 10.1128/AEM.02576-16.Editor.

Community Ecology of Oomycetes and Fungi in Douglas-fir Foliage

Lilah Gonen and Jared LeBoldus

Department of Botany and Plant Pathology, Oregon State University

In April and May 2019, we sampled needles from three Douglas-fir common gardens across coastal Oregon and Washington (Fig. 1) in order to survey the fungi and oomycetes living endophytically in the trees' foliage, including the pathogens *Nothophaeocryptopus gaeumannii* and *Phytophthora pluvialis.* We intend to characterize these microbial communities by amplifying, metabarcoding, and sequencing fungi- and oomycete-specific DNA (ITS1 and rps10, respectively). We will then compare these communities to the common gardens' environmental and weather data, as well as Douglas-fir seed sources and phenology to address whether variation in endophyte diversity among trees and sites reflect environmental characteristics and host genotype x environment interactions. Further, after surface sterilizing needles in 5% bleach solution, we cultured 18 *Pythium* isolates in oomycete-specific agar media (CARP) from two of the common gardens (Fig. 2). This spring, we plan to inoculate 180 Douglas-fir seedlings with three of these isolates with the intent of re-culturing isolates from needle tissue to verify Koch's postulates and compare any differences in host fitness. *Pythium* spp. have yet to be described inhabiting Douglas-fir needle tissue, and we hope to either name new species or improve upon the existing description of known *Pythium* species. Results from these experiments will shed new light on the ecology of recognized and cryptic foliar microbes of Douglas-fir, including known pathogens, thereby improving our understanding of the environment and host characteristics that influence disease.
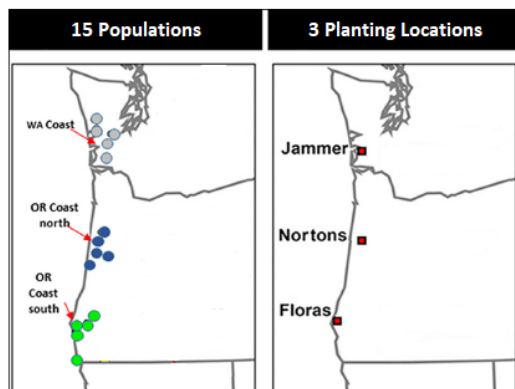
Figure 1. locations of seed sources and common gardens of the Douglas-fir Seed-Source Movement Trial.

Figure 2. *Pythium* sp. Culture growing out of surface-sterilized Douglas-fir needles on CARP.

References

Wilhelmi, N. P., D. C. Shaw, C. A. Harrington, J. B. St. Clair, and L. M. Ganio. 2017. Climate of seed source affects susceptibility of coastal Douglas-fir to foliage diseases. Ecosphere 8(12):e02011. 10.1002/ecs2.2011

List of Refereed Publications

Disease Distribution, Severity and Epidemiology

Agne, MC, Beedlow PA, Shaw DC, Woodruff DR, Lee EH, Cline S, Comeleo RL. 2018. Interactions of predominant insects and diseases with climate change in Douglas-fir forests of western Oregon and Washington, U.S.A.. Forest Ecology and Management. 409:317-332.

Hansen, E. M., Stone, J. K., Capitano, B. R., Rosso, P., Sutton, W., Winton, L., Kanaskie, A. and M. G. McWilliams. 2000. Incidence and impact of Swiss needle cast in forest plantations of Douglas-fir in coastal Oregon. Plant Disease. 84: 773-779.

Lan Y-H, Shaw D.C., Beedlow P.A., Lee E.H., Waschmann R.S.. 2019. Severity of Swiss needle cast in young and mature Douglas-fir forests in western Oregon, USA. Forest Ecology and Management. 442:79-95.

Manter, D. K., Reeser, P. W., and J. K. Stone. 2005. A climate-based model for predicting geographic variation in Swiss needle cast severity in the Oregon coast range. Phytopathology. 95: 1256-1265.

Ritóková, G, Shaw DC, Filip GM, Kanaskie A, Browning J, Norlander D. 2016. Swiss Needle Cast in Western Oregon Douglas-Fir Plantations: 20-Year Monitoring Results. Forests. 7(155)

Rosso, P. H. and E. M. Hansen. 2003. Predicting Swiss needle cast disease distribution and severity in young Douglas-fir plantations in coastal Oregon. Phytopathology. 93: 790-798.

Stone, J. K., Hood, I. A., Watt, M. S. and J. L. Kerrigan. 2007. Distribution of Swiss needle cast in New Zealand in relation to winter temperature. Australasian Plant Pathology. 36: 445-454.

Stone, J. K., Capitano, B. R. and J. L. Kerrigan. 2008. The histopathology of *Phaeocryptopus gaeumannii* on Douglas-fir needles. Mycologia. 100: 431-444.

Stone, J. K., Coop, L. B. and D. K. Manter. 2008. Predicting the effects of climate change on Swiss needle cast disease severity in Pacific Northwest forests. Canadian Journal of Plant Pathology. 30: 169-176.

Watt, M. S., Stone, J. K., Hood, I. A. and D. J. Palmer. 2010. Predicting the severity of Swiss needle cast on Douglas-fir under current and future climate in New Zealand. Forest Ecology and Management (*in press*).

Forest Protection Issues

Kelsey, R. G. and D. K. Manter. 2004. Effect of Swiss needle cast on Douglas-fir stem ethanol and monoterpene concentrations, oleoresin flow, and host selection by the Douglas-fir beetle. Forest Ecology and Management. 190: 241-253.

Shaw, D. C., Filip, G. M., Kanaskie, A., Maguire, D. A. and W. Littke. 2011. Managing an epidemic of Swiss needle cast in the Douglas-fir region of Oregon: The Swiss Needle   Cast Cooperative. Journal of Forestry (*in press*).

Genetic Resistance/Tolerance in Douglas-fir

Jayawickrama, K.J.S., D. Shaw, and T.Z. Ye. 2012. Genetic Selection in Coastal Douglas-fir for tolerance to Swiss Needle Cast Disease. Proceedings of the fourth international workshop on the genetics of host-parasite interactions in forestry: Disease and insect resistance in forest trees. Gen. Tech. Rep. PSW-GTR-240. Albany, CA: Pacific Southwest Research Station, Forest Service, U.S. Department of Agriculture. 372 p.

Johnson, G. R. 2002. Genetic variation in tolerance of Douglas-fir to Swiss needle cast as assessed by symptom expression. Silvae Genetica. 51: 80-86.

Kastner, W., Dutton, S. and D. Roche. 2001. Effects of Swiss needle cast on three Douglas-fir seed sources on a low-elevation site in the northern Oregon Coast Range: Results after five growing seasons. Western Journal of Applied Forestry. 16 (1): 31-34.

Temel, F., Johnson, G. R. and J. K. Stone. 2004. The relationship between Swiss needle cast symptom severity and level of *Phaeocryptopus gaeumannii* colonization in coastal Douglas-fir (*Pseudotsuga menziesii var. menziesii*). Forest Pathology. 34: 383-394.

Temel, F., Johnson, G. R. and W. T. Adams. 2005. Early genetic testing of coastal Douglas-fir for Swiss needle cast tolerance. Canadian Journal of Forest Research. 35: 521-529.

Wilhelmi, N.P., Shaw D.C., Harrington C.A., St. Clair J.B., Ganio L.M. 2017. Climate of seed source affects susceptibility of coastal Douglas-fir to foliage diseases. Ecosphere. 8(12):e02011.

Genetics of *Nothophaeocryptopus gaeumannii*

Bennett P, Hood P.I, Stone J.K.. 2018. The genetic structure of populations of the Douglas-fir Swiss needle cast fungus *Nothophaeocryptopus gaeumannii* in New Zealand. Phytopathology. 109:446-455.

Bennett P, Stone J.K.. 2019. Environmental variables associated with *Nothophaeocryptopus gaeumannii* population structure and Swiss needle cast severity in Western Oregon and Washington. Ecology and Evolution. 9(19):11379-11394.

Winton, L. M., Hansen, E. M. and J. K. Stone. 2006. Population structure suggests reproductively isolated lineages of *Phaeocryptopus gaeumannii*. Mycologia. 98 (5): 781-791.

Winton. L. M., Stone, J. K. and E. M. Hansen. 2007. The systematic position of *Phaeocryptopus gaeumannnii*. Mycologia. 99: 240-252.

Hydrology

Bladon KD, Bywater-Reyes S, LeBoldus JM, Keriö S, Segura C, Ritóková G, Shaw D.C.. 2019. Increased streamflow in catchments affected by a forest disease epidemic. Science of The Total Environment. 691:112-123.

Mensuration and growth effects

Lee, E.H., Beedlow P.A., Waschmann R.S., Tingey D.T., Cline S., Bollman M., Wickham C., Carlile C. 2017. Regional patterns of increasing Swiss needle cast impacts on Douglas-fir growth with warming temperatures. Ecology and Evolution. 7(24):11167–11196.

Maguire D. A., Kanaskie, A., Voelker, W., Johnson, R. and G. Johnson. 2002. Growth of young Douglas-fir plantations across a gradient in Swiss needle cast severity. Western Journal of Applied Forestry. 17: 86-95.

Maguire, D. A. and A. Kanaskie. 2002. The ratio of live crown length to sapwood area as a measure of crown sparseness. Forest Science. 48: 93-100.

Maguire, D. A., Mainwaring, D. B. and Kanaskie A. 2011. Ten-year growth and mortality in young Douglas-fir stands experiencing a range in Swiss needle cast severity. Can. J. For. Res. 41: 2064-2076.

Weiskittel, A. R., Garber, S. M., Johnson, G. P., Maguire, D. A. and R.A. Monserud. 2007. Annualized diameter and height growth equations for Pacific Northwest plantation-grown Douglas-fir, western hemlock, and red alder. Forest Ecology and Management. 250: 266-278.

Weiskittel, A. R., Maguire, D. A., Garber, S. M. and A. Kanaskie. 2006. Influence of Swiss needle cast on foliage age class structure and vertical distribution in Douglas-fir plantations of north coastal Oregon. Canadian Journal of Forest Research. 36: 1497-1508.

Weiskittel, A. R., Maguire, D. A. and R. A. Monserud. 2007. Modeling crown structural responses to competing vegetation control, thinning, fertilization, and Swiss needle cast in coastal Douglas-fir of the Pacific Northwest, USA. Forest Ecology and Management. 245: 96-109.

Weiskittel, A. R., Maguire, D. A. and R. A. Monserud. 2007. Response of branch growth and mortality to silvicultural treatments in coastal Douglas-fir plantations: Implications for predicting tree growth. Forest Ecology and Management. 251: 182-194.

Weiskittel, A. R. and D. A. Maguire. 2007. Response of Douglas-fir leaf area index and litterfall dynamics to Swiss needle cast in north coastal Oregon, USA. Annals of Forest Science. 64: 121-132.

Weiskittel, A. R. and D. A. Maguire. 2006. Branch surface area and its vertical distribution in coastal Douglas-fir. Trees. 20: 657-667.

Weiskittel, A. R., Temesgen, H., Wilson, D. S. and D. A. Maguire. 2008. Sources of within and between-stand variability in specific leaf area of three ecologically distinct conifer species. Annals of Forest Science. 65: 103-112.

Zhao, J., Maguire, D. A., Mainwaring, D. B., Kanaskie, A. 2012. Climatic influences on needle cohort survival mediated by Swiss needle cast in coastal Douglas-fir. Trees 26: 1361-1371

Zhao, J., Mainwaring, D. B., Maguire, D. A., Kanaskie, A. 2011. Regional and annual trends in Douglas-fir foliage retention: Correlations with climatic variables. For. Ecol. And Management 262: 1872-1886

Zhao, J, Maguire DA, Mainwaring DB, Kanaskie A. 2015. The effect of within-stand variation in Swiss needle cast intensity on Douglas-fir stand dynamics. Forest Ecology and Management. 347:75-82.

Zhao, J., Maguire, D. A., Mainwaring, D. B., Wehage, J., Kanaskie, A. 2013. Thinning Mixed Species Stands of Douglas-Fir and Western Hemlcok in the Presence of Swiss Needle Cast: Guidelines Based on Relative Basal Area Growth of Individual Trees. For. Sci. 60 (1): 191-199.

Nutrition and soil interactions

El-Hajj, Z., Kavanagh, K., Rose, C., and Z. Kanaan-Atallah. 2004. Nitrogen and carbon dynamics of a foliar biotrophic fungal parasite in fertilized Douglas-fir. New Phytologist. 163: 139-147.

Lan Y-H, Shaw D.C., Ritóková G, Hatten J. 2019. Associations between Swiss Needle Cast Severity and Foliar Nutrients in Young-Growth Douglas-Fir in Coastal Western Oregon and Southwest Washington, USA. For. Sci. 65(5):537-542.

Mulvey, R.L., Shaw, D.C., Maguire, D.A. 2013. Fertilization impacts on Swiss needle cast disease severity in Western Oregon. Forest Ecology and Management 287: 147-158.

Perakis, S. S., Maguire, D. A., Bullen, T. D., Cromack, K., Waring, R. H. and J. R. Boyle. 2005. Coupled nitrogen and calcium cycles in forests of the Oregon Coast Range. Ecosystems. 8: 1-12.

Waring, R. H., Boyle, J., Cromack, K. Jr., Maguire, D. and A. Kanaskie. 2000. Researchers offer new insights into Swiss needle cast. Western Forester. 45 (6): 10-11.

Pathology and physiological host effects

Bennett, P., Stone, J. 2016. Assessments of Population Structure, Diversity, and Phylogeography of the Swiss Needle Cast Fungus (*Phaeocryptopus gaeumannii*) in the U.S. Pacific Northwest. Forests: 7, 14.

Black, B. A., Shaw, D. C. and J. K. Stone. 2010. Impacts of Swiss needle cast on overstory Douglas-fir forests of western Oregon Coast Range. Forest Ecology and Management. 259: 1673-1680.

Lee, H.E., Beedlow, P.A., Waschamnn, R.S., Burdick, C.A., Shaw, D.C. 2013. Tree-ring analysis of the fungal disease Swiss needle cast in western Oregon coastal forests. Can Journal of For. 43(8):677-690.

Manter, D. K., Bond, B. J., Kavanagh, K. L., Rosso, P. H. and G. M. Filip. 2000. Pseudothecia of Swiss needle cast fungus, *Phaeocryptopus gaeumannii,* physically block stomata of Douglas-fir, reducing CO_2 assimilation. New Phytologist. 148 (3): 481-491.

Manter, D. K. 2002. Energy dissipation and photoinhibition in Douglas-fir needles with a fungal-mediated reduction in photosynthetic rates. Phytopathology. 150: 674-679.

Manter, D. K., Bond, B. J., Kavanagh, K. L., Stone, J. K. and G. M. Filip. 2003. Modeling the impacts of the foliar pathogen, *Phaeocryptopus gaeumannii*, on Douglas-fir physiology: net canopy carbon assimilation, needle abscission and growth. Ecological Modeling. 164: 211-226.

Manter, D. K. and Kavanagh, K. L. 2003. Stomatal regulation in Douglas-fir following a fungal-mediated chronic reduction in leaf area. Trees. 17: 485-491.

Manter, D. K., Kelsey, R. G., and J. K. Stone. 2001. Quantification of *Phaeocryptopus gaeumannii* colonization in Douglas-fir needles by ergosterol analysis. Forest Pathology. 31: 229-240.

Manter, D. K., Winton, L. M., Filip, G. M. and J. K. Stone. 2003. Assessment of Swiss needle cast disease: temporal and spatial investigations of fungal colonization and symptom severity. Phytopathology. 151: 344-351.

Saffell, B.J., Meinzer, R.C., Voelker, S.L., Shaw, D.C., Brooks, R.J., Lachenbruch, B, McKay, J. 2014. Tree-ring stable isotopes record the impact of a foliar fungal pathogen on CO_2 assimilation and growth in Douglas-fir. Plant, Cell & Environment. doi: 10.1111/pce.12256

Winton, L. M., Manter, D. K., Stone, J. K. and E. M. Hansen. 2003. Comparison of biochemical, molecular and visual methods to quantify *Phaeocryptopus gaeumannii* in Douglas-fir foliage. Phytopathology. 93: 121-126.

Winton, L. M., Stone, J. K., Watrud, L. S. and E. M. Hansen. 2002. Simultaneous one-tube quantification of host and pathogen DNA with real-time polymerase chain reaction. Phytopathology. 92: 112-116.

Winton, L. M., Stone, J. K. and E. M. Hansen. 2007. Polymorphic microsatellite markers for the Douglas-fir pathogen *Phaeocryptopus gaeumannii*, causal agent of Swiss needle cast disease. Molecular Ecology. 7: 1125-1128.

Silviculture and Control

Filip, G., Kanaskie, A., Kavanagh, K., Johnson, G., Johnson, R. and D. Maguire. 2000. Research Contribution 30, Forest Research Laboratory, College of Forestry, Oregon State University, Corvallis, Oregon.

Mainwaring, D. B., Maguire, D. A., Kanaskie, A. and J. Brandt. 2005. Growth responses to commercial thinning in Douglas-fir stands with varying intensity of Swiss needle cast. Canadian Journal of Forest Research. 35: 2394-2402.

Stone, J. K., Reeser, P. W. and A. Kanaskie. 2007. Fungicidal suppression of Swiss needle cast and pathogen reinvasion in a 20-year-old Douglas-fir stand. Western Journal of Applied Forestry. 22: 248-252.

Wood Quality

Johnson, G. R., Gartner, B. L., Maguire, D. and A. Kanaskie. 2003. Influence of Bravo fungicide applications on wood density and moisture content of Swiss needle cast affected Douglas-fir trees. Forest Ecology and Management. 186: 339-348.

Johnson, G. R., Grotta, A. T., Gartner, B. L. and G. Downes. 2005. Impact of the foliar pathogen Swiss needle cast on wood quality of Douglas-fir. Canadian Journal of Forest Research. 35: 331-339.

Grotta, A. T., Leichti, R. J., Gartner, B. L. and G. R. Johnson. 2004. Effect of growth ring orientation and placement of earlywood and latewood on MOE and MOR of very-small clear Douglas-fir beams. Wood and Fiber Science. 37: 207-212.

ORIGINAL RESEARCH

Ecology and Evolution WILEY

Environmental variables associated with *Nothophaeocryptopus gaeumannii* population structure and Swiss needle cast severity in Western Oregon and Washington

Patrick I. Bennett 🟢 | Jeffrey K. Stone

Department of Botany and Plant Pathology, Oregon State University, Corvallis, OR, USA

Correspondence
Patrick I. Bennett, Department of Botany and Plant Pathology, Oregon State University, 2082 Cordley Hall, 2701 SW Campus Way, Corvallis 97331, OR, USA.
Email: bennetpa@oregonstate.edu

Abstract

The environment has a strong influence on the abundance and distribution of plant pathogenic organisms and plays a major role in plant disease. Climatological factors may also alter the dynamics of the interactions between plant pathogens and their hosts. *Nothophaeocryptopus* (=*Phaeocryptopus*) *gaeumannii*, the causal agent of Swiss needle cast (SNC) of Douglas-fir, is endemic to western North America where it exists as two sympatric, reproductively isolated lineages. The abundance of this fungus and the severity of SNC are strongly influenced by climate. We used statistical and population genetic analyses to examine relationships between environment, pathogen population structure, and SNC severity. Although *N. gaeumannii* Lineage 2 in western Oregon and Washington was most abundant where SNC symptoms were most severe, we did not detect a significant relationship between Lineage 2 and disease severity. Warmer winter temperatures were inversely correlated with foliage retention (*AFR*) and positively correlated with the relative abundance of Lineage 2 (*PL2*). However when distance inland, which was strongly correlated with both *AFR* and *PL2*, was included in the model, there was no significant relationship between Lineage 2 and *AFR*. Spring/early summer dew point temperatures also were positively associated with total *N. gaeumannii* abundance (colonization index (*CI*)) and inversely correlated with *AFR*. Warmer summer mean temperatures were associated with lower *CI* and higher *AFR*. Our results suggest that the two lineages have overlapping environmental optima, but slightly different tolerance ranges. Lineage 2 was absent from more inland sites where winters are colder and summers are warm and dry, while Lineage 1 occurred at most sites across an environmental gradient suggesting broader environmental tolerance. These relationships suggest that climate influences the abundance and distribution of this ecologically important plant pathogen and may have played a role in the evolutionary divergence of these two cryptic fungal lineages.

KEYWORDS
environmental adaptation, evolutionary divergence, forest pathology, population genetics, Swiss needle cast

1 | INTRODUCTION

Climate plays a major role in influencing the geographic distributions of plant pathogens and their hosts and may lead to changes in host–pathogen dynamics (Sturrock et al., 2011). Climate change is predicted to directly affect pathogens most strongly, and fungi causing foliage diseases in particular are most likely to be influenced by environmental variables (Harvell et al., 2002). Outbreaks of damaging forest pathogens such as *Dothistroma septosporum*, which causes foliage loss, growth reductions, and mortality of native and introduced *Pinus* species, have been linked to regional weather patterns (Kliejunas et al., 2009; Welsh, Lewis, & Woods, 2014). The recent emergence of this major forest disease and others around the globe may be attributable, at least in part, to climate change (Harvell et al., 2002; Kliejunas et al., 2009; Welsh et al., 2014; Woods, Coates, & Hamann, 2005; Woods et al., 2016). Microbial pathogens and insects, because of their shorter generation times, respond more rapidly to environmental changes than forest communities and may amplify the effects of climate change on forest health (Kliejunas et al., 2009). Changes to forest disturbance regimes due to the influences of climate on the interactions between disease, fire, and insects are expected to impact the future ecological trajectories of forested landscapes (Agne et al., 2018; Sturrock et al., 2011).

Swiss needle cast (SNC) is a foliar disease specific to Douglas-fir (*Pseudotsuga menziesii* (Mirb.) Franco) caused by the ascomycete *Nothophaeocryptopus* (=*Phaeocryptopus*) *gaeumannii* (T. Rohde) Videira, C. Nakash., U. Braun & Crous. The inhibition of gas exchange and CO_2 assimilation resulting from the cumulative occlusion of stomata by the pseudothecia of *N. gaeumannii* causes premature needle abscission (Manter, Bond, Kavanagh, Rosso, & Filip, 2000; Manter, Winton, Filip, & Stone, 2003). Impaired carbon assimilation and reduced photosynthetic capacity due to foliage loss result in height and diameter growth reductions of 20%–50% relative to healthy trees (Maguire, Kanaskie, Voelker, Johnson, & Johnson, 2002; Maguire, Mainwaring, & Kanaskie, 2011; Manter et al., 2003). The physiological stress caused by this disease rarely leads to mortality, as even the most severely diseased trees retain the current year's foliage (Hansen et al., 2000; Maguire et al., 2002). However, the loss of vigor associated with SNC may diminish the ability of Douglas-fir to compete with other conifer species (e.g., *Tsuga heterophylla*), thereby altering the ecology and successional trajectory of Douglas-fir in mixed natural stands (Lee et al., 2017; Stone, Coop, & Manter, 2008; Zhao, Maguire, Mainwaring, & Kanaskie, 2014).

Although the disease was first described from a Douglas-fir plantation in Switzerland in 1925, *Nothophaeocryptopus gaeumannii* is presumed to be native to the Pacific Northwest (Hansen et al., 2000) where the population is subdivided into two reproductively isolated lineages (Bennett & Stone, 2016; Winton, Hansen, & Stone, 2006). Lineage 1 occurs throughout the natural range of Douglas-fir and worldwide where Douglas-fir is grown as an exotic (Winton et al., 2006). Lineage 2 has a more restricted distribution (Bennett & Stone, 2016; Winton et al., 2006) and is most abundant along the western Coast Ranges in Oregon and Washington within a few kilometers of the coast. The abundance of Lineage 2 decreases further inland, where it is often supplanted entirely by Lineage 1 (Bennett & Stone, 2016; Winton et al., 2006). The factors influencing the spatial distributions of these lineages are not currently understood. Previous studies have identified strong genetic differentiation between these two lineages (Bennett & Stone, 2016; Winton et al., 2006). Despite the fact that there is circumstantial evidence for reproductive isolation between the two lineages, there is currently insufficient evidence to describe them as distinct biological or phylogenetic species.

Prior to the late 1970s, SNC had not caused any serious damage in Pacific Northwest forests (Hansen et al., 2000). However, symptoms of SNC have been intensifying in this region since 1990s, and a 2016 aerial survey identified approximately 200,000 hectares of affected land in Oregon (Hansen et al., 2000; Ritóková et al., 2016). Its proliferation and subsequent emergence as a threat to Douglas-fir forest health and productivity in western North America is thought to have been perpetuated by the widespread planting of Douglas-fir where the climate is particularly conducive to disease in a narrow band of low-elevation coastal forests along the western slopes of the Coast Ranges in Oregon and Washington that has historically been considered the *Picea sitchensis* vegetation zone (Franklin & Dyrness, 1973; Hansen et al., 2000).

Because the distribution of Lineage 2 in the western Coast Ranges in Oregon and Washington corresponds to the region where the most severe SNC symptoms (foliage loss and growth reduction) have been documented, a causal relationship between Lineage 2 and the recent intensification and expansion of SNC in this region has been suggested (Winton et al., 2006). Compared to Lineage 1, recovery of Lineage 2 isolates from diseased foliage was twice as likely in severely diseased stands, and only half as likely in healthier stands (Winton et al., 2006). In coastal Oregon, Douglas-fir stands with higher relative proportions of Lineage 2 had more sparse canopies, suggesting less foliage retention due to SNC (Winton et al., 2006). Visual estimates of foliage discoloration as an indicator of disease severity also suggested a causal relationship with the relative abundance of Lineage 2 in the stand (Winton et al., 2006). Isolates of *N. gaeumannii* collected from sites with severe disease also seemed to cause more severe SNC symptoms in an inoculation study, suggesting that more virulent or aggressive genotypes may be more prevalent in the low-elevation coastal forests in Oregon and Washington where SNC is most severe (Winton, 2001). These observations informed our hypotheses about the potential relationships between the distribution of *N. gaeumannii* Lineage 2 and SNC severity.

The regional climate in the western Coast Ranges in Oregon and Washington has a strong influence on the distribution and severity of SNC, and variation in *N. gaeumannii* abundance and SNC symptom severity in relation to site-specific climate factors has been well documented (Coop & Stone, 2010; Hansen et al., 2000; Lee, Beedlow, Waschmann, Burdick, & Shaw, 2013; Lee et al., 2017; Manter, Reeser, & Stone, 2005; Rosso & Hansen, 2003; Stone, Coop, et al., 2008; Stone, Hood, Watt, & Kerrigan, 2007; Watt, Stone, Hood, & Palmer, 2010; Zhao, Maguire, Mainwaring, & Kanaskie, 2012;
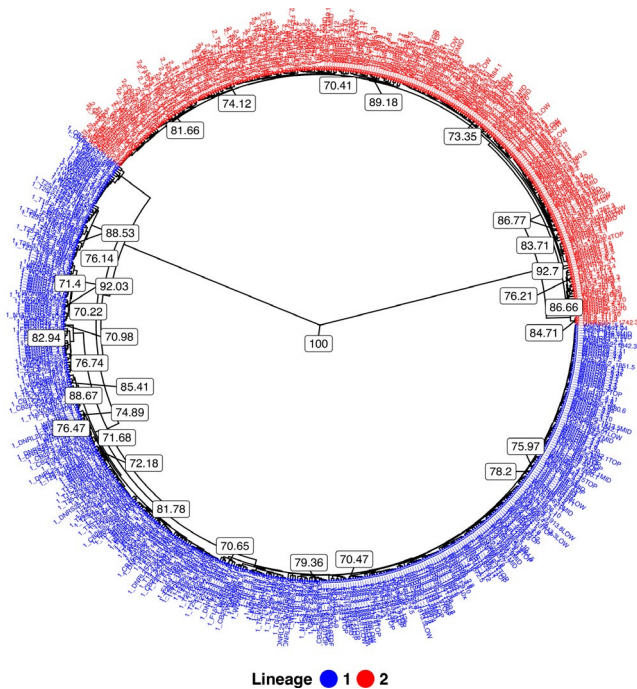
FIGURE 1 Genetic distance dendrogram (UPGMA, unweighted pair-group method with arithmetic means) from bootstrap analysis of Nei's genetic distance showing divergence between genotypes corresponding to two *Nothophaeocryptopus gaeumannii* lineages from Oregon and Washington (clone-censored, N = 663). Node labels represent bootstrap statistics (≥ 70%) from 10,000 replicate trees

Zhao, Mainwaring, Maguire, & Kanaskie, 2011). Winter temperature consistently has been identified as being strongly correlated with *N. gaeumannii* abundance, and thus SNC severity, given that needle colonization and the development of pseudothecia continue throughout winter following the spring/summer infection period (Capitano, 1999; Manter et al., 2005; Stone, Capitano, & Kerrigan, 2008). Colder winter temperatures limit the colonization of needles by *N. gaeumannii* (Manter et al., 2005). Leaf wetness and free moisture (as precipitation, fog, or dew) during the spring and early summer are necessary for spore dispersal, adhesion, and germination on the needle surface (Capitano, 1999; Manter et al., 2005), and thus are highly influential in predictive spatial models of SNC severity when severity estimates are based on the abundance of *N. gaeumannii*. Temperatures above 30°C inhibit the growth of *N. gaeumannii*, and thus, warmer average summer temperatures also are associated with less severe SNC symptoms (Capitano, 1999; Lee et al., 2017; Rosso & Hansen, 2003; Zhao et al., 2011). Predictive models based on combinations of these factors explain much of the variability (R^2 = 57%–78%) in SNC severity in western Oregon and Washington forests (Lee et al., 2017; Manter et al., 2005; Rosso & Hansen, 2003; Stone, Coop, et al., 2008). A trend of increasing mean winter temperatures and spring precipitation in the Pacific Northwest in recent decades has resulted in conditions conducive to the intensification and expansion of SNC (Abatzoglou, Rupp, & Mote, 2014; Lee et al., 2017; Stone, Coop, et al., 2008).

Our objectives for this study were to (a) assess the spatial distributions of the two *N. gaeumannii* lineages in relation to SNC severity in the Oregon (OR) and Washington (WA) Coast Ranges, (b) determine whether any relationship exists between SNC severity and the relative abundance of *N. gaeumannii* Lineage 2, and (c) examine the relationships between the genetic structure of *N. gaeumannii* populations, SNC severity, and key environmental variables with a multivariate statistical ordination. Given previous observations of the relationship between the spatial distribution of *N. gaeumannii* Lineage 2 and SNC severity, we aimed to test the hypothesis that the relative abundance of Lineage 2 within sites is positively correlated with disease severity. The analyses performed here were also designed to test the hypothesis that SNC severity and the spatial distributions of the two lineages (and thus the spatial genetic structure of *N. gaeumannii* populations) are correlated with environmental variables that have been previously identified as being critical for the development of *N. gaeumannii*.

2 | MATERIALS AND METHODS

2.1 | Foliage sampling

Douglas-fir foliage was collected from 23 sites in the western Oregon Coast Range in a plot network maintained by the Oregon State University Swiss Needle Cast Cooperative (SNCC) (Ritóková et al., 2016; Shaw, Filip, Kanaskie, Maguire, & Littke, 2011). For these sites, the sampling was concurrent with annual disease assessments performed 2014–2016. In 2015, foliage was also collected from 11 sites in Washington managed by the Washington Department of Natural Resources (WA DNR) (Figure 1). With the exception of the WA DNR sites in southwest Washington and those near Gold Beach, OR, the sampling sites were generally arranged in transects stratified by distance inland, with sites ranging from the shoreline to 56 km inland (Figure 1). At each site, foliage was collected from second- and third-year internodes on secondary branches in the upper crowns of five randomly selected 10- to 30-year-old Douglas-fir trees. From one of the five trees sampled at each of the SNCC sites, foliage samples were also collected from the lower, middle, and upper crowns to assess within-tree diversity. The foliage was stored on ice and promptly returned to the campus of Oregon State University for storage in a cold room for no longer than 7 days prior to processing.

2.2 | Isolation of *N. gaeumannii* from Douglas-fir Foliage

The protocol for isolating *N. gaeumannii* from infected Douglas-fir needles is described in detail in Bennett and Stone (2016). Briefly, needles with pseudothecia of *N. gaeumannii* were attached to the lids of Petri dishes with double-sided adhesive tape, placed over water agar, and incubated for 48–72 hr. Individual ascospores were removed from the agar with sterilized forceps and transferred onto 2% malt agar (MA) (Difco Laboratories). Cultures were

incubated at 18°C for a minimum of 2 months, and often up to 6 months.

2.3 | Molecular techniques

The protocols for DNA extraction, PCR amplification, and genotyping of simple sequence repeats (SSRs) are described in Bennett and Stone (2016). The DNeasy Plant Kit (Qiagen) was used to extract genomic DNA from vegetative mycelium. The manufacturer's protocol was modified with the addition of a maceration procedure (Bennett & Stone, 2016). For each isolate, ten SSR loci (Winton, Stone, & Hansen, 2007) were amplified in three multiplexed PCR reactions (Bennett & Stone, 2016). The Qiagen Type-It Microsatellite PCR kit (Qiagen, Hilden, Germany) and its associated protocols were used, but with reaction volumes of 12.5 µl. The amplification was performed with the thermal cycling protocol described in Bennett and Stone (2016).

The PCR amplicons were submitted to the Center for Genome Research and Biocomputing (CGRB, Oregon State University) for SSR genotyping via capillary electrophoresis with an ABI 3730 DNA Analyzer (Applied Biosystems, Thermo Fisher Scientific Corporation). Allele sizes and genotypes were assigned with ABI GeneMapper 4.1 (Applied Biosystems, Thermo Fisher Scientific Corporation) and were also visually examined for each locus and isolate to confirm accuracy. A positive control isolate was included with each PCR and genotyping run to ensure that the results were consistent and reproducible. One of the loci, Pgdi5, did not amplify reliably for all isolates and therefore was omitted from the dataset prior to analysis. The actual number of trees per site represented by the isolates in the SSR dataset was often less than five due to a number of steps that may have resulted in sample loss, such as variation in the presence of pseudothecia, contamination during isolation and culturing, and inconsistent amplification during PCR. The genotypes used for this study included those analyzed in Bennett and Stone (2016) (i.e., those sampled in 2014) along with additional isolates that were collected in 2015 and 2016.

2.4 | Data analysis

All statistical and population genetic analyses were performed with the R statistical computing software version 3.4.1 (R Core Team, 2017). The multilocus genotypes (MLGs) consisting of alleles for the 9 SSR loci were formatted in Microsoft Excel 2016 with GenAlEx 6.503 (Peakall & Smouse, 2012, 2006). The MLGs were then imported into R version 3.4.1 (R Core Team, 2017) with the R package _poppr_ version 2.5.0. The MLGs were organized in a stratified population hierarchy that included levels for lineages, states within lineages, sites within states, and trees within sites.

Estimates of genetic diversity, including genotypic diversity (Shannon-Weiner index, H) and Nei's unbiased gene diversity (expected heterozygosity, H_e) (Nei, 1978), were calculated with the R package _poppr_ 2.5.0 (Kamvar et al., 2015, 2014). The Shannon-Weiner diversity index, H, was estimated from 1,000 iterations of

a bootstrap analysis with rarefaction. Genotypic richness was estimated as the number of expected multilocus genotypes (eMLG) with a rarefaction sample size ≥ 10 (Kamvar et al., 2014).

The membership of each isolate in either Lineage 1 or Lineage 2 was visualized as a UPGMA dendrogram constructed from 10,000 bootstrap replicates of Nei's genetic distance (Nei, 1978). This analysis was performed with the R packages _poppr_ 2.5.0 (Kamvar et al., 2015, 2014) and visualized with _ggtree_ version 1.12.0 (Yu, Smith, Zhu, Guan, & Lam, 2017). Genetic differentiation between the two _N. gaeumannii_ lineages was estimated by calculating a standardized differentiation metric, G'_{ST} (Hedrick, 2005), with the R package mmod (Winter, 2012). This measure is scaled such that the value for two populations that do not share any alleles is one, and the value for population pairs that share all alleles is equal to zero (Hedrick, 2005). This metric is also corrected for the observed population heterozygosity and the number of subpopulations being compared (Hedrick, 2005; Winter, 2012). If we assume that the rate of gene flow between populations is higher than the mutation rate within populations, indices such as G'_{ST} can provide a reasonable estimate of migration (Balloux & Lugon-Moulin, 2002; Hedrick, 2005).

Aerial disease survey data were obtained from the Oregon Department of Forestry (https://www.oregon.gov/ODF/ForestBenefits/Pages/ForestHealth.aspx) (Ritóková et al., 2016), and from the Washington Department of Natural Resources (Ramsey, Omdal, Dozic, Kohler, & Boderck, 2015). Researchers with the Oregon State University Swiss Needle Cast Cooperative (SNCC, http://sncc.forestry.oregonstate.edu/) and the Washington Department of Natural Resources provided estimates of both average foliage retention (_AFR_) and colonization index (_CI_) for sites in OR and WA (Ramsey et al., 2015; Ritóková et al., 2016). These disease severity metrics were measured using methods similar to those described in Manter et al. (2005) and Watt et al. (2010). For this study, _AFR_ was expressed as the average percentage of foliage remaining across four needle age classes from secondary branches collected in the midcanopies of 10 trees from each site. An estimate of the average percentage of stomata occluded by pseudothecia, _CI_, was calculated as the product of incidence (the proportion of needles bearing pseudothecia, $N = 50$ needles) and the percentage of stomata occluded by pseudothecia ($N = 10$ needles). The percentage of stomata occluded was calculated by averaging the numbers of pseudothecia from 100 stomata in each of three sections per needle (base, middle, and tip) for each sample of ten 2-year-old needles from each of three canopy sections per tree (lower, middle, and upper) for ten trees from each site.

Pearson correlation coefficients were calculated for all pairwise correlations between geographic and disease variables (for the 34 sites for which disease severity data were available) with the R package _Hmisc_ version 4.1-1 (Harrell, 2017). Scatter plots associated with these statistical analyses were constructed with _ggplot2_ (Wickham, 2016). To account for the possibility that Douglas-fir foliage retention, SNC severity, and the relative proportion of _N. gaeumannii_ Lineage 2 may vary independently along the west–east sampling gradient (due to climatic and other spatial geographic factors), a linear mixed model was utilized to

investigate the influence of the proportion of Lineage 2 on *AFR* with the distance inland from the coast held at its mean value (26 km). Distance inland is related to continentality and serves as a proxy for a complex combination of environmental variables (i.e., average temperature, precipitation, RH, dew point deficit, fog, wind speed, and other unknown factors) that are expected to influence Swiss needle cast severity and foliage retention (Zhao et al., 2011). The following model was designed to test the null hypothesis that the proportion of Lineage 2 had no effect on *AFR* after accounting for distance inland (H_0: $\beta_1 = 0$):

$$Y_i = \beta_0 + \beta_1 X_{1i} + \beta_2 X_{2i} + \varepsilon_i$$

where Y_i is the average foliage retention of the ith site. The intercept β_0 is the mean average foliage retention when the relative proportion of Lineage 2 recovered at the site is 0 and the distance inland is 0 km, β_1 is the coefficient for the effect of the relative proportion of Lineage 2 on mean average foliage retention, X_{1i} is the relative proportion of Lineage 2 recovered from the ith site, β_2 is the coefficient for the effect of the distance inland (km) on mean average foliage retention, X_{2i} is the distance inland (km) of the ith site, and ε_i is the random effect of the ith site on mean average foliage retention, $\varepsilon_i \sim N(0, \sigma^2)$.

Nonmetric multidimensional scaling (NMDS) was used to visualize genetic differentiation between each of the sample sites. Roger's euclidean genetic distance (Rogers, 1972) was calculated pairwise between each of the sampling sites with the R package *adegenet* (Jombart, 2008). The NMDS ordination based on this genetic distance matrix was performed with the function *metaMDS* in the R package *vegan* version 2.4-5 (Oksanen et al., 2017). This method ranks sample units according to their dissimilarity and then attempts to minimize the stress in the relationship between ordination distances and genetic distances (McCune, Grace, & Urban, 2002). Correlations between the ordination, SNC severity, and the environmental/geographic variables associated with each site were calculated with the function *envfit* from the R package *vegan version 2.4-5* (Oksanen et al., 2017). The environmental and geographic overlays were displayed as a

series of radiating vectors, with the direction of the vector corresponding to its relationship to the ordination axes, and the length of the vector proportional to the strength of the correlation between the variable and the ordination. Included as vectors on the joint plot were SNC severity (*AFR* and *CI*), the relative proportion of Lineage 2, latitude, longitude, elevation, and several environmental variables related to SNC severity and *N. gaeumannii* abundance (Lee et al., 2017; Manter et al., 2005; Rosso & Hansen, 2003; Stone, Coop, et al., 2008; Stone et al., 2007; Watt et al., 2010; Zhao et al., 2011). Interpolated spatial climatic data were obtained for each of the sample sites from the Parameter-elevation Regressions on Independent Slopes Model (PRISM) data explorer (PRISM Climate Group, Oregon State University, http://prism.oregonstate.edu).

3 | RESULTS

3.1 | Genetic diversity and population structure

This study included a total of 663 unique multilocus genotypes (MLGs) from 1,061 isolates collected from 35 sites in western Oregon and Washington. This includes 492 isolates collected in 2014 (Bennett & Stone, 2016), as well as an additional 579 isolates collected in 2015 and 2016. There was an average of 23.67 alleles per locus, with an average of 0.93% missing data per locus. Total gene diversity (H_e) for the 1,061 isolates was 0.82 (Tables 1 and 2). There were 403 distinct Lineage 1 MLGs and 260 distinct Lineage 2 MLGs (Table 1). The number of private alleles was 88 for Lineage 1 and 55 for Lineage 2. Overall, Lineage 1 had greater genotypic diversity, genotypic richness, and gene diversity than Lineage 2, even after correcting for the difference in sample sizes by rarefaction (Table 1). The two *N. geaumannii* lineages were strongly differentiated ($G'_{ST} = 0.941$) (Table 1). In the UPGMA dendrogram constructed from a bootstrap analysis of Nei's distance, isolates from the two lineages clustered into two distinct groups (Figure 1). The branch lengths and topologies reflected strong genetic differentiation between the lineages and high genetic diversity within each lineage. Of the 657 isolates collected in Oregon, 384 had distinct MLGs, and of the 404 isolates

TABLE 1 Sample sizes and diversity estimates for the two *Nothophaeocryptopus gaeumannii* lineages

	N_{sites}	$N_{isolates}$	MLG[a]	eMLG[b]	SE[c]	H[d,e]	H_e[f]	G'_{ST}[g]
Lineage 1	28	646	403	290	5.66	5.48	0.70	
Lineage 2	31	415	260	260	0.00	5.35	0.63	
Total	35	1,061	663	323	6.74	5.66	0.82	0.941

[a]MLG = number of multilocus genotypes.
[b]eMLG = expected number of multilocus genotypes in rarefied sample ($n \geq 10$).
[c]SE = standard error of eMLG estimate.
[d]H = Shannon-Weiner diversity index.
[e]Estimated genotypic diversity from 1,000 bootstrap replicates with rarefaction ($n \geq 10$).
[f]H_e = Nei's unbiased gene diversity.
[g]Hedrick's G'_{ST}, a standardized measure of population differentiation calculated here to reflect genetic differentiation between Lineage 1 and Lineage 2.

TABLE 2 Site variables, sample sizes, genetic diversity, and disease severity estimates for each of the sites from which Douglas-fir foliage was collected for isolation of *Nothophaeocryptopus gaeumannii*

Site	Year	Distance inland (km)	Elevation (m)	N_{trees}	$N_{isolates}$	MLG	eMLG	SE	H*	H_e	L1[a]	L2[b]	CI[c]	AFR (%)[d]
Oregon														
Tillamook														
TO-1	2014	5.3	134	9	53	36	9.26	0.78	2.2	0.79	26	27	23.1	42.3
TO-2	2014	4.2	169	5	16	8	5.96	0.91	1.61	0.55	3	13	19.6	52.3
TO-3	2014	8.3	127	5	26	19	8.79	0.9	2.13	0.75	13	13	24.9	30.5
T5-3	2014	16.7	158	5	28	24	9.44	0.67	2.23	0.75	22	6	42.8	32.8
T5-5	2014	17.9	293	5	24	18	8.92	0.83	2.15	0.73	19	5	36.3	46.3
T15-1	2014	28.1	459	4	49	37	9.27	0.79	2.19	0.75	27	22	16.1	67.1
T15-2	2014	36.2	576	5	31	25	9.35	0.71	2.21	0.79	17	14	6.7	88.5
T25-2	2014	49.5	591	5	101	40	8.56	1.03	2.09	0.6	101	0	3.7	88.8
T25-3	2014	49.2	521	5	63	38	8.93	0.93	2.14	0.67	62	1	6.4	88.5
Newport														
N0-1	2015	4.7	146	4	28	9	5.85	1.01	1.59	0.56	0	28	22.9	37.3
N5-2	2015	14.2	457	3	23	17	8.71	0.89	2.12	0.59	0	23	8.8	64
N15-3	2015	32.3	411	3	13	6	5.3	0.66	1.54	0.66	6	7	8.3	83.2
N25-5	2015	50.8	251	2	10	6	6	0	1.61	0.65	10	0	9.6	89.3
Florence														
F0-2	2015	2.7	31	5	11	11	10	0	2.3	0.56	0	11	19.2	43.3
F5-1	2015	11.2	160	3	13	4	3.73	0.45	1.16	0.49	0	13	12.7	37.8
F15-1	2014	40.6	595	5	32	21	8.57	0.97	2.09	0.75	28	4	15.3	77.8
F15-3	2014	38	223	2	15	11	8.12	0.83	2.03	0.68	4	11	17.4	85
F25-2	2014	50	498	5	38	22	8.07	1.11	2	0.74	25	13	18.5	78.8
Coos Bay														
CB0-1	2015	8	51	2	11	5	4.73	0.45	1.34	0.32	0	11	29.3	56.5
CB5-2	2015	25	114	2	8	3	3	0	0.97	0.42	8	0	34.4	57
CB15-2	2015	42	283	5	12	9	7.82	0.65	1.97	0.82	7	5	17.4	71.3
CB25-2	2015	57	549	1	23	12	7.32	1.01	1.9	0.75	16	7	4.1	76.5
Gold beach														
G0-1	2015	1.8	159	3	19	8	6	0.9	1.62	0.58	0	19	18.3	56.5
G0-2	2016	2.2	98	2	10	6	6	0	1.7	0.52	0	10	21.7	40.5
Washington														

(Continues)

TABLE 2 (Continued)

Site	Year	Distance inland (km)	Elevation (m)	N_{trees}	$N_{isolates}$	MLG	eMLG	SE	H^*	H_e	L1[a]	L2[b]	CI[c]	AFR (%)[d]
N Olympic Peninsula														
WDNR70	2015	5.9	16	5	37	29	9.05	0.91	2.16	0.78	20	17	21.8	78.9
WDNR71	2015	12.6	105	5	39	28	9.04	0.87	2.17	0.81	21	18	27.2	71.1
WDNR49	2015	20.4	163	5	41	32	9.38	0.72	2.21	0.78	30	11	27	76.7
WDNR68	2015	34.6	116	5	31	27	9.61	0.56	2.25	0.65	29	2	23.5	70.1
WDNR66	2015	43.7	47	5	53	36	8.93	0.94	2.15	0.6	52	1	32.8	60
S Olympic Peninsula														
WDNRQ	2015	4.3	37	5	31	24	9.18	0.79	2.19	0.65	2	29	NA	NA
WDNR64	2015	11.8	67	5	38	26	8.99	0.86	2.16	0.64	2	36	22.4	51.7
WDNR63	2015	21.9	265	5	40	28	9.13	0.82	2.18	0.76	17	23	8.4	75.2
WDNR32	2015	30.6	482	5	46	33	9.1	0.87	2.17	0.64	46	0	14.2	86.5
SW Washington														
DNRL25-2	2014	58	228	5	25	24	9.85	0.36	2.28	0.74	19	6	18.1	80.3
DNRS25-1	2014	48	355	5	23	15	8.07	1.01	2.02	0.73	14	9	19.4	78.8
Total				150	1,061	663[e]					646	415		

Abbreviation: NA, data not available.

[a]L1 = number of *Nothophaeocryptopus gaeumannii* Lineage 1 isolates recovered from the site.

[b]L2 = number of *N. gaeumannii* Lineage 2 isolates recovered from the site.

[c]CI = colonization index (average percentage of stomata occluded by pseudothecia).

[d]AFR (%) = average foliage retention (average percentage of needles remaining across four needle age classes).

[e]Total MLG not equal to sum of population totals due to shared MLGs. The genotypes of isolates collected in 2014 were analyzed previously in Bennett and Stone (2016).

*Estimated genotypic diversity from 1,000 bootstrap replicates with rarefaction ($n \geq 10$).
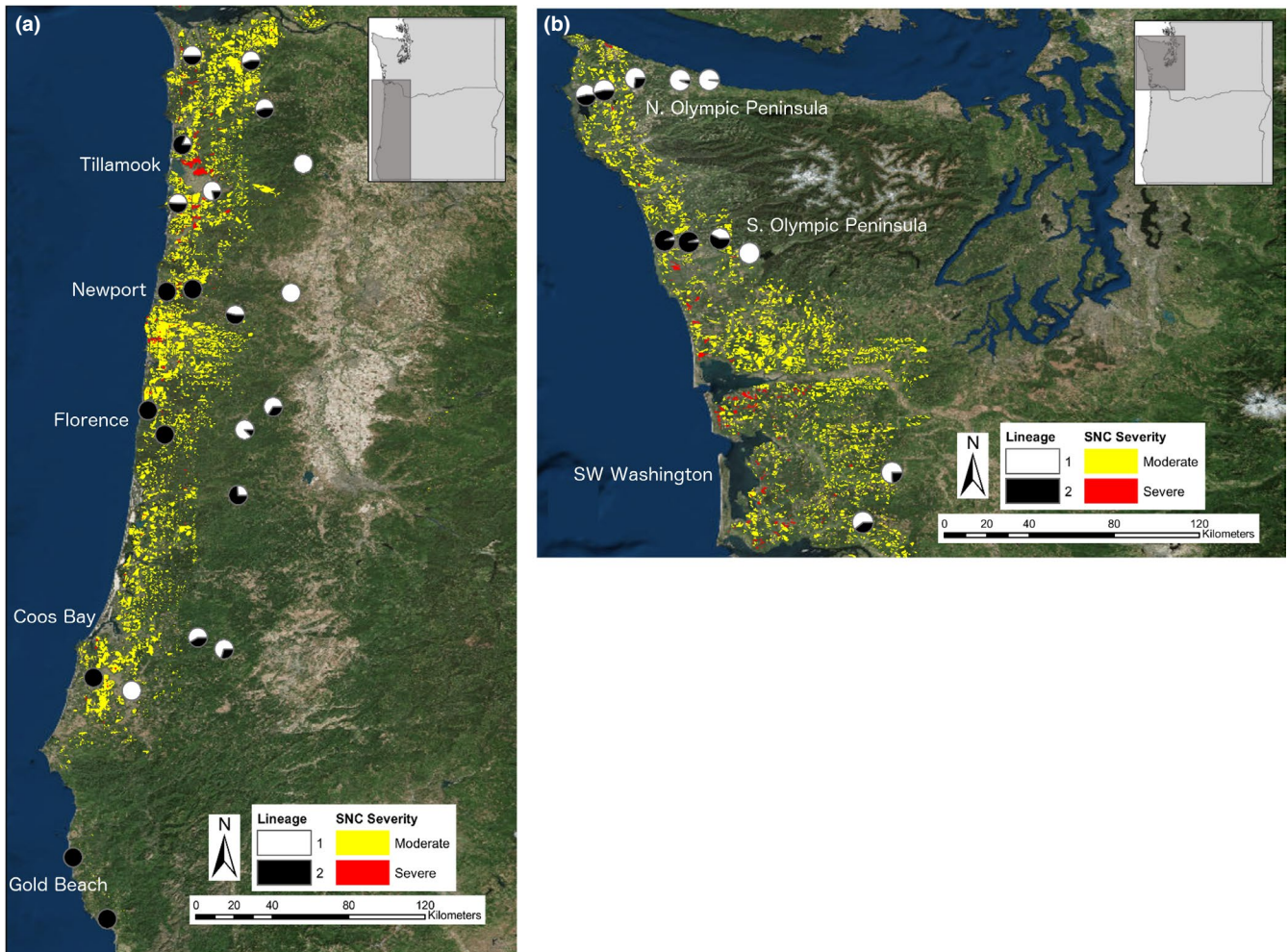
FIGURE 2 Swiss needle cast aerial survey maps with pie charts showing the geographic distributions of *Nothophaeocryptopus gaeumannii* lineages (a) 24 sites in western Oregon (for two of the pie charts, data from adjacent sites were pooled to avoid overlap), and (b) 11 sites in western Washington. Maps were produced with GIS data from the Washington Department of Natural Resources (Ramsey et al., 2015) and the Oregon Department of Forestry (https://www.oregon.gov/ODF/ForestBenefits/Pages/ForestHealth.aspx)

collected in Washington, 282 had distinct MLGs (Table 2). There were 39 private alleles in the Oregon population and 24 in the Washington population.

3.2 | Spatial distributions of *N. gaeumannii* lineages in relation to SNC severity

There was a strong association between the geographic distributions of *N. gaeumannii* Lineage 2 and SNC symptom severity assessed by aerial surveys (Figure 2). With few exceptions, sites nearest the coast had the highest proportions of Lineage 2 and occurred in areas where moderate-to-severe SNC symptoms were observed in the aerial surveys. Sites further inland, where Lineage 2 was generally rare or absent, had less severe SNC, or symptoms were not visible (Figure 2). However, aerial surveys did not detect symptoms of SNC in southwestern Oregon, where only Lineage 2 was isolated from foliage samples and Lineage 1 was not recovered (Figure 2).

3.3 | Variation in geography, environment, and disease severity across sites

The 35 sampling sites in Oregon and Washington covered a latitudinal range from 42°N to 48°N, and a longitudinal range from −124.6°W to −123.3°W (Table 3). Sampling sites ranged from 16 to 595 m elevation and were located from 1.8 to 57.6 km inland (Table 3). Across sampling sites, mean average May–July dew point temperature (MADT) ranged from 7.3° to 10.5°, average spring/ early summer precipitation (PPT) varied from approximately 11.6–132.3 mm, mean summer temperature (TmSummer) ranged from 14.2° to 17.8°, and mean winter temperature (TmWinter) ranged from 4.1° to 10.3° (Table 3).

Disease severity varied across the 34 sites for which disease severity data were available. Estimates of *AFR* ranged from 30.5% to 89.2%, with a mean of 65.3% (Table 2). *CI* ranged from 3.7 to 42.8, with a mean of 19.2. The most severe SNC symptoms occurred at sites in the vicinity of Tillamook, OR (Table 2), where the lowest *AFR* was at site T0-3 (127 m elevation, 8.3 km inland), and the highest

TABLE 3 Summary of variation in geography, disease severity, and environment across sites in Oregon and Washington from which Douglas-fir foliage was sampled for isolation of *Nothophaeocryptopus gaeumannii*

Variable	Mean	SD	Min	Max
Disease				
CI[a]	19.2	9.4	3.7	42.8
AFR[b]	65.3	18.4	30.5	89.3
PL2[c]	0.5	0.4	0.0	1.0
Environment				
MADT[d]	9.2	0.8	7.3	10.5
PPT[e]	70.6	28.0	11.6	132.3
TmSummer[f]	15.9	0.9	14.2	17.8
TmWinter[g]	6.4	1.9	4.1	10.3
Geography				
Lat[h]	45.5	1.8	42.1	48.2
Long[i]	−123.9	0.4	−124.6	−123.3
Elev[j]	261.7	185.3	16.0	595.0
Dist[k]	26.0	18.3	1.8	57.6

[a]CI = colonization index (average percentage of stomata occluded by pseudothecia).
[b]AFR (%) = average foliage retention (average percentage of needles remaining across four needle age classes).
[c]PL2 = relative proportion of *Nothophaeocryptopus gaeumannii* Lineage 2 recovered from a site (number of Lineage 2 isolates/ total isolates).
[d]MADT = mean average dew point temperature (°C) (May–July year prior to sampling).
[e]PPT = average precipitation (mm) (May–July year prior to sampling).
[f]TmSummer = mean summer temperature (°C) (May–September year prior to sampling).
[g]TmWinter = mean winter temperature (°C) (November–March prior to sampling).
[h]Lat = latitude (decimal degrees).
[i]Long = longitude (decimal degrees).
[j]Elev = elevation (meters).
[k]Dist = distance inland (km).

CI was at site T5-3 (158 m elevation, 16.7 km inland; Table 2). The sites with the least severe SNC symptoms were at higher elevations and further inland. The highest AFR was at site N25-5 (251 m elevation, 51 km inland), and the lowest CI was at T25-2 (591 m elevation, 49.5 km inland; Table 2).

3.4 | Correlations between environment, disease, and the genetic structure of *N. Gaeumannii* populations

Pearson's coefficient (*r*) was calculated pairwise between the environmental, geographic, and disease variables in our dataset. *PL2* was negatively correlated with distance inland (Figure 3) and elevation (Table 4), and was positively correlated with mean winter temperature (Table 4). *AFR* was positively correlated with elevation and distance inland (Figure 3, Table 4). *CI* was negatively correlated with elevation and distance inland (Figure 3, Table 4) and was positively

correlated with *MADT* (Table 4). *AFR* was negatively correlated with the relative proportion of *N. gaeumannii* Lineage 2 isolates recovered from the site (*PL2*) (Figure 3), *CI* (Figure 5), and *MADT* (Table 4).

The linear model described the site-level *AFR* as a function of the relative proportion of *N. gaeumannii* Lineage 2 (*PL2*) recovered from the site, after accounting for distance inland (a variable that was strongly correlated with both *PL2* and SNC severity; Figure 4, Table 4). Although it initially appeared that there was a significant correlation between *AFR* and *PL2* (Figure 3d), this association was not significant when distance inland was held at its mean (25.95 km) ($t_{31} = -0.01$, $p = .99$) (Figure 4). There was a significant negative association between *AFR* and *CI*, but there also was considerable variation in *AFR* for a given value of *CI* (Figure 5), though foliage retention may be affected by a combination of environmental variables in addition to colonization by *N. gaeumannii*.

In initial runs of NMDS that included all of the 34 sites for which disease severity data were available, site CB5-2 appeared as an outlier in the periphery of the plot and had a disproportionate influence on the ordination (see Section 4). For this reason, CB5-2 was removed from subsequent analyses. The NMDS ordination of the 33 remaining sites for which disease severity data were available (Table 2) had a final stress of 0.095 (Figure 6). *PL2* had the strongest relationship with the NMDS ordination ($R^2 = .947$, $p = .001$) (Figure 6, Table 5). Therefore sites were aligned along NMDS axis 1 according to the relative proportion of the isolates recovered from the site that were identified as *N. gaeumannii* Lineage 2.

In addition to the genetic differentiation across sites related to the divergence between lineages, there also appeared to be genetic variation between sites that was correlated with environment and SNC severity (Figure 6). Disease severity varied along NMDS axis 2 (Figure 6), and *AFR* was most strongly correlated with the ordination of genetic distance between the sites ($R^2 = .569$, $p = .001$) (Figure 6, Table 5). *CI* was inversely related to *AFR*, but was not correlated as strongly with the ordination ($R^2 = .228$, $p = .016$) (Figure 6, Table 5). Winter temperature (*TmWinter*) was the environmental variable most strongly correlated with the genetic differentiation between sites ($R^2 = .513$, $p = .001$), and with *PL2* (Figure 6, Table 5). Mean summer temperature (*TmSummer*) ($R^2 = .284$, $p = .012$) and average spring/early summer dew point temperature (*MADT*) ($R^2 = .247$, $p = .015$) had much weaker, but nonetheless significant, correlations with the ordination, while average precipitation in the spring and early summer was not significantly correlated with the ordination (Figure 6, Table 5). Latitude was the geographic variable with the strongest correlation with the ordination ($R^2 = .342$, $p = .004$), followed by elevation ($R^2 = .283$, $p = .009$), and longitude ($R^2 = .253$, $p = .017$) (Table 5). *AFR* and *TmSummer* were positively correlated with elevation and longitude, while *CI* was positively correlated with latitude and *MADT* (Figure 6, Table 5).

4 | DISCUSSION

The population of *N. gaeumannii* in Oregon and Washington is diverse with a genetic structure that reflects the presence of two strongly
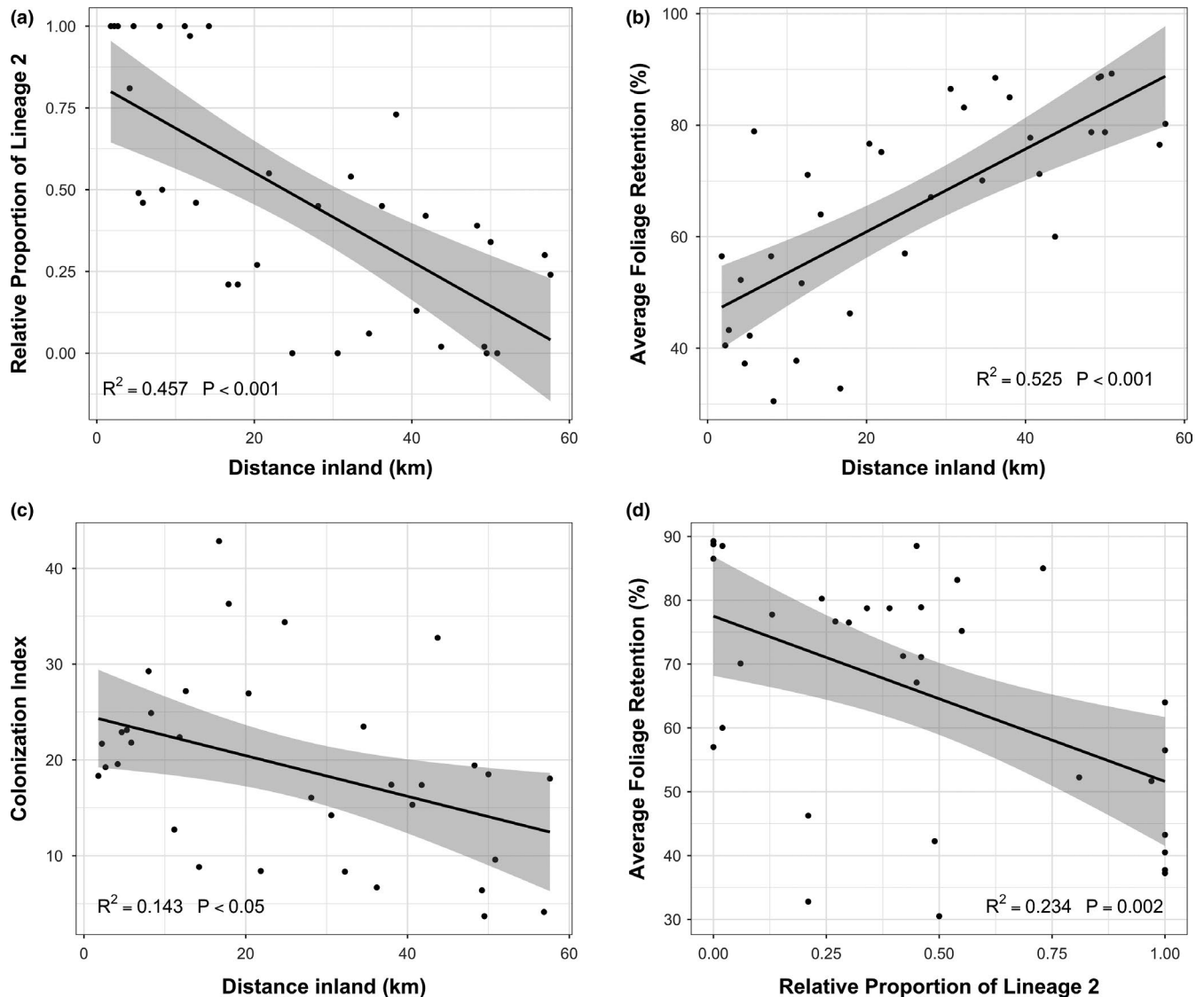
FIGURE 3 The relationships between distance inland (km) and (a) the relative proportion of isolates corresponding to *Nothophaeocryptopus gaeumannii* Lineage 2, (b) average foliage retention (AFR) (%), and (c) the colonization index (i.e., the average proportion of stomata occluded by *N. gaeumannii* pseudothecia). (d) The relationship between the relative proportion of Lineage 2 and average foliage retention when the distance inland (a major confounding variable) is not taken into account. Shaded regions represent 95% confidence intervals for the fitted lines

differentiated noninterbreeding lineages (Figure 1) (Bennett & Stone, 2016; Winton et al., 2006). These characteristics are consistent with the presumed endemism of *N. gaeumannii* in northwestern North America (Hansen et al., 2000; Winton et al., 2006). The presence of repeated multilocus genotypes (i.e., clones) within the two lineages (Tables 1 and 2) likely reflects reproduction via homothallism, as *N. gaeumannii* is not known to reproduce asexually (Winton et al., 2006; Winton, 2001). This reproductive mode likely contributes to the genetic structure of *N. gaeumannii* populations, but the level of genetic variation observed suggests that outcrossing also occurs.

Although the two *N. gaeumannii* lineages have overlapping distributions, it appears that each is adapted to slightly different environmental conditions and thus exhibit different habitat distributions that are determined, directly or indirectly, by climate.

The spatial distribution of *N. gaeumannii* Lineage 2 corresponded to the regions where SNC symptoms were most severe suggesting that some variation in aggressiveness between the two lineages might exist, as suggested by previous authors (Winton et al., 2006). However, we found no evidence to suggest that *N. gaeumannii* Lineage 2 is more aggressive than Lineage 1. After accounting for distance inland, a confounding variable in the relationship between *PL2* and *AFR*, there was no significant correlation between Lineage 2 and SNC severity. Thus, the association between Lineage 2 and greater defoliation can be attributed to overall abundance of *N. gaeumannii* rather than dominance of Lineage 2 genotypes.

The separation of sites along axis 2 in the NMDS analysis (Figure 6) reflects genetic differentiation between the isolates collected at sites with severe disease (higher CI and lower AFR) and

TABLE 4 Pearson's correlation coefficients (r) for the relationships between SNC severity and each of the environmental and geographic variables used for this study

	CI[a]	AFR[b]	PL2[c]	MADT[d]	PPT[e]	TmSummer[f]	TmWinter[g]	Elev[h]	Dist[i]
CI	–								
AFR	−.59 (.000)	–							
PL2	−.03 (.857)	−.51 (.002)	–						
MADT	.65 (.000)	−.58 (.000)	.26 (.144)	–					
PPT	.32 (.062)	−.32 (.067)	.06 (.757)	.17 (.339)	–				
TmSummer	−.33 (.053)	.38 (.025)	−.21 (.236)	−.2 (.257)	−.28 (.109)	–			
TmWinter	.2 (.262)	−.48 (.004)	.51 (.002)	.6 (.000)	−.04 (.821)	.07 (.707)	–		
Elev	−.66 (.000)	.6 (.000)	−.38 (.027)	−.8 (.000)	−.19 (.272)	.39 (.023)	−.48 (.004)	–	
Dist	−.41 (.016)	.73 (.000)	−.69 (.000)	−.55 (.001)	−.14 (.423)	.49 (.004)	−.47 (.005)	.63 (.000)	–

Note: Numbers in parentheses represent computed *p*-values for the correlation coefficient.
[a]colonization index (average proportion of stomata occluded by pseudothecia).
[b]Average foliage retention (%).
[c]Relative proportion of Lineage 2 isolates from sample site (Lineage 2 isolates/total isolates).
[d]Mean average dew point temperature (°C).
[e]Spring/early summer precipitation (mm).
[f]Mean summer temperature (°C).
[g]Mean winter temperature (°C).
[h]Elevation (meters).
[i]Distance inland (km).

those collected at sites with lower disease severity (lower CI and higher AFR). This genetic differentiation was not related to the relative abundances of Lineages 1 and 2. This suggests that some variation in aggressiveness among isolates exists that is not related to the genetic differentiation between the two lineages. These observations also suggest that adaptation to local climate or natural selection for advantageous genotypes has occurred in the geographic regions where SNC is most severe. Whether *N. gaeumannii* populations in

the coastal SNC epidemic zone are in fact more aggressive or have increased fitness (and thus cause more severe symptoms) is still unclear and should be the focus of future studies.

The relative abundances of the lineages varied along a west–east gradient, with Lineage 2 more abundant relative to Lineage 1 in sites near the coast and decreasing in relative abundance further inland. At sites approximately 40–56 km inland, Lineage 2 was supplanted entirely by Lineage 1 in some sites. The correspondence between the geographic distributions of *N. gaeumannii* Lineage 2 and severe SNC symptoms in western Oregon and Washington (Figure 2)
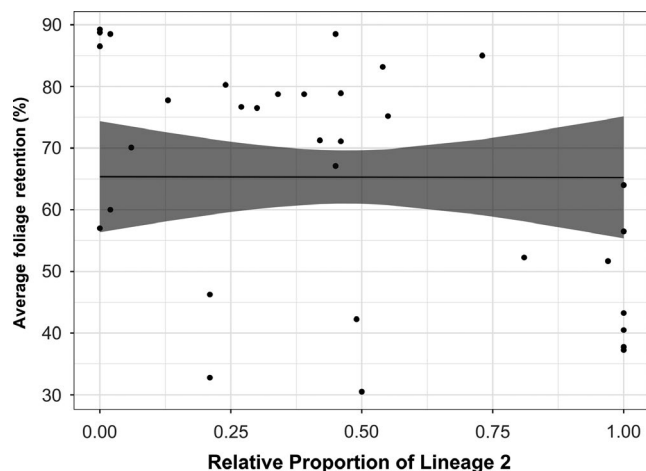
FIGURE 4 The relationship between average foliage retention (AFR) (%) and the relative proportion of *Nothophaeocryptopus gaeumannii* Lineage 2, after accounting for distance inland. Each point corresponds to one of the 34 sites for which disease severity data were available. The line corresponds to predicted values from the model when the distance inland is fixed at its mean (26 km), with the shaded region representing the 95% confidence intervals for the predicted values
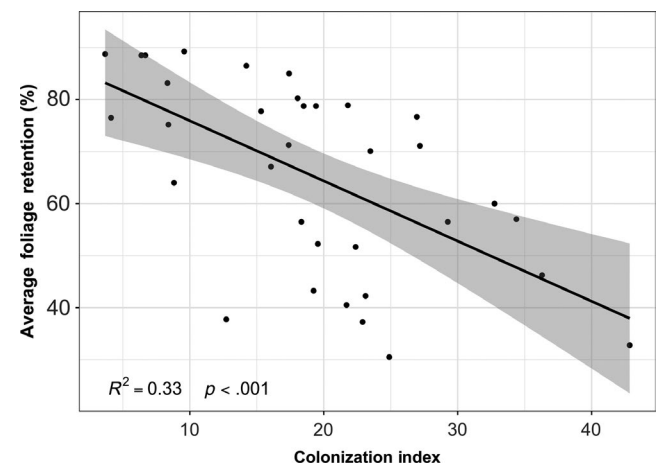
FIGURE 5 The relationship between average foliage retention (AFR) (%) and the colonization index (CI), an estimate of the average percentage of stomata occluded by pseudothecia of *Nothophaeocryptopus gaeumannii*. AFR and CI were measured for ten Douglas-fir trees from each site. The data here reflect only the 34 sites for which disease severity data were available
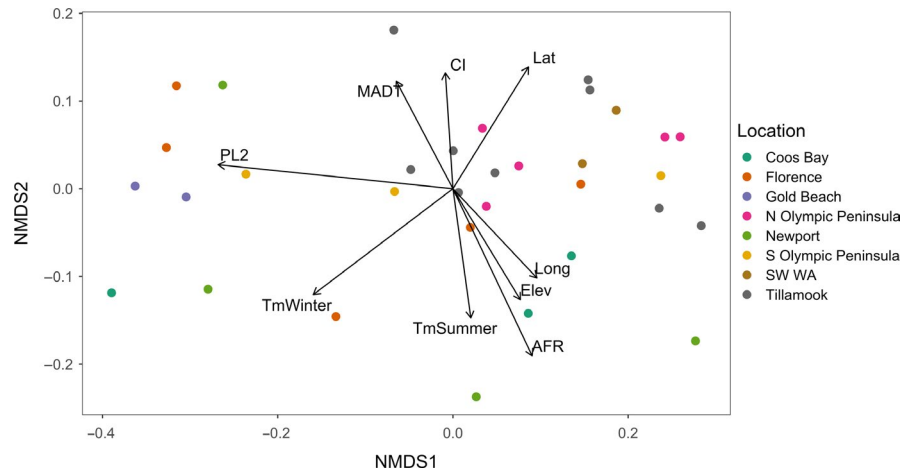
FIGURE 6 Nonmetric multidimensional scaling (NMDS) ordination based on the genetic distances between 33 sample sites calculated from multilocus SSR genotypes of *Nothophaeocryptopus gaeumannii* isolates. Joint plot vectors show correlations between environmental variables and the ordination. Only environmental variables with statistically significant correlations ($p < .05$) are shown. Vector labels correspond to the variables listed in Table 4. Final stress = 0.095. Locations in legend correspond to the sampling blocks. One Coos Bay site was removed from the ordination because it was an outlier, and one S Olympic Peninsula site was not included because disease severity estimates were not available

initially suggested a causal relationship between the relative abundance of this lineage and disease severity. At the landscape level, the SNC symptoms documented by aerial surveys were most prevalent along the western slopes of the Coast Ranges, where Lineage 2 was generally more abundant, or where the two lineages coexisted within ~30 km of the coast (Figure 2). This trend was observed in the low-elevation forests along the western slopes of the Coast Ranges in Oregon and Washington from Coos Bay, OR to the northern Olympic Peninsula (Figure 2, Table 2). Further inland, Lineage 2

was generally less abundant, or absent, and SNC symptoms were generally less severe or not detected (Figure 2).

The observation that the regions where distributions of the two *N. gaeumannii* lineages overlap correspond to the regions with severe SNC is in agreement with previous studies (Winton et al., 2006). The apparent association between *PL2* and *AFR* when distance inland was not included in the model (Figure 3, Table 4) also supports the interpretation by Winton et al. (2006) that SNC symptoms were more severe in Douglas-fir stands with higher proportions of Lineage

TABLE 5 Environmental, geographic, and disease variables used in the joint plot for the NMDS analysis based on the genetic distance *Nothophaeocryptopus gaeumannii*

Variable	Description	R^{2a}	p^b
CI	Colonization index (average percentage of stomata occluded by pseudothecia)	.228	.016
AFR	Average foliage retention (% foliage remaining across four needle age classes from branches in the midcanopy)	.569	.001
PL2	Relative proportion of Lineage 2 isolates in sample site (Number of Lineage 2 Isolates/Total Number of Isolates)	.947	.001
MADT	Mean average dew point temperature (°C) (May–July year prior to sampling)	.247	.015
PPT	Average precipitation (mm) (May–July year prior to sampling)	.147	.100
TmSummer	Mean summer temperature (°C) (May–September year prior to sampling)	.284	.012
TmWinter	Mean winter temperature (°C) (November–March prior to sampling)	.513	.001
Lat	Latitude (decimal degrees)	.342	.004
Long	Longitude (decimal degrees)	.253	.017
Elev	Elevation (meters)	.283	.009

[a]R^2 reflects the correlation between environmental variables and ordination scores.
[b]p-values calculated from 999 permutations of the data.

2. However, *PL2* was not correlated with the colonization index (*CI*) (Table 4), the variable that should have the strongest mechanistic relationship with foliage retention (Manter et al., 2005, 2003). Given the current understanding of the mechanisms of disease in this pathosystem, where premature foliage loss associated with SNC results from cumulative occlusion of the stomata by the pseudothecia of *N. gaeumannii* (Manter et al., 2000, 2005, 2003; Stone, Capitano, et al., 2008), the most plausible mechanism by which Lineage 2 could cause more severe defoliation than Lineage 1 would be by colonizing the host needle more rapidly and subsequently producing more abundant pseudothecia relative to Lineage 1. Our analyses do not support such a mechanism.

Lineage 1 was not isolated from the Douglas-fir foliage samples collected at the two southernmost sites in Oregon near Gold Beach (Figure 2). These sites were composed exclusively of *N. gaeumannii* Lineage 2. To date, aerial surveys have documented very low incidence of SNC symptoms along the Oregon coast south of Port Orford (Figure 2), although Douglas-fir is abundant (Lavender & Hermann, 2014) and *N. gaeumannii* is relatively common. The fact that we only recovered isolates of *N. gaeumannii* Lineage 2 from those sites, yet symptoms of SNC are not observed there, provides further evidence that Lineage 2 is not in fact associated with increased SNC severity.

The NMDS ordination of sites in relation to genetic distance revealed strong spatial genetic differentiation between inland and coastal sample sites (Figure 6). This approach allowed for a visualization of relationships between genetic variation and environmental, geographic, and disease variables. The spatial distribution of genetic variation was strongly correlated with *Tmwinter*, *Tmsummer*, and *MADT* in the year prior to sampling, but not *PPT* (Figure 6, Table 5). Precipitation in the western Coast Ranges is generally abundant during the period of sporulation and infection by *N. gauemannii*, so spatial variation in spring/summer precipitation has not been a useful variable for modeling *N. gaeumannii* abundance in this region (Manter et al., 2005). The distribution of *N. gaeumannii* Lineage 2 was most strongly correlated with *Tmwinter* (Figure 6, Table 5). Foliage retention varied most strongly with *Tmsummer*, elevation, and longitude, and was negatively correlated with *MADT* (Figure 6, Table 5). Sites with lower *AFR* values and higher *CI* values generally occurred at lower elevations nearest the coast where summers were cooler and spring/early summer dew point temperatures were warmer (Figure 6). The *N. gaeumannii* populations occurring in these sites appeared to be genetically differentiated from the higher elevation inland sites where the winters were colder, summers were hotter, and *AFR* was greater (Figure 6).

The environmental variable most strongly correlated with the spatial distribution of Lineage 2 (*Tmwinter*) is also strongly correlated with *MADT*, the variable most strongly associated with needle colonization by both lineages (Table 4). This suggests that the environment most conducive to needle colonization is also optimal for *N. gaeumannii* Lineage 2, but that Lineage 1 has a broader range of environmental tolerance than Lineage 2. These apparent differences in environmental tolerance may be related to the underlying causes of reproductive isolation and evolutionary divergence between the two lineages. These results also suggest that the distribution of genetic variability within and between *N. gaeumannii* populations is influenced by environmental factors, possibly due to the influences of natural selection and local adaptation. Although the SSR markers used here are presumed to be selectively neutral, and thus are not directly influenced by the environment, they provided a tool with which to detect genetic differentiation between populations that may be associated with adaptation to local climate.

Previous studies have identified significant associations between environmental variables, colonization by *N. gaeumannii*, and SNC symptoms (Coop & Stone, 2010; Hansen et al., 2000; Lee et al., 2013, 2017; Manter et al., 2005; Rosso & Hansen, 2003; Shaw, Woolley, & Kanaskie, 2014; Stone, Coop, et al., 2008; Stone et al., 2007; Watt et al., 2010; Zhao et al., 2012, 2011). Thus it was expected that *Tmwinter* and variables associated with moisture availability would be correlated with the abundance of *N. gaeumannii*, measured here as *CI*. However, in the present study *Tmwinter* was significantly associated with *AFR* ($r = -.48$, $p < .05$) but not *CI* ($p > .05$), and *PPT* was not significantly associated with either *AFR* ($p > .05$) or CI ($p > .05$) (Table 4). However, spring and early summer dew point temperature (*MADT*) was significantly correlated with *CI* suggesting that *N. gaeumannii* colonization is highest where moisture is abundant at warmer temperatures (Table 4).

Given that the occlusion of stomata causes the foliage loss associated with SNC, we expected the correlation between *AFR* and *CI* to be stronger, as reported in previous studies (Manter et al., 2003; Watt et al., 2010). In our dataset, there was considerable variation in *AFR* for a given value of *CI*, suggesting genetic variation in host tolerance (i.e., some host genotypes can tolerate higher levels of infection before needle abscission occurs) and/or that *AFR* may be affected by environmental factors in combination with SNC severity. This variation in *AFR* in relation to *N. gaeumannii* abundance has been investigated for SNC in coastal Douglas-fir (Temel, Johnson, & Stone, 2004). In that study, the authors concluded that some genetic variation in host tolerance reflected the historical SNC pressure in the environment where the host genotype evolved (Temel et al., 2004). Generally, Douglas-fir provenances from regions where rainfall and humidity are low are less tolerant of SNC because natural selection has not favored tolerant individuals where disease pressure is historically low (Hood, 1982; Mcdermott & Robinson, 1989; Temel et al., 2004). The variation in *AFR* observed in our study may also reflect some direct interaction between environment and disease; SNC is one of several factors that may affect *AFR*. It seems reasonable to assume that some unfavorable environmental conditions may lead to greater foliage loss at lower levels of infection and that favorable conditions may allow hosts to maintain a healthy level of foliage with higher levels of infection.

Distance inland and elevation are two geographic variables that had significant associations with both *PL2* and disease severity in our data. While these geographic variables may not directly affect biological processes that influence *N. gaeumannii* abundance or SNC severity, their effects on the biological system are a reflection of interacting climatic and environmental factors along a gradient from the low-elevation forests

along the western slopes of the Coast Range to the higher elevation forests further inland along the Coast Range (Hansen et al., 2000; Shaw et al., 2014; Zhao et al., 2011). In fact, distance inland and elevation were collinear with several environmental variables examined in this study. We therefore used distance inland as a proxy for continentality, a complex combination of multicollinear environmental factors that vary along this geographic gradient (Zhao et al., 2011). A synthesis of the results from this study provides a framework for understanding the factors influencing SNC severity and the genetic structure of *N. gaeumannii* populations. In general, the sites with the most severe SNC and the highest *PL2* were at low elevations (<300 m) within ~20 km of the coast along the western slopes of the Oregon and Washington Coast Ranges where winter temperatures were the warmest (~6–10°C), summers were coolest (~14–16°C), and the dew point temperatures (the temperature at which the air was saturated with water vapor) were warmest (~9–11°C). These observations are in agreement with previous studies that demonstrated that warmer winter temperatures and abundant moisture in the spring/early summer, though not necessarily as precipitation, favor *N. gaeumannii* abundance and thus SNC severity (Lee et al., 2013, 2017, 2016; Manter et al., 2005; Stone, Coop, et al., 2008; Stone et al., 2007; Watt et al., 2010). Our observations are also in agreement with studies that suggested that high summer temperatures inhibit the growth of *N. gaeumannii* (Rosso & Hansen, 2003), resulting in lower SNC severity (Lee et al., 2017; Manter et al., 2005; Stone, Coop, et al., 2008; Stone et al., 2007; Watt, Stone, Hood, & Manning, 2011; Watt et al., 2010; Zhao et al., 2012). Climate change (i.e., increasingly warmer winter temperatures) will likely exacerbate SNC severity in the western Coast Range leading to an intensification of symptoms in areas already affected by SNC, as well as an expansion of the area affected by SNC (Coop & Stone, 2010; Lee et al., 2017; Stone, Coop, et al., 2008; Watt et al., 2011, 2010).

One site near Coos Bay, Oregon (CB5-2) did not fit with the overall trends observed for the geographic distributions of the two lineages in relation to coastal proximity. This site was within 25 km of the coast, but all of the isolates recovered from two separate trees were Lineage 1 (Table 2, Figure 2). This was unexpected, considering that the isolates sampled from a site just a few kilometers to the west were all Lineage 2, and both lineages were recovered from the closest sites to the northeast (Figure 2, Table 2). This suggests that little gene flow is occurring between these sites, even though they are only a few kilometers apart. There were only eight isolates sampled from this site, and thus the estimated *PL2* (and the estimated relationships between *PL2* and other variables) may have been affected by sampling bias. The sample of eight isolates from this site had MLGs that were very dissimilar from those collected from nearby sites. Because all isolates collected from CB5-2 were Lineage 1, but Lineage 2 should have been relatively abundant given the site location, this site disproportionately influenced the fitting of the geographic variables in the NMDS, especially latitude. This suggests that the isolates at CB5-2 were more similar to sites further north, even though this site is near the southern coast of Oregon.

The results of our analyses suggest that climate influences the population structure of this ecologically important Douglas-fir pathogen. Not only does the environment influence SNC severity through direct effects on growth rate and reproduction of *N. gaeumannii*, but environmental variables were also correlated with spatial genetic differentiation in the *N. gaeumannii* population. This suggests that climate may play a role in the evolutionary divergence of these cryptic fungal lineages. Climate change has the potential to be a driver of further genetic change in *N. gaeumannii* populations.

The strong genetic differentiation between the two *N. geaumannii* lineages observed in this study is in agreement with the results of previous analyses that suggested that the lineages were reproductively isolated (Bennett & Stone, 2016; Winton et al., 2006). Although the reproductive incompatibility of these two lineages cannot be definitively demonstrated, as this fungus does not produce ascomata in culture, the divergence observed suggests that the two lineages constitute separate ecological species. However, designation of Lineage 1 and Lineage 2 as distinct species will require phylogenetic or phylogenomic analyses to evaluate the degree of evolutionary divergence between the lineages.

The scope of this study was limited due to the use of highly variable neutral markers, which are useful for identifying populations and estimating genetic differentiation but cannot be used for analyses of evolutionary processes such as natural selection and adaptation. Thus, a thorough demonstration of the role of environment in structuring populations of *N. gaeumannii* was not possible with the available molecular tools. Recent advances in population genomics have enabled the identification of the molecular mechanisms involved in adaptation to local environmental conditions. This analytical framework could be applied to *N. gaeumannii* as a next step toward elucidating the environmental factors contributing to spatial genetic variability in its populations and identifying the mechanistic influences of these environmental factors on its biology.

ACKNOWLEDGMENTS

CONFLICT OF INTEREST

The authors have no competing interests to declare.

AUTHOR CONTRIBUTIONS

PIB and JKS designed the study, PIB performed all laboratory work and data analyses, produced all figures, and drafted the manuscript. Editing of the manuscript was performed collaboratively by PIB and JKS.

DATA AVAILABILITY STATEMENT

Microsatellite genotypes, environmental data, and R scripts for re-producing analyses and figures: Dryad https://doi.org/10.5061/dryad.2p7r5g6.

ORCID

Patrick I. Bennett iD https://orcid.org/0000-0002-1042-2157

REFERENCES

Abatzoglou, J. T., Rupp, D. E., & Mote, P. W. (2014). Seasonal climate variability and change in the pacific northwest of the United States. *Journal of Climate*, *27*, 2125–2142. https://doi.org/10.1175/JCLI-D-13-00218.1

Agne, M. C., Beedlow, P. A., Shaw, D. C., Woodruff, D. R., Lee, E. H., Cline, S. P., & Comeleo, R. L. (2018). Interactions of predominant insects and diseases with climate change in Douglas-fir forests of western Oregon and Washington, U.S.A. *Forest Ecology and Management*, *409*, 317–332. https://doi.org/10.1016/j.foreco.2017.11.004

Balloux, F., & Lugon-Moulin, N. (2002). The estimation of population differentiation with microsatellite markers. *Molecular Ecology*, *11*, 155–165.

Bennett, P., & Stone, J. (2016). Assessments of population structure, diversity, and phylogeography of the Swiss needle cast fungus (*Phaeocryptopus gaeumannii*) in the U.S. Pacific Northwest. *Forests*, *7*, 14. https://doi.org/10.3390/f7010014

Capitano, B. R. (1999). *The infection and colonization of Douglas-fir needles by the Swiss needle cast pathogen*, Phaeocryptopus gaeumannii *(Rhode) Petrak (MS Thesis)*. Oregon State University, Corvallis, OR.

Coop, L. B., & Stone, J. K. (2010). Climate models for predicting distribution and severity of Swiss needle cast. In R. Mulvey & D. Shaw (Eds.), *Swiss needle cast cooperative annual report 2010* (pp. 66–80). Corvallis, OR: College of Forestry, Oregon State University.

Franklin, J. F., & Dyrness, C. T. (1973). *Natural vegetation of Oregon and Washington*. Corvallis, OR: Oregon State University Press.

Hansen, E. M., Stone, J. K., Capitano, B. R., Rosso, P., Sutton, W., Winton, L., ... McWilliams, M. G. (2000). Incidence and impact of Swiss needle cast in forest plantations of Douglas-fir in coastal Oregon. *Plant Disease*, *84*, 773–778. https://doi.org/10.1094/PDIS.2000.84.7.773

Harrell, F. E. J. (2017). *Hmisc: Harrell miscellaneous. R package version 4.0-3*. Retrieved from https://CRAN.R-project.org/package=Hmisc

Harvell, C. D., Mitchell, C. E., Ward, J. R., Altizer, S., Dobson, A. P., Ostfeld, R. S., & Samuel, M. D. (2002). Climate warming and disease risks for terrestrial and marine biota. *Science*, *296*, 2158–2162. https://doi.org/10.1126/science.1063699

Hedrick, P. W. (2005). A standardized genetic differentiation measure. *Evolution*, *59*, 1633–1638. https://doi.org/10.1111/j.0014-3820.2005.tb01814.x

Hood, I. A. (1982). *Phaeocryptopus gaeumannii* on *Pseudotsuga menziesii* in Southern British Columbia. *New Zealand Journal of Forestry Science*, *12*, 415–424.

Jombart, T. (2008). adegenet: A R package for the multivariate analysis of genetic markers. *Bioinformatics*, *24*, 1403–1405. https://doi.org/10.1093/bioinformatics/btn129

Kamvar, Z. N., Brooks, J. C., & Grunwald, N. J. (2015). Novel R tools for analysis of genome-wide population genetic data with emphasis on clonality. *Frontiers in Genetics*, *6*, 208. https://doi.org/10.3389/fgene.2015.00208

Kamvar, Z. N., Tabima, J. F., & Grünwald, N. J. (2014). *Poppr*: An R package for genetic analysis of populations with clonal, partially clonal, and/or sexual reproduction. *PeerJ*, *2*, e281. https://doi.org/10.7717/peerj.281

Kliejunas, J. T., Geils, B. W., Glaeser, J. M., Goheen, E. M., Hennon, P., Kim, M.-S., ... Frankel, S. J. (2009). *Review of literature on climate change and forest diseases of western North America*. Gen. Tech. Rep. PSW-GTR-225 (54 p). Albany, CA: US Department of Agriculture, Forest Service, Pacific Southwest Research Station.

Lavender, D. P., & Hermann, R. K. (2014). *Douglas-Fir: The Genus Pseudotsuga*. Corvallis, OR: OSU College of Forestry, Oregon State University.

Lee, E. H., Beedlow, P. A., Waschmann, R. S., Burdick, C. A., & Shaw, D. C. (2013). Tree-ring analysis of the fungal disease Swiss needle cast in western Oregon coastal forests. *Canadian Journal of Forest Research*, *43*, 677–690. https://doi.org/10.1139/cjfr-2013-0062

Lee, E. H., Beedlow, P. A., Waschmann, R. S., Tingey, D. T., Cline, S., Bollman, M., ... Carlile, C. (2017). Regional patterns of increasing Swiss needle cast impacts on Douglas-fir growth with warming temperatures. *Ecology and Evolution*, *7*, 1167–1196. https://doi.org/10.1002/ece3.3573

Lee, E. H., Beedlow, P. A., Waschmann, R. S., Tingey, D. T., Wickham, C., Cline, S., ... Carlile, C. (2016). Douglas-fir displays a range of growth responses to temperature, water, and Swiss needle cast in western Oregon, USA. *Agricultural and Forest Meteorology*, *221*, 176–188. https://doi.org/10.1016/j.agrformet.2016.02.009

Maguire, D. A., Kanaskie, A., Voelker, W., Johnson, R., & Johnson, G. (2002). Growth of young Douglas-fir plantations across a gradient in Swiss needle cast severity. *Western Journal of Applied Forestry*, *17*, 86–95. https://doi.org/10.1093/wjaf/17.2.86

Maguire, D. A., Mainwaring, D. B., & Kanaskie, A. (2011). Ten-year growth and mortality in young Douglas-fir stands experiencing a range in Swiss needle cast severity. *Canadian Journal of Forest Research*, *41*, 2064–2076. https://doi.org/10.1139/x11-114

Manter, D. K., Bond, B. J., Kavanagh, K. L., Rosso, P. H., & Filip, G. M. (2000). Pseudothecia of Swiss needle cast fungus, *Phaeocryptopus gaeumannii*, physically block stomata of Douglas fir, reducing CO_2 assimilation. *The New Phytologist*, *148*, 481–491. https://doi.org/10.1046/j.1469-8137.2000.00779.x

Manter, D. K., Reeser, P. W., & Stone, J. K. (2005). A climate-based model for predicting geographic variation in Swiss needle cast severity in the Oregon Coast Range. *Phytopathology*, *95*, 1256–1265. https://doi.org/10.1094/PHYTO-95-1256

Manter, D. K., Winton, L. M., Filip, G. M., & Stone, J. K. (2003). Assessment of Swiss needle cast disease: Temporal and spatial investigations of fungal colonization and symptom severity. *Journal of Phytopathology*, *151*, 344–351. https://doi.org/10.1046/j.1439-0434.2003.00730.x

McCune, B., Grace, J. B., & Urban, D. L. (2002). Analysis of ecological communities. *Journal of Experimental Marine Biology and Ecology*, *289*(2), 303–305. https://doi.org/10.1016/S0022-0981(03)00091-1

Mcdermott, J. M., & Robinson, R. A. (1989). Provenance variation for disease resistance in *Pseudotsuga menziesii* to the Swiss needle-cast

pathogen, *Phaeocryptopus gaeumannii*. *Canadian Journal of Forest Research*, *19*, 244–246.

Nei, M. (1978). Estimation of average heterozygosity and genetic distance from a small number of individuals. *Genetics*, *89*, 583–590.

Oksanen, J., Guillaume, B., Friendly, M., Kindt, R., Legendre, P., McGlinn, D., … Wagner, H. (2017). *Vegan: Community ecology package. R package version 2.4-5*. https://CRAN.R-project.org/package=vegan

Peakall, R., & Smouse, P. E. (2006). GenAlEx 6: Genetic analysis in Excel. Population genetic software for teaching and research. *Molecular Ecology Notes*, *6*, 288–295. https://doi.org/10.1111/j.1471-8286.2005.01155.x

Peakall, R., & Smouse, P. E. (2012). GenAlEx 6.5: Genetic analysis in Excel. Population genetic software for teaching and research–an update. *Bioinformatics*, *28*, 2537–2539. https://doi.org/10.1093/bioinformatics/bts460

PRISM Climate Group (2017). PRISM climate data *Oregon State University*. Retrieved from http://prism.oregonstate.edu

R Core Team (2017). *R: A language and environment for statistical computing*. Vienna, Austria: R Foundation for Statistical Computing. Retrieved from https://www.R-project.org/

Ramsey, A., Omdal, D., Dozic, A., Kohler, G., & Boderck, M. (2015). Swiss needle cast aerial and ground survey coastal Washington. In G. Ritóková & D. Shaw (Eds.), *Swiss needle cast cooperative annual report 2015* (pp. 12–18). Corvallis, OR: College of Forestry, Oregon State University. Retrieved from http://sncc.forestry.oregonstate.edu/annual-reports

Ritóková, G., Shaw, D., Filip, G., Kanaskie, A., Browning, J., & Norlander, D. (2016). Swiss needle cast in western Oregon Douglas-fir plantations: 20-year monitoring results. *Forests*, *7*, 155. https://doi.org/10.3390/f7080155

Rogers, J. S. (1972). Measures of genetic similarity and genetic distances. In M. R. Wheeler (Ed.), *Studies in Genetics* (pp. 145–153). Austin, TX: University of Texas Publication.

Rosso, P. H., & Hansen, E. M. (2003). Predicting Swiss needle cast disease distribution and severity in young Douglas-fir plantations in coastal Oregon. *Phytopathology*, *93*, 790–798. https://doi.org/10.1094/PHYTO.2003.93.7.790

Shaw, D. C., Filip, G. M., Kanaskie, A., Maguire, D. A., & Littke, W. A. (2011). Managing an epidemic of swiss needle cast in the Douglas-fir region of Oregon: The role of the Swiss needle cast cooperative. *Journal of Forestry*, *109*, 109–119.

Shaw, D. C., Woolley, T., & Kanaskie, A. (2014). Vertical foliage retention in Douglas-fir across environmental gradients of the Western Oregon coast range influenced by Swiss needle cast. *Northwest Science*, *88*, 23–32. https://doi.org/10.3955/046.088.0105

Stone, J. K., Capitano, B. R., & Kerrigan, J. L. (2008). The histopathology of *Phaeocryptopus gaeumannii* on Douglas-fir needles. *Mycologia*, *100*, 431–444.

Stone, J. K., Coop, L. B., & Manter, D. K. (2008). Predicting effects of climate change on Swiss needle cast disease severity in Pacific Northwest forests. *Canadian Journal of Plant Pathology*, *30*, 169–176. https://doi.org/10.1080/07060661.2008.10540533

Stone, J. K., Hood, I. A., Watt, M. S., & Kerrigan, J. L. (2007). Distribution of Swiss needle cast in New Zealand in relation to winter temperature. *Australasian Plant Pathology*, *36*, 445. https://doi.org/10.1071/AP07049

Sturrock, R. N., Frankel, S. J., Brown, A. V., Hennon, P. E., Kliejunas, J. T., Lewis, K. J., … Woods, A. J. (2011). Climate change and forest diseases. *Plant Pathology*, *60*, 133–149. https://doi.org/10.1111/j.1365-3059.2010.02406.x

Temel, F., Johnson, G. R., & Stone, J. K. (2004). The relationship between Swiss needle cast symptom severity and level of *Phaeocryptopus gaeumannii* colonization in coastal Douglas-fir (*Pseudotsuga menziesii var. menziesii*). *Forest Pathology*, *34*, 383–394. https://doi.org/10.1111/j.1439-0329.2004.00379.x

Watt, M. S., Stone, J. K., Hood, I. A., & Manning, L. K. (2011). Using a climatic niche model to predict the direct and indirect impacts of climate change on the distribution of Douglas-fir in New Zealand. *Global Change Biology*, *17*, 3608–3619. https://doi.org/10.1111/j.1365-2486.2011.02486.x

Watt, M. S., Stone, J. K., Hood, I. A., & Palmer, D. J. (2010). Predicting the severity of Swiss needle cast on Douglas-fir under current and future climate in New Zealand. *Forest Ecology and Management*, *260*, 2232–2240. https://doi.org/10.1016/j.foreco.2010.09.034

Welsh, C., Lewis, K. J., & Woods, A. J. (2014). Regional outbreak dynamics of Dothistroma needle blight linked to weather patterns in British Columbia, Canada. *Canadian Journal of Forest Research*, *44*, 212–219. https://doi.org/10.1139/cjfr-2013-0387

Wickham, H. (2016). *ggplot2: Elegant graphics for data analysis*. New York, NY: Springer-Verlag. Retrieved from http://ggplot2.org

Winter, D. J. (2012). mmod : An R library for the calculation of population differentiation statistics. *Molecular Ecology Resources*, *12*, 1158–1160. https://doi.org/10.1111/j.1755-0998.2012.03174.x

Winton, L. M. (2001). *Phylogenetics, population genetics, molecular epidemiology, and pathogenicity of the Douglas-fir Swiss needle cast pathogen* Phaeocryptopus gaeumannii. PhD dissertation. Oregon State University, Corvallis, OR.

Winton, L. M., Hansen, E. M., & Stone, J. K. (2006). Population structure suggests reproductively isolated lineages of *Phaeocryptopus gaeumannii*. *Mycologia*, *98*, 781–791. https://doi.org/10.3852/mycologia.98.5.781

Winton, L. M., Stone, J. K., & Hansen, E. M. (2007). Polymorphic microsatellite markers for the Douglas-fir pathogen *Phaeocryptopus gaeumannii*, causal agent of Swiss needle cast disease. *Molecular Ecology Notes*, *7*, 1125–1128. https://doi.org/10.1111/j.1471-8286.2007.01802.x

Woods, A., Coates, K. D., & Hamann, A. (2005). Is an unprecedented Dothistroma needle blight epidemic related to climate change? *BioScience*, *55*, 761–769. https://doi.org/10.1641/0006-3568(2005)055[0761:IAUDNB]2.0.CO;2

Woods, A. J., Martín-García, J., Bulman, L., Vasconcelos, M. W., Boberg, J., La Porta, N., … Diez, J. J. (2016). Dothistroma needle blight, weather and possible climatic triggers for the disease's recent emergence. *Forest Pathology*, *46*, 443–452. https://doi.org/10.1111/efp.12248

Yu, G., Smith, D. K., Zhu, H., Guan, Y., & Lam, T.-T.-Y. (2017). ggtree: An r package for visualization and annotation of phylogenetic trees with their covariates and other associated data. *Methods in Ecology and Evolution*, *8*, 28–36. https://doi.org/10.1111/2041-210X.12628

Zhao, J., Maguire, D. A., Mainwaring, D. B., & Kanaskie, A. (2012). Climatic influences on needle cohort survival mediated by Swiss needle cast in coastal Douglas-fir. *Trees*, *26*, 1361–1371. https://doi.org/10.1007/s00468-012-0711-x

Zhao, J., Maguire, D. A., Mainwaring, D. B., & Kanaskie, A. (2014). Western hemlock growth response to increasing intensity of Swiss needle cast on Douglas-fir: Changes in the dynamics of mixed-species stands. *Forestry*, *87*, 697–704. https://doi.org/10.1093/forestry/cpu030

Zhao, J., Mainwaring, D. B., Maguire, D. A., & Kanaskie, A. (2011). Regional and annual trends in Douglas-fir foliage retention: Correlations with climatic variables. *Forest Ecology and Management*, *262*, 1872–1886. https://doi.org/10.1016/j.foreco.2011.08.008

BRIEF COMMUNICATION

forest ecology

Associations between Swiss Needle Cast Severity and Foliar Nutrients in Young-Growth Douglas-Fir in Coastal Western Oregon and Southwest Washington, USA

Yung-Hsiang Lan, David C. Shaw, Gabriela Ritóková, and Jeff A. Hatten

Swiss needle cast (SNC) is a foliage disease of Douglas-fir (*Pseudotsuga menziesii*) caused by *Nothophaeocryptopus gaeumannii*, an ascomycete fungus (Mycosphaerellaceae) that causes tree growth reductions in the Pacific Northwest. The epidemiology of the fungus is generally well known, but the relations between disease expression and foliar nutrition are unclear. In this study, we used data from the Swiss Needle Cast Cooperative research and monitoring plot network in western Oregon and SW Washington to assess associations between SNC severity, carbon, and nine foliage nutrients (nitrogen, Na, K, P, Ca, Mg, Mn, Al, S). Foliage samples were collected from midcrown of selected Douglas-firs from each plot. SNC severity was determined on 2-year-old needles by multiplying disease incidence and fungal reproductive (pseudothecia) density. Disease severity and nutrient relations were determined using linear mixed models. SNC severity showed statistically significant positive trends with concentrations of carbon, nitrogen, Na, K, and S, no relation with concentrations of Ca, Mg, or Al, and slightly negative trends that were not significant for P and Mn. This is the first such analysis of associations between a conifer foliage disease and foliage nutrients across a landscape; subsequently, there is little published literature on how or why these nutrients may interact with disease.

Keywords: conifer foliage diseases, forest disease, forest nutrition

Swiss needle cast (SNC) is a foliage disease of Douglas-fir (*Pseudotsuga menziesii* [Mirb.] Franco) caused by a native fungus, *Nothophaeocryptopus gaeumannii* (T. Rohde) Videira et al. (Ascomycete: Mycosphaerellaceae) (Videira et al. 2017). The disease causes growth losses in Douglas-fir plantations across coastal Oregon and Washington (Shaw et al. 2011). Swiss needle cast was unimportant in forest plantations until the 1990s when it emerged as a significant concern (Hansen et al. 2000). The first aerial survey conducted in 1996 detected 53,050 hectares of forest with visible disease symptoms in coastal Oregon, which increased to 238,705 hectares in 2015 (Ritóková et al. 2016). Although mortality from SNC is rare, growth loss of wood volume was estimated at ~23 percent within the NW Coast Range portion of the epidemic area, whereas some plantations experienced up to 52 percent growth losses (Maguire et al. 2002). Management of Douglas-fir stands

infected with SNC requires a nuanced approach because impacts vary with geographical setting, climate, and other plantation attributes. Foliage nutrition is a plantation scale attribute that may influence foliage disease, but research on this topic is quite limited.

Nothophaeocryptopus gaeumannii is a widespread, endophytic fungus that plugs the stomates with fungal reproductive structures (pseudothecia). Needles with 50 percent or more plugged stomates will likely die and fall ("cast") from the tree (Hansen et al. 2000). Disease severity is usually determined by assessment of 2-year-old needles because this age class is best correlated with a disease effect (Manter et al. 2005). If pseudothecia occur on needles older than 4 years, there is no significant disease expression or growth impacts.

Nitrogen and Ca in the soil and foliage are hypothesized to play an important role in SNC disease severity (El-Hajj et al. 2004, Perakis et al. 2006, Mulvey et al. 2013). Perakis et al. (2006) showed

a correlation between increased soil nitrogen and decreased soil Ca following the pattern of increasing SNC severity from east to west across the Oregon Coast Range. El-Hajj et al. (2004) suggested that *N. gaeumannii* might acquire nitrogen and carbon from apoplastic spaces within Douglas-fir needles. In El-Hajj et al.'s (2004) study, 10-year-old trees were fertilized, and the authors found a positive association between the concentration of nitrogen in conifer needles and the concentration in the pseudothecia of the fungus, but there was only a weak relation between carbohydrates in pseudothecia and infected needles.

Furthermore, El-Hajj et al. (2004) hypothesized that fertilization might be associated with increasing disease severity in Douglas-fir forests. In their study, *N. gaeumannii* disease severity was positively associated with host nutrient levels, especially increased nitrogen concentration. In contrast, Mulvey et al. (2013) found no increase in disease severity associated with standard amounts of fertilization with nitrogen, Ca, P, and custom blends of fertilizers in the Oregon Coast Range, even though there were increases detected in foliar nutrient concentrations. Therefore, the direct relations between foliage nutrition and SNC severity remain equivocal.

There is a general lack of information on foliage disease and foliage nutrition in forestry. This study investigated the associations between SNC severity and common foliar nutrients in a network of research plots established by the Swiss Needle Cast Cooperative (SNCC) (http://sncc.forestry.oregonstate.edu/) in coastal Oregon and southwest Washington, as a first step in assessing the relation between nutrients and SNC on the landscape. The plot network represents a range of disease severity and therefore allows us to ask: Are foliar nutrients in Douglas-fir associated with disease severity caused by *N. gaeumannii*? Based on the results of previous studies (El-Hajj et al. 2004, Perakis et al. 2006, Mulvey et al. 2013), we hypothesized that higher nitrogen and lower Ca in the needle are associated with SNC severity. Associations were also examined between SNC severity and concentrations of other elements in our study, including Na, K, S, P, Mg, Mn, and Al. Carbon was included because it is related to foliar nitrogen and site productivity.

Methods

The study was conducted in Douglas-fir plantations, located within 50 km (35 miles) of the Pacific Ocean, from the California border to southwest Washington (Figure 1). Each plot consisted of a 0.08-hectare (0.2-acre) area of uniform-age trees 10–30 years old. The targeted composition was a minimum of 80 percent Douglas-fir and 740–1,000 trees per hectare (300–400 trees per acre). All plots were established plantations that had not been precommercially thinned or fertilized 5 years prior to establishment. The research plots are located across diverse elevation, latitude, and rain shadow, and so precipitation and temperature vary. Annual precipitation ranges from 1,200 to 4,800 mm, and occurs primarily from October to May. The mean annual temperature ranges from 13 to 18°C, and the elevation of the research plots ranges from 40 to 800 m.

A midcrown branch was destructively sampled on the south side of five to 10 of the largest trees by diameter at breast height in each plot and was used for evaluation of SNC severity and foliar nutrients. Disease severity (Manter et al. 2005) was assessed using 50 individual needles from the 2-year-old needle cohort from each tree sample branch. Needles facing underside up were taped on an index card

and stored at –20°C. Each needle was closely inspected for stomatal occlusion of pseudothecia (presence or absence). The percentage of 50 needles with psuedothecia was noted as incidence. On each index card, the first 10 needles with pseudothecia present were then examined with a microscope to determine the number of occluded stomates in three regions (base, mid, and tip) of each needle. The proportion of pseudothecial occlusion for these 10 needles was noted as pseudothecia density. The SNC severity index was calculated as the incidence multiplied by the pseudothecia density (in percentage) (Mulvey et al. 2013), and averaged for all five to 10 trees in each plot.

The concentrations of carbon and nine nutrients (nitrogen, Na, K, S, Ca, P, Mg, Mn, Al) were measured in 1-year-old needles from the midcrown samples. One-year old needles were used because that is the leaf condition that the fungus would find as it colonizes foliage in the first year. These nutrients were chosen because some of their roles are in tree growth (N and P), cell wall stability, solute transport across the cell wall, or general disease resistance (Na, K, S, Ca, Mg, Mn, and Al) (Datnoff et al. 2007). After transporting foliage samples to the lab, approximately 200 one-year-old needles were randomly selected from the midcrown samples of five to 10 trees from each plot and dried for 48 h in a drying oven at 40°C. The dried samples were then ground with a ball grinder and stored in combustion vials to avoid contamination.

The measurement of nutrient concentration was based on dry needle weight. Total nitrogen and carbon were determined on dried and ground foliar material using dry combustion on a Thermo FlashEA 1112 (Thermo Fisher Scientific). Foliar samples were digested using 30 percent H_2O_2 and a 1:10 nitric acid–hydrochloric acid (HNO_3–HCl) acid digestion in conjunction with external heating (EPA method 3050; Benton and Wolf, 1997). Digests and extracts were analyzed for Na, K, S, Ca, P, Mg, Mn, and Al with inductively coupled plasma atomic emission spectrometry (ICP-AES) using a Thermo Scientific ICP-OES 61E.

Mixed linear models were used to test the association of nutrients with disease severity by using R (v. 3.4.3, R Core Team 2017) packages dplyr (Wickham et al. 2017), ggplot2 (Wickham 2009), and nlme (Pinheiro et al. 2017). Separate models were run for each nutrient variable. Nutrient concentration was treated as

---

Management and Policy Implications

Foliage diseases are thought to be influenced by foliage nutritional status. However, there is very little research on the topic. In Douglas-fir forest plantations of coastal Oregon and Washington, Swiss Needle Cast (SNC) has been at epidemic levels since 1996. It has been hypothesized that the severity of SNC is related to high foliage nitrogen and low foliage calcium, therefore we do not recommend fertilization of Douglas-fir plantations with N. Our new research shows that there is a positive association between N, Na, K, and S in foliage and disease severity across the Coast Range of western Oregon and SW Washington, while Ca, Mg, Al, Mn, and P were not significantly associated. This paper does not describe cause and effect, but managers should be aware that high N sites are at higher risk for disease, while the implications of the positive association with Na, K, and S are more difficult to interpret. We feel that more research is needed to better understand the relationship between foliage nutrition and foliage diseases because nutrient inputs are commonly managed by foresters. Fertilization activities in plantations should include an assessment of how these nutrient additions might predispose trees to foliage diseases.
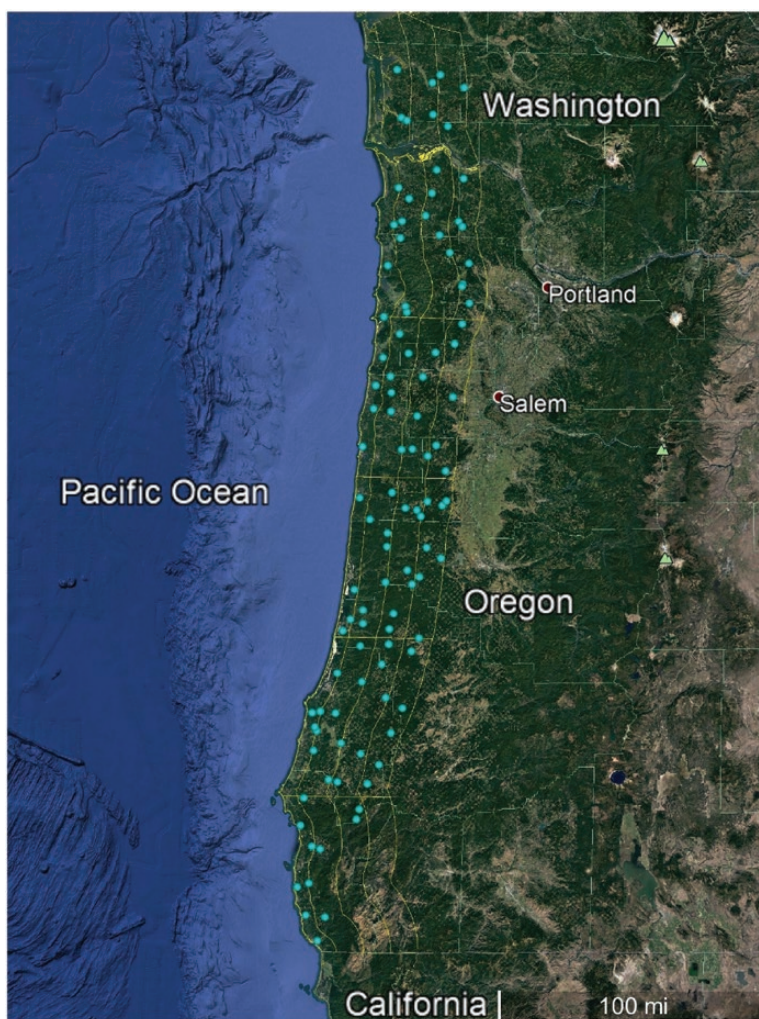
Figure 1. Distribution of 106 research plots established in 2013–15 by the Swiss Needle Cast Cooperative (SNCC) in western Oregon and southwestern Washington ([Ritóková et al. 2017](#)). The yellow lines show the geographical grids, and the blue dots represent the research plots. (Photo credit: Google Earth.)

Table 1. Associations between nutrients and SNC disease severity index in 106 plots in coastal Oregon and southwestern Washington, 2013–15.

Nutrient	*F*-value	*P*-value	Estimate of intercept	Estimate of slope
N	20.4	**<.001**	−6.34 (5.55)	14.94 (3.31)
C	25.6	**<.001**	−232.69 (49.18)	5.00 (0.99)
Na	44.0	**<.001**	12.12 (2.17)	0.03 (0.01)
K	8.7	**.004**	−2.01 (6.75)	0.00 (0.00)
S	20.8	**<.001**	−15.76 (7.40)	0.04 (0.01)
Ca	0.0	.84	16.50 (3.84)	−0.00 (0.00)
P	2.3	.13	22.67 (5.08)	−0.01 (0.00)
Mg	0.8	.36	21.41 (3.48)	−0.01 (0.01)
Mn	5.7	**.02**	20.15 (2.83)	−0.01 (0.00)
Al	2.5	.12	19.83 (3.59)	−0.03 (0.02)

Note: Statistical number (*F*-value), significance (*P*-value), and the estimates of intercept and slope were calculated from linear mixed model. Standard errors are shown in parentheses followed by the estimates. Bold value indicates significant of *P*-value ($P < .05$).

the fixed effect, and plots were treated as random effects, which assumed all 106 plots were independent.

Results and Discussion

Concentrations of nitrogen, carbon, Na, K, and S were significantly positively associated with SNC severity index on 2-year-old needles, and concentrations of Ca, P, Mg, Mn, and Al did not show a statistically significant association with mean SNC severity index ([Table 1](#), [Figure 2](#)). The research examining relations between foliage diseases and foliar nutrients in conifers is lacking, and much of the information regards response to fertilization ([Datnoff et al. 2007](#)) ([Table 2](#)). We studied unfertilized plantations across a geographic and climate gradient and found that the higher foliar nitrogen was positively associated with the SNC severity index.
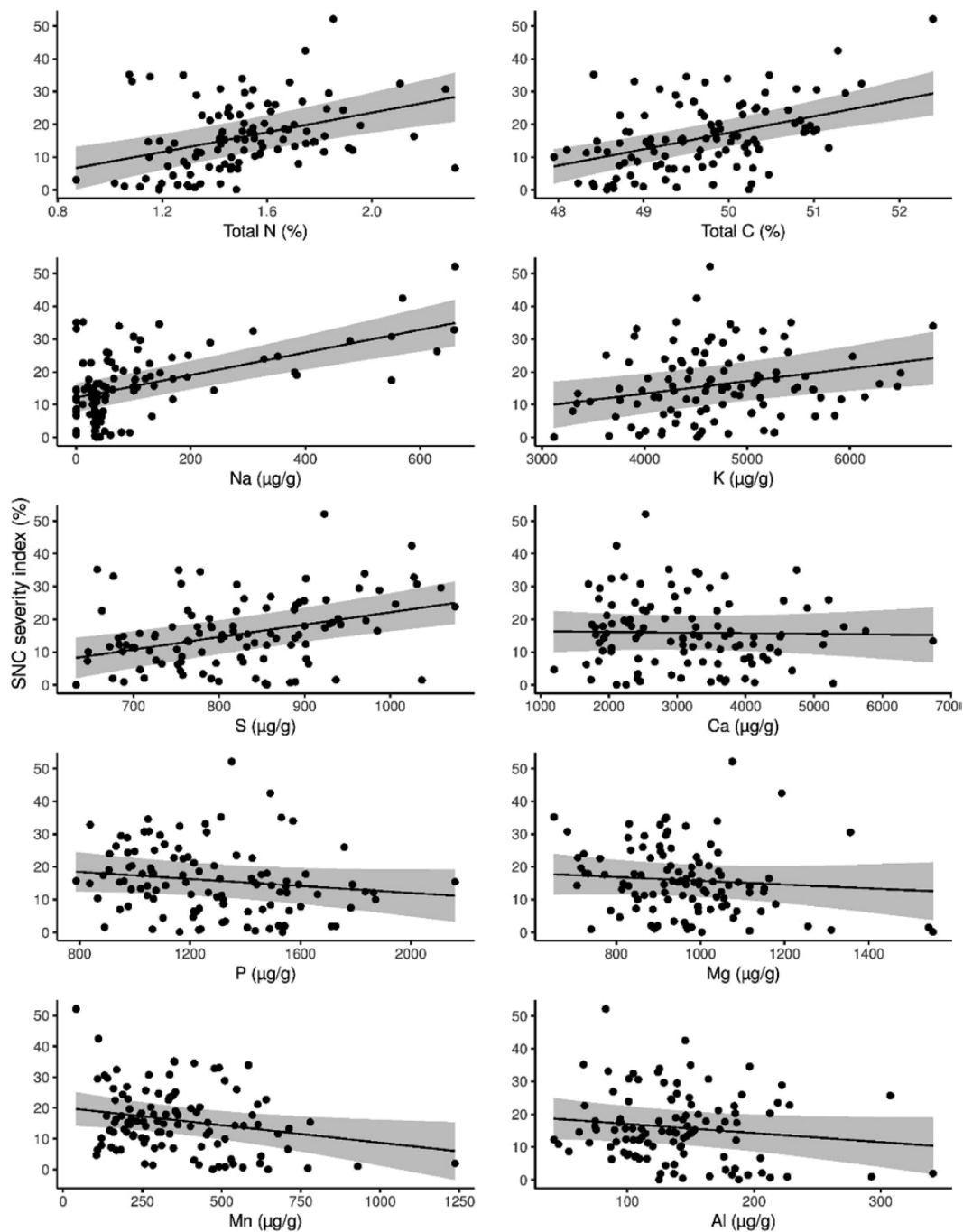
Figure 2. Estimated relations between mean SNC severity index and foliage nutrients at midcrown level in young Douglas-fir plantations in western Oregon southwestern Washington, 2013–15. Shaded areas indicate 95 percent confidence intervals. SNC severity index (percent) is calculated as the incidence (percentage of 50 needles with psuedothecia) multiplied by the pseudothecia density (proportion of pseudothecial occlusion), and represented as a mean of all 5–10 trees in the same plot. Significant positive relations were found for nitrogen, carbon, Na, K, and S ($P < .01$).

The linkage between foliar nitrogen and SNC susceptibility has been suggested since the beginning of the outbreak in the Pacific Northwest (Waring et al. 2000). El-Hajj et al. (2004) used isotopes to find that a high percentage of nitrogen in fungal pseudothecia was from the host needles. Perakis et al. (2006) suggested that higher soil nitrogen and lower soil Ca were associated with severe SNC, and we found higher foliar nitrogen was positively associated with the SNC severity index. However, we found no evidence that

the SNC severity index was associated with the concentration of foliar Ca.

Total nitrogen and total carbon concentrations in foliage were positively associated with SNC severity. Foliar carbon concentration is commonly related to foliar nitrogen concentration, as carbohydrates are products of photosynthesis. However, Saffell et al. (2014) found that foliar concentrations of non-structural carbohydrates (NSC) were unrelated to SNC severity.

Table 2. Summary of literature on relations between conifer foliage diseases and key foliage nutrients within the leaf, including results from our study.

Nutrient	Effect	Citation	Our study
N	Generally thought to increase disease but not always	Conifer literature rare Mulvey et al. (2013): no impacts of fertilization SNC El Hajj et al. (2004): yes there was an impact on SNC from fertilization Lambert (1986): *Dothistroma* infection increased in N fertilized plot	Positive
C	Correlated with N Foliar NSC retains high in infected needles	Saffell et al. (2014)	Positive
K	Pinus needle shedding, K decreases in shedding needle *Pinus strobu* rust (*Peridermium* spp.), K decreases in disease	Bruning 1965, cited in Prabhu et al. (2007a) Hutchinson 1935, cited in Prabhu et al. (2007a)	Positive
Na	Conifer foliage disease relations unknown		Positive
Ca	No effect in fertilization and SNC Conifer foliage disease relations unknown	Mulvey et al. (2013)	None
P	Fusiform rust on pine, P increases in disease No response to fertilization and SNC	Prabhu et al. (2007b) Mulvey et al. (2013)	None
Mg	Included in custom fertilizer blends and no response Conifer foliage disease relations unknown	Mulvey et al. (2013)	None
Mn	Included in custom fertilizer blends and no response Conifer foliage disease relations unknown	Mulvey et al. (2013)	None
Al	Conifer foliage disease relations unknown		None
S	S related to *Dothistroma* severity Conifer foliage disease relations unknown	Lambert (1986), S deficiency related to increased *Dothistroma*	Positive

One possible explanation for the positive relation between nitrogen concentration in 1-year-old needles and SNC severity could be that severe SNC infection on 2-year-old needles causes retranslocation of nitrogen to 1-year-needles. Nitrogen in plants is very mobile and usually concentrated in active tissues (Pallardy 2008). Typically, nitrogen is retranslocated to woody tissues in perennial species (Taiz and Zeiger 2010), but severe SNC infection might cause heavy defoliation on the second-year needles, thereby causing nitrogen translocation from older needles to juvenile needles. Thus, the tree may be actively moving nitrogen to 1-year-old needles as 2-year-old needles die and fall off. Something similar may also be occurring with other highly mobile nutrients (Kimmins 1987), such as Na, K, and S, which also showed associations with disease.

The nutrient, Na, K, and S, may influence the ability of the fungus to access nutrients within the cell. Stone et al. (2008) have shown that *N. gaeumannii* does not penetrate host cell walls but that hypha are appressed to the cell wall of palisade parenchyma and the spongy mesophyll. Sodium and K are known to influence solute transport across the cell wall, and S may increase the availability of other nutrients and plant resistance to disease (Datnoff et al. 2007). In addition, these elements are high in seawater and in areas affected by sea salt deposition (Vet et al. 2014), so the correlation of these compounds with SNC severity could be a result of collinear relations such as soil nitrogen and climatic factors not analyzed here.

Fertilization and management of nutrients to maximize tree growth are fundamental aspects of forestry. Our assessment of young forest plantation foliage nutrients and their relation to foliage disease is important because it can influence management decisions regarding whether to fertilize or not (Mulvey et al. 2013). Mulvey et al. (2013) investigated fertilization response with a variety of applications that included nitrogen, two forms of Ca, P, and custom fertilizer blends (with Mg and Mn), and did not see a response in SNC severity with any treatment, although management recommendations for Douglas-fir forests impacted by SNC have discouraged the use of nitrogen fertilizer based partially on financial merits.

The scope of inference for this study was limited to Douglas-fir plantations in Oregon and SW Washington coastal regions. Although there are associations between foliar nutrients (nitrogen, Na, K, S) and disease severity, we did not show cause-effect, which would require experimental treatments. Explanatory relations between foliar nutrients and *N. gaeumannii* are still unknown, but this study narrowed down the potential nutrients related to SNC severity for further consideration of *N. gaeumannii* infection ecology. It is important to consider that foliar fungi could be influenced by foliar nutrients.

Literature Cited

Benton, J., and B. Wolf. 1997. *Plant analysis handbook II: A practical sampling, preparation, analysis, and interpretation guide.* Micro-Macro Publishing, Incorporated, Athens, GA.

Datnoff, L.E., W.H. Elmer, and D.M. Huber (eds.). 2007. *Mineral nutrition and plant disease.* The American Phytopathological Society, St. Paul, MN.

El-Hajj, Z., K. Kavanagh, C. Rose, and Z. Kanaan-Atallah. 2004. Nitrogen and carbon dynamics of a foliar biotrophic fungal parasite in fertilized Douglas-fir. *New Phytol.* 163(1):139–147.

Hansen, E.M., J.K. Stone, B.R. Capitano, P. Rosso, W. Sutton, A. Kanaskie, and M.G. McWilliams. 2000. Incidence and impact of Swiss needle cast in forest plantations of Douglas-fir in coastal Oregon. *Plant Dis.* 84:773–779.

Kimmins, J.P. 1987. *Forest ecology.* Macmillan Publishing Company, New York.

Lambert, M.J. 1986. Sulphur and nitrogen nutrition and their interactive effects on *Dothistroma* infection in *Pinus radiata. Can. J. Forest Res.* 16(5):1055–1062.

Maguire, D.A., A. Kanaskie, W. Voelker, R. Johnson, and G. Johnson. 2002. Growth of young Douglas-fir plantations across a gradient in Swiss needle cast severity. *West. J. Appl. For.* 17(2):86–95.

Maguire, D.A., D.B. Mainwaring, and A. Kanaskie. 2011. Ten-year growth and mortality in young Douglas-fir stands experiencing a range in Swiss needle cast severity. *Can. J. Forest Res.* 41:2064–2076.

Manter, D.K., P.W. Reese, and J.K. Stone. 2005. A climate-based model for predicting geographic variation in Swiss needle cast severity in the Oregon coast range. *Phytopathology* 95(11):1256–1265.

Mulvey, R.L., D.C. Shaw, and D.A. Maguire. 2013. Fertilization impacts on Swiss needle cast disease severity in western Oregon. *Forest Ecol. Manag.* 287:147–158.

Pallardy, S.G. 2008. *Physiology of woody plants.* 3rd ed. Academic Press, Cambridge, MA.

Perakis, S.S., D.A. Maguire, T.D. Bullen, K. Cromack, R.H. Waring, and J.R. Boyle. 2006. Coupled nitrogen and calcium cycles in forests of the Oregon coast range. *Ecosystems* 9(1):63–74.

Pinheiro, J., D. Bates, S. DebRoy, D. Sarkar, and R Core Team. 2017. *nlme: Linear and nonlinear mixed effects models_. R package version 3.1–131*. Available online at https://CRAN.R- project.org/package=nlme; last accessed June 15, 2018.

Prabhu, A.S., N.K. Fageria, D.M. Huber, and F.A. Rodrigues. 2007a. Potassium and plant disease. P. 57–78 in *Mineral nutrition and plant disease*, Datnoff, L.E., W.H. Elmer, and D.M. Huber (eds.). The American Phytopathological Society, St. Paul, MN.

Prabhu, A.S., N.K. Fageria, F. Berni, and F.A. Rodrigues. 2007b. Phosphorus and plant disease. P. 45–55 in *Mineral nutrition and plant disease*, Datnoff, L.E., W.H. Elmer, and D.M. Huber (eds.). The American Phytopathological Society, St. Paul, MN.

R Core Team. 2017. *R: A language and environment for statistical computing.* R Foundation for Statistical Computing, Vienna, Austria. Available online at https://www.R-project.org/; last accessed April 4, 2019.

Ritóková, G., D.C. Shaw, G. Filip, A. Kanaskie, J. Browning, and D. Norlander. 2016. Swiss needle cast in western Oregon Douglas-Fir plantations: 20-year monitoring results. *Forests* 7:155.

Ritóková, G., D.C. Shaw, D. Maguire, D. Mainwaring, J. Browning, M. Gourley, G. Filip, A. Kanaskie, and B. Marshall. 2017. *Swiss needle cast cooperative research and monitoring plot network in coastal Oregon, southwestern Washington and Oregon Cascade Foothills.* Swiss needle cast Cooperative Annual Report. Oregon State University, Corvallis, OR. 8–15 p.

Saffell, B.J., F.C. Meinzer, D.R. Woodruff, D.C. Shaw, S.L. Voelker, B. Lachenbruch, and K. Falk. 2014. Seasonal carbohydrate dynamics and growth in Douglas-fir trees experiencing chronic, fungal-mediated reduction in functional leaf area. *Tree Physiol.* 34(3):218–228.

Shaw, D.C., G.M. Filip, A. Kanaskie, D.A. Maguire, and W.A. Littke. 2011. Managing an epidemic of Swiss needle cast in the Douglas-fir region of Oregon: The role of the Swiss Needle Cast Cooperative. *J. For.* 109(2):109–119.

Stone, J.K., B.R. Capitano, and J.L. Kerrigan. 2008. The histopathology of *Phaeocrytopus gaeumannii* on Douglas-fir needles. *Mycologia* 100(3):431–444.

Taiz, L., and E. Zeiger. 2010. *Plant physiology.* 5th ed. Sinauer Associates, Sunderland, MA.

Vet, R., R.S. Artz, S. Carou, M. Shaw, C.U. Ro, W. Aas, A. Baker, V.C. Bowersox, F. Dentener, C. Galy-Lacaux, and A. Hou. 2014. A global assessment of precipitation chemistry and deposition of sulfur, nitrogen, sea salt, base cations, organic acids, acidity and pH, and phosphorus. *Atmos. Environ.* 93:3–100.

Videira, S.I.R., J.Z. Groenewald, C. Nakashima, U. Braun, R.W. Barreto, P.J.G.M. de Wit, and P.W. Crous. 2017. Mycosphaerellaceae—Chaos or clarity? *Stud. Mycol.* 87:257–421.

Waring, R.H., J. Boyle, K. Cromack, D. Maguire Jr., and A. Kanaskie. 2000. Researchers offer new insights into Swiss needle cast. *West. For.* 45:10–11.

Wickham, H. 2009. *ggplot2: Elegant graphics for data analysis.* Springer, New York.

Wickham, H., R. Francois, L. Henry, and K. Müller. 2017. *dplyr: A grammar of data manipulation. R package version 0.7.4.* Available online at https://CRAN.R-project.org/package=dplyr; last accessed April 4, 2019.
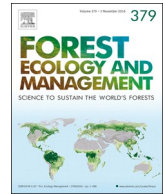
Severity of Swiss needle cast in young and mature Douglas-fir forests in western Oregon, USA

Yung-Hsiang Lan[a,*], David C. Shaw[b], Peter A. Beedlow[c], E. Henry Lee[c], Ronald S. Waschmann[c]

[a] *Department of Forest Ecosystems and Society, Oregon State University, USA*
[b] *Department of Forest Engineering, Resources and Management, Oregon State University, USA*
[c] *U.S. Environmental Protection Agency, Western Ecology Division, Corvallis, OR, USA*

ABSTRACT

Swiss needle cast (SNC), caused by *Nothophaeocryptopus gaeumannii*, is an important foliage disease of Douglas-fir (*Pseudotsuga menziesii*) forests of the Pacific Northwest. The fungus lives endophytically within the foliage, until forming reproductive structures (pseudothecia) that plug stomates and cause carbon starvation. When pseudothecia appear on one- and two-year-old foliage, significant needle abscission can occur, which reduces productivity of the tree. While there is considerable evidence of SNC disease in coastal Douglas-fir plantations, the severity of SNC in mature and old-growth forests is poorly understood. We compared tree crowns of mature and old-growth conifer forests and nearby young forests at three locations in the Oregon Coast Range and four locations in the western Cascade Range of Oregon. We assessed disease severity for *N. gaeumannii* on two-year-old foliage, incidence by presence of *N. gaeumannii* on all foliage, foliage retention for the first four years, and foliar nitrogen of one-year-old foliage. We also compared leaf wetness at three heights in one mature and one young tree at five of the seven sites. Disease severity was greater in young forests than mature forests at all sites except for high elevation Cascade Range areas. Incidence of disease was highest for two-year-old needles in young trees and 3–5 year-old needles in mature trees, except for one coastal site. Retention of 1–4 year-old needle cohorts differed between young and mature trees, and mature trees had much larger complements of > four-year-old needles. Total foliar nitrogen (TN) concentration did not differ in needles of young and mature trees, but at some locations total N differed between canopy positions. Leaf wetness differences were not consistent between young and mature tree crowns. However, at one study site in the core epidemic area, the younger stand had longer periods of wetness in the upper crowns than a nearby old stand. Leaf wetness and foliar N were hypothesized to play a role in SNC disease severity, but they do not explain differences in adjacent young and mature trees. Although the fungus is present in old and young trees, the likelihood of disease expression and lower foliage retention appears to be greater in younger plantation trees than mature and older trees in western Oregon Douglas-fir forests.

1. Introduction

Swiss needle cast (SNC), caused by *Nothophaeocryptopus gaeumannii* (T. Rohde) Videira et al. (2017) (Ascomycete: Mycosphaerellaceae), is an important foliage disease of Douglas-fir (*Pseudotsuga menziesii* (Mirb.) Franco) plantations in the coastal region of the Pacific Northwest (Hansen et al., 2000; Shaw et al., 2011). *Nothophaeocryptopus gaeumannii* is a common native fungus that occurs everywhere Douglas-fir grows. The fungus does not spread per se, but intensifies when conditions allow. Aerial detection surveys across coastal Oregon and Washington have shown the disease symptoms to be intensifying, with

1996 aerial survey in Oregon detecting 53,050 ha of forest land having disease symptoms, increasing to 238,705 ha in 2015 (Ritóková et al., 2016). Rather than directly attacking host cells, *N. gaeumannii* is an endophyte that causes disease by carbon starvation when the reproductive structures (pseudothecia) plug the stomates and inhibit carbon uptake and transpiration (Manter et al., 2000). Disease impact in forest plantations is associated with loss of foliage. Foliage retention of less than three years results in reduced tree volume growth < 25%, and foliage retention of two years is associated with a volume loss > 25% (Maguire et al., 2002; 2011). Mortality is rare but stands with ~one year or less of foliage retention are associated with the most
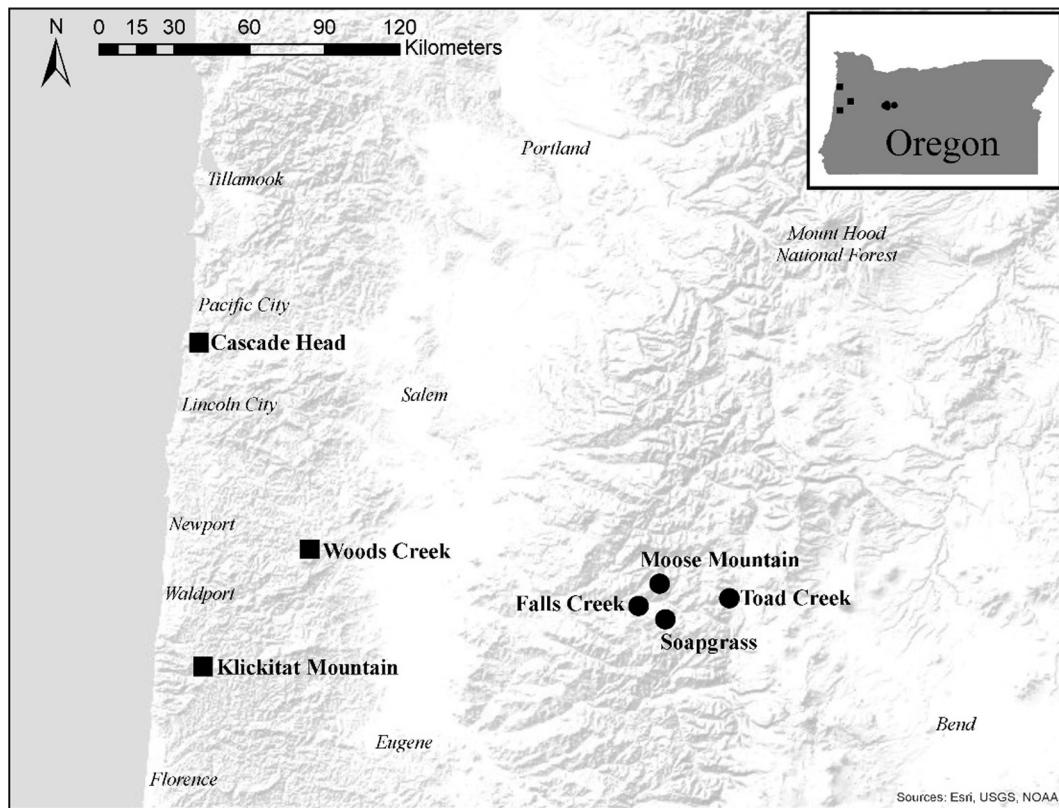
Fig. 1. Northwestern Oregon study area showing the seven study sites and major cities. The Oregon Coast Range adjacent to the coast, and the Cascade Range to the east.

severe disease impacts observed (Maguire et al., 2011).

Foliage retention is a common metric for assessing disease severity in young Douglas-fir plantations (Maguire et al., 2011). Foliage retention is known to vary with site productivity and elevation, the lowest productivity and highest elevation sites have the greatest foliage retention (Ewers and Schmid, 1981; Reich et al., 1995). The overall effect of SNC is to lower foliage retention in forest plantations across this gradient (Shaw et al., 2014), but the influence of SNC on foliage retention in older stands is not known.

Disease severity, assessed on two-year-old needles, varies with canopy position in younger forests, with severity greatest in the upper crown (Hansen et al., 2000; Manter et al., 2003; Shaw et al., 2014). This is unusual because foliage disease severity is typically greatest in the most humid portion of the crown, which for conifers is typically the lower and inner crown. Therefore, the assumption has been that leaf wetness is not a limiting factor within the epidemic area (~within 50 km of the coast). However, leaf wetness and humidity are necessary for spore dispersal, germination on the leaf, and growth of the hyphae into stomates (Manter et al., 2005).

Epidemiology of SNC has focused on winter temperature and leaf wetness during spore dispersal from May through August (Manter et al., 2005). Subsequent models using foliage retention found that needle survival was positively related to minimum winter temperature (December-February) and spring (March-May) precipitation (Zhao et al., 2012). Dendrochronological analysis has shown that mature forests in the coastal mountains are susceptible to growth reduction by SNC, specifically associated with warmer spring and summer temperature (Black et al., 2010). Forests further from the coast in the Cascade Mountains also have been reported with SNC, particularly the low elevation foothills (Ritóková et al., 2016), and it has been shown that disease severity decreases with increasing elevation. Lee et al. (2013, 2017) demonstrated that current- and previous-year's winter and summer temperatures and summer precipitation were strongly

correlated with SNC impacts on radial stem growth in mature and old-growth forests of western Oregon. In addition, the relative importance of these climate variables varied by elevation and distance from the coast (Lee et al., 2013; 2016; 2017).

Anecdotal observations suggest that SNC is more severe in young trees than in mature trees, however, this has not been measured quantitatively. SNC has been well studied in young-growth stands but there is still uncertainty regarding what controls disease severity. Data on SNC severity in mature and old-growth forests are rare and there is little understanding of SNC disease epidemiology in older forests. We hypothesized that the vertical and horizontal complexity of older stands would lead to differentiation of microclimate within the vertical profile of older tree crowns and that would lead to less uniform infection of the crown by *N. gaeumannii*. We predicted that this could result in less severe SNC disease in old forests.

Two factors thought to be influential in fungal disease epidemiology in conifer forests are leaf wetness during spore dispersal (Capitano, 1999) and nitrogen content of the leaf (El-Hajj et al., 2004). These factors are expected to be different in crowns of young versus older trees because of differences in tree morphology, needle age composition and microclimate within the tree. Given that, we hypothesized that wetter needles and greater nitrogen content would be associated with greater disease severity.

We investigated SNC disease patterns in tree crowns of mature and old-growth forests and nearby young forests at three locations in the Oregon Coast Range and four locations in the western Cascade Range. We compared needle samples from young and old trees at each site to determine if SNC disease severity differed between tree age. We also compared infection incidence in different needle age classes, foliage retention for first 4 years, and foliage nitrogen patterns and leaf wetness (May – August) to determine if these variables differed between tree age classes. We expected that (1) Severity of SNC would be greater in younger than adjacent older trees; (2) Incidence of *N. gaeumannii* would

vary by tree age, needle age, and canopy position; (3) Foliage retention would be greatest in older trees; (4) Total nitrogen would be greater in foliage with higher SNC severity; and (5) Leaf wetness would be higher where SNC was more severe.

2. Methods

2.1. Study sites

Foliage samples were collected in 2016 and again in 2017 at seven sites in western Oregon, including five sites at long-term ecological monitoring plots established by the Environmental Protection Agency (hereafter EPA; Beedlow et al., 2013, Lee et al., 2016) and two sites in the Siuslaw National Forest (Fig. 1). Four sites were located on the west slope of the Cascade Range (Moose Mountain, Fall Creek, Toad Creek, and Soapgrass Mountain), and three sites were in the Coast Range (Cascade Head, Woods Creek, and Klickitat Mountain). Forests at each site included a mixture of old stands of Douglas-fir that were 114–470 years old and young stands of Douglas-fir that were 20–30 years old. The old forests were unmanaged stands that regenerated after fires, whereas the young stands were plantations, growing on areas that had been clear-cut and replanted. Elevation ranged from 140 m at the lowest plot in the Coast Range to 1200 m at the highest plot in the Cascade Range. Precipitation varied from 1300 to 2700 mm (Table 1). Associated tree species included western hemlock (*Tsuga heterophylla*) and western red cedar (*Thuja plicata*), as well as Pacific silver fir (*Abies amabilis*) and noble fir (*Abies procera*) at higher elevations in the Cascades (Table 2).

Two weather stations were previously installed at each of the five mature stands managed by EPA (Environmental Protection Agency, Western Ecology Division) (Cascade Head, Moose Mountain, Falls Creek, Soapgrass Mountain and Toad Creek), one at the base and another at the top of a dominant tree which had been rigged for climbing. At these mature stands, branch samples were collected from the instrumented tree and two nearby dominant or co-dominant trees which were previously rigged for climbing (5 sites × 3 mature trees). In each adjacent young stand, the EPA installed a single weather station that was placed 2 m above ground and three trees were selected for

sampling near the weather station (5 sites × 3 young trees). Branch samples from mature and young trees were collected from upper, middle and lower crown. Leaf wetness sensors were connected to the datalogger of the weather station and placed along the vertical gradient of one study tree at the upper, middle and lower parts of the canopy at each old and young EPA site. Five old trees and five young trees had leaf wetness sensors.

In each of the two sites that were not instrumented with weather stations (Klickitat Mountain and Woods Creek), we selected sample trees that had well-developed crowns and were easily accessible without placing leaf wetness sensors in canopies (2 sites × 3 trees = 6 old trees and 6 young trees). Branch samples from mature and young trees were collected from the upper, middle and lower parts of the crown.

2.2. Field sampling

We collected 1–3 branches from three canopy positions (lower, middle, and upper crown) in each tree (total of 21 mature trees and 21 young trees). Samples were collected on the south side of the tree in late May through early June in both 2016 and 2017, after bud-break and before new branchlets were elongated. At least one branch > 1 m in length was selected to ensure sufficient needle material for measurements and foliage nutrient analysis. Several shorter branches were chosen if there were no branches > 1 m in length. Branches were transported to the lab and stored in a 5℃ cold room. Foliage retention was determined by estimating the number of years (annual cohorts) of foliage present on 1–4 year-old branches (Maguire et al., 2011). We rated the needle amount present within each age class along the branch on a scale from 0 to 1, With a 1 indicating all needles were still present. We combined the four age classes for analysis with needle retention possible from 0 to 4.

2.3. Lab analysis

For each canopy height position of 21 mature trees and 21 young trees, 50 individual needles were randomly selected from each cohort of all foliar age classes. Needles were taped on an index card and stored at

Table 1

Location, tree age, elevation, and climate variables of the seven research sites. Cascade Head, Woods Creek, and Klickitat Mountain are in the Oregon Coast Range, and Moose Mountain, Falls Creek, Soapgrass Mountain, and Toad Creek are in the western Cascade Range.

Site	Stand	Latutude	Longitude	Elev (m)	Tree age (year)	Annual mean temperature[6] (℃)	Annual precipitation[6] (mm)	Dec-Feb average temperature[6] (℃)	May-Aug precipitation[6] (mm)
Cascade Head	Mature	45°02′26.82″	123°55′08.13″	147	~150[1]	10.5	2517	5.9	301
	Young	45°02′14.75″	123°51′06.65″	171	~30[2]	10.1	2760	5.4	310
Klickitat Mountain	Mature	44°14′38.03″	123°56′16.52″	383	~130[1]	10.8	2198	5.9	247
	Young	44°14′10.89″	123°56′33.86″	610	~15[3]	10.4	2236	5.6	252
Woods Creek	Mature	44°32′00.67″	123°32′59.30″	523	~150[1]	10.6	2353	4.7	183
	Young	44°32′12.13″	123°33′21.58″	496	~10[4]	10.7	2253	4.9	181
Moose Mountain	Mature	44°24′52.92″	122°23′39.48″	664	~120[1]	9.7	1786	2.7	274
	Young	44°24′40.95″	122°23′52.26″	679	~20[5]	9.7	1868	2.8	273
Falls Creek	Mature	44°23′44.24″	122°22′25.47″	556	~130[1]	10.1	1922	2.9	276
	Young	44°23′42.38″	122°22′35.08″	562	~30[2]	10	1908	2.8	274
Soapgrass Mountain	Mature	44°20′52.67″	122°17′30.45″	1169	~470[1]	7.9	2541	1.8	372
	Young	44°20′42.66″	122°17′38.10″	1193	~30[2]	8.2	2489	2.1	360
Toad Creek	Mature	44°25′32.86″	122°01′57.65″	1210	~200[1]	7.4	2279	0.9	286
	Young	44°25′32.98″	122°02′19.68″	1193	~30[2]	7.4	2280	0.9	293

[1] Tree age of mature trees were determined by coring trees using increment borer in a previous study (Lee et al. 2016), except for Klickitat Mountain. Mature trees in Klickitat Mountain were newly estimated by coring trees using increment borer in this study.

[2] Young trees in Cascade Head, Falls Creek, Soapgrass Mountain, and Toad Creek were planted in the early 1990′s.

[3] Young trees in Klickitat Mountain were cored by increment borer and estimated the tree age is about 15 years old.

[4] Young trees in Woods Creek were planted in 2005.

[5] Young trees in Moose Mountain were replanted within the next year after a clear cut in 1997–1998.

[6] Climate data were collected from PRISM at Oregon State University (http://www.prism.oregonstate.edu/explorer/, accessed 11 December 2018) by providing study site coordinates. Using 30 year average climate database and 800 m special resolution.

Table 2

Stand structure, density, diameter, basal area, and tree height attributes of the seven research sites where we conducted studies of SNC severity in western Oregon, 2016–2017.

Site	Plot	Trees per plot[2]		Trees per Ha		Average DBH (cm)		Basal Area (m²/Ha)		Average Tree Height (m)	
		Douglas-fir	Other Trees	Douglas-fir	Other Trees	Douglas-fir	Other Trees	Douglas-fir	Other Trees	Douglas-fir	Other Trees
CH[1]	Mature	3	4	133	160	112.9	43.6	119.5	34.4	54.7	29.5
	Young	17	0	680	0	28.3	NA[3]	42.9	NA	20.0	NA
KT[1]	Mature	2	1	93	27	158.4	43.7	176.3	6.0	62.3	28.0
	Young	3	0	120	0	23.8	NA	5.4	NA	14.6	NA
WC[1]	Mature	2	8	93	307	107.0	21.2	68.3	11.0	57.7	NA
	Young	9	1	360	40	10.3	2.9	3.0	0.0	6.0	4.0
MM[1]	Mature	4	6	173	253	85.1	15.7	93.7	5.6	53.5	12.0
	Young	15	19	600	760	9.8	8.7	4.6	4.5	8.1	7.7
FC[1]	Mature	4	10	173	400	78.6	9.4	83.6	2.2	66.0	6.4
	Young	6	36	240	1440	24.4	4.0	11.2	1.8	10.6	5.9
SG[1]	Mature	2	5	67	213	156.4	42.6	133.2	30.8	54.1	21.4
	Young	10	8	400	320	15.5	14.9	7.5	5.5	9.4	8.8
TC[1]	Mature	4	13	173	533	81.4	18.3	88.4	13.8	45.7	11.5
	Young	4	32	160	1280	9.7	8.5	1.2	7.2	7.8	7.1

[1] The abbreviation of study sites is Cascade Head (CH), Woods Creek (WC), and Klickitat Mountain (KT), Moose Mountain (MM), Falls Creek (FC), Soapgrass Mountain (SG), and Toad Creek (TC).

[2] For each of mature stands, we investigated three 8.9 m radius plots centered with our sample tree, and averaged all 3 plots data to represent mature stand. For each of young stands, because the trees are closed to EPA weather station and the young trees grow evenly in stand, so we only investigated one 8.9 m radius plot centered with EPA weather station. Dead trees and saplings were not included.

[3] "NA" means no data or not sufficient data to present.

[4] Three sampled trees for the mature stands are spaced at least 10 m apart from each other (mostly > 20 m), and the three sampled trees for the young stands were located in proximity to a weather station at different orientations and were spaced at least 3 m apart from each other (mostly > 5 m).

−20 °C. The SNC incidence is defined as the percentage of the 50 needles with pseudothecia present. All needle ages were examined for SNC incidence under a microscope for presence or absence of pseudothecia occluding the stomates. The SNC disease severity index was calculated based on the two-year old needles as the product of the incidence and the pseudothecia density. Pseudothecia density was determined by selecting the first 10 two-year-old needles with pseudothecia present and then counting the % of stomates occluded in three regions (base, middle, and tip) of the needle. In each region evenly divided along length of needle, we picked a random starting point from the needle base and examined 100 stomates from the starting point to determine the number that were occluded by pseudothecia. Pseudothecial occlusion in the three regions was then averaged for each needle and then averaged for 10 needles per canopy position per tree.

Foliar nitrogen was determined on dried and ground foliar material using dry combustion in a FlashEA 1112 NC Analyzer (Thermo Fisher Scientific Inc. USA). Only one-year-old needles were collected for foliage nitrogen measurements. After transporting branches to the lab, we randomly selected ~200 needles from each canopy position of each sample tree, dried them for 48 h in a drying oven at 40 °C, and ground them with a ball grinder and stored in clean vials. We then placed 3–5 mg of the powder into a tin capsule and used FlashEA1112 to measure total nitrogen concentration (%).

2.4. Leaf wetness data collection

We estimated leaf wetness duration during May-August as the ratio of total wet hours in each month/total hours in each month. Only May-August leaf wetness data were examined because that is the primary period of spore dispersal and leaf colonization (Michaels and Chastagner, 1984). Leaf wetness data were collected every 5 min with a PHYTOS31 sensor (Decagon Devices, Inc. USA) then averaged and recorded as hourly data in mV with a CR1000 datalogger (Campbell Scientific Inc. USA). Based on the excitation voltage for our datalogger (2.5 V), we assumed that leaf surfaces were wet when resistance values were > 280 mV (The manual of leaf wetness sensor is available at http://library.metergroup.com/Manuals/20434_PHYTOS31_Manual_Web.pdf accessed 14 March 2019). In addition, as a quality control of the sensors, we also compared the leaf wetness data with rainfall and

humidity sensor data that were collected on site, and 280 mV was the mean value from all sensors when no rainfall was present, and the needle surface was dry.

2.5. Statistical analysis

Multivariate analysis of variance (MANOVA) was used to test for the main effects of canopy position (upper, middle, and lower), tree age (mature or young), sites, and years (2016 and 2017), and their interactions on the SNC severity index, foliage retention, and total foliar nitrogen at the 0.05 level of significance. Canopy position and year were treated as within-subject factors in the MANOVA whereas tree age and sites were between-subject factors where the subject was an individual tree. The SNC severity index data from Soapgrass Mountain and Toad Creek were excluded from the analysis because almost all SNC values from those sites were zeros (Figs. 2 and 3). In the preliminary results (Table 3), there were interactions involving sites, so we also ran the MANOVA on individual sites, to test for differences in SNC severity index between canopy position, year, and tree age (Table 4). When one or more main effects but not their interactions were statistically significant, we conducted a Bonferroni mean separation test to infer which treatment means were different. MANOVA tests were performed using R (v. 3.4.3, R Core Team, 2017) and package car (Fox and Weisberg, 2011), dplyr (Wickham et al., 2017), emmeans (Lenth, 2018), ggplot2 (Wickham, 2009), and nlme (Pinheiro et al., 2017).

3. Results

3.1. SNC incidence patterns

Graphical exploration showed that the percentage of needles with pseudothecia (i.e., SNC incidence) varied by site, tree age, and canopy position (Fig. 2). SNC incidence was least in mature trees at high-elevation sites in the Cascades (Soapgrass Mountain and Toad Creek), and greatest in young and mature trees at Cascade Head in the Coast Range. At all study sites SNC incidence was greater in young stands than in the adjacent old forest stands. At all sites excluding Soapgrass Mountain and Toad Creek, nearly 100% of the two-year-old and older needles in young trees had *N. gaeumannii* present, whereas the peak incidence in

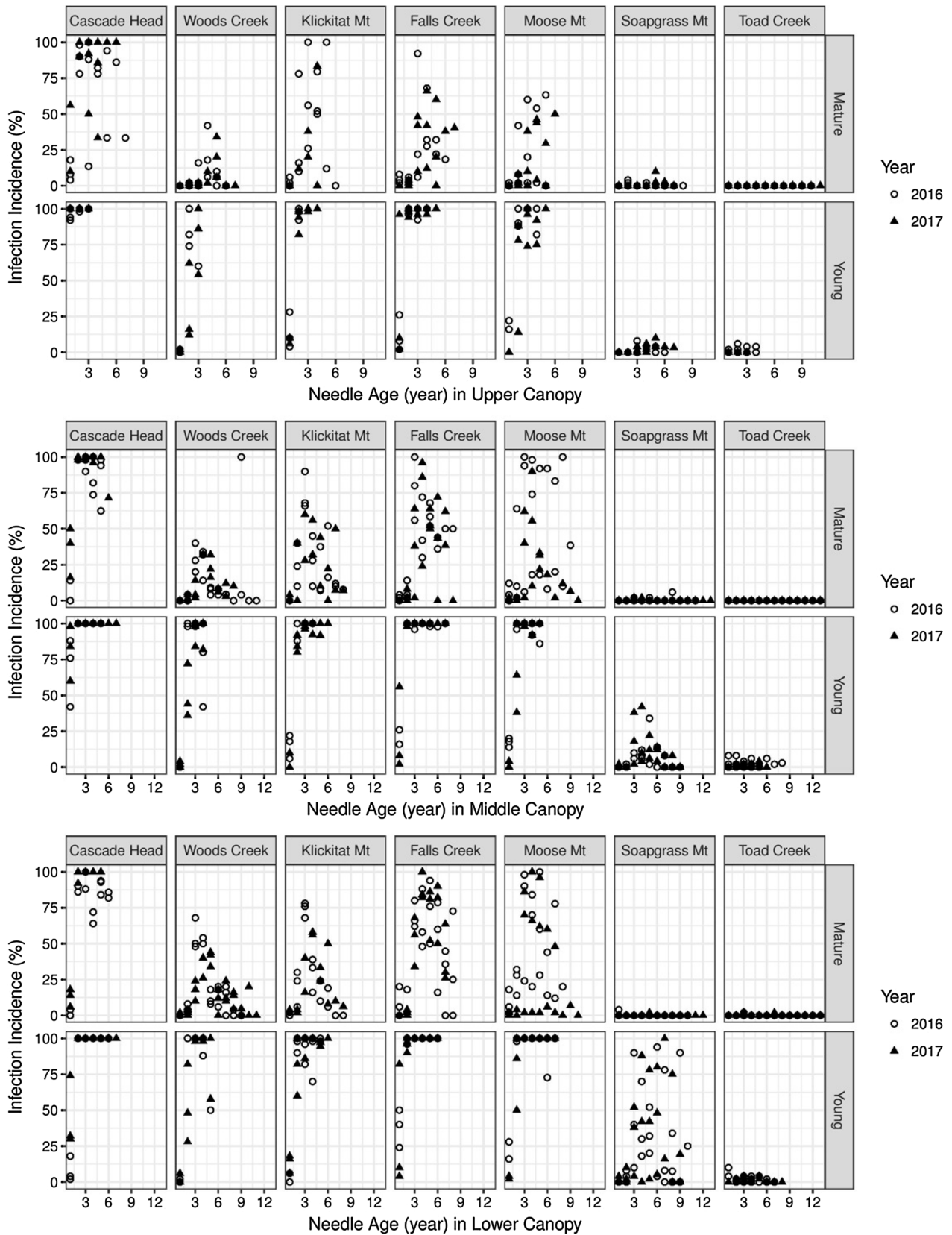**Fig. 2.** Incidence of *Nothophaeocryptopus gaeumannii* pseudothecia along needle age at three canopy positions and seven sites in western Oregon in 2016–2017. Panels are in sets of upper, middle and lower canopy positions, for mature and young stands. Needle age was determined by counting the number of internodes on twigs from the current year needles. All classes of needle age are included in the figure.
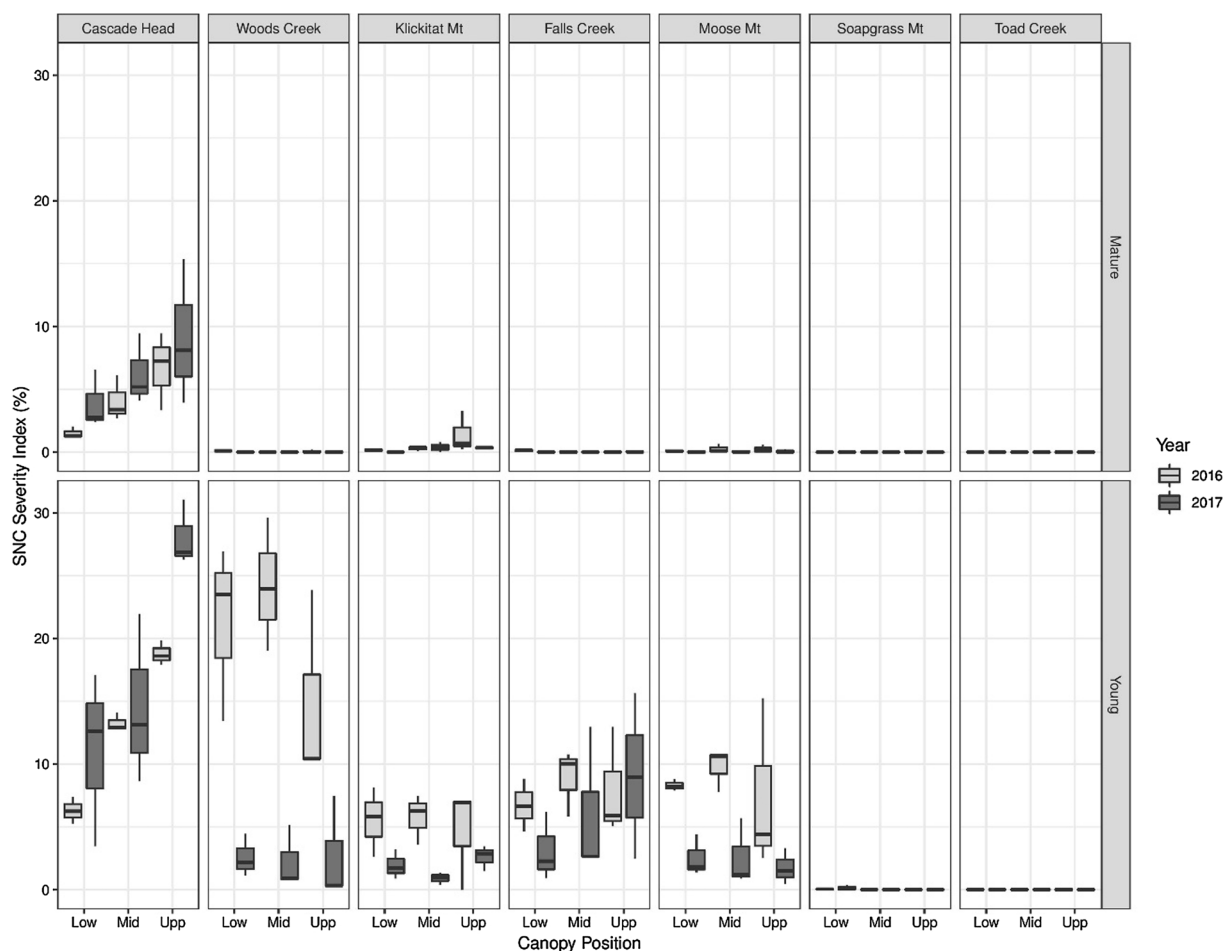
Fig. 3. Swiss needle cast disease severity index for mature and young trees at three canopy positions (x-axis) across seven sites in western Oregon in 2016–2017. Only two-year-old needles were used for SNC disease severity index. The whiskers represented the range of mean values.

Table 3
Results of preliminary MANOVA tests for the main effects of tree age, site, year and canopy position and their interactions on SNC severity index, foliage retention, and foliage nitrogen (TN) in study areas in western Oregon.

| | SNC Severity Index (5 sites[2]) | | | Foliage retention (7 sites[3]) | | | Foliage TN (7 sites[3]) | | |
	F-value	p-value		F-value	p-value		F-value	p-value	
(Intercept)	295.9	< **0.001**	***	4197.1	< **0.001**	***	3705.1	< **0.001**	***
Tree age	172.6	< **0.001**	***	5.1	**0.033**	*	0.0	0.865	
Site	28.9	< **0.001**	***	21.4	< **0.001**	***	7.1	**0.001**	**
Tree age × Site	6.7	**0.002**	**	2	0.098	.	0.4	0.794	
Year	12.1	**0.003**	**	0.1	0.740		74.0	< **0.001**	***
Tree age × Year	17.1	**0.001**	***	0	0.886		2.2	0.156	
Site × Year	10.9	< **0.001**	***	0.6	0.740		3.6	**0.024**	*
Tree age × Site × Year	7.7	**0.001**	***	2.5	**0.046**	*	0.3	0.857	
Canopy	7.1	**0.006**	**	18.9	< **0.001**	***	17.8	< **0.001**	***
Tree age × Canopy	1.5	0.260		3.4	**0.050**[1]	*	3.5	0.053	.
Site × Canopy	3.5	**0.004**	**	2	**0.050**[1]	*	0.9	0.516	
Tree age × Site × Canopy	2.1	0.057	.	1.4	0.180		1.3	0.287	
Year × Canopy	2.8	0.086	.	1.5	0.248		2.6	0.100	
Tree age × Year × Canopy	2.8	0.086	.	2.0	0.153		0.2	0.785	
Site × Year × Canopy	0.4	0.923		0.7	0.736		0.2	0.992	
Tree age × Site × Year × Canopy	0.3	0.944		1.5	0.159		0.8	0.636	

P-values < 0.05 are in bold.

[1] The tree age × canopy and site × canopy interaction terms were not statistically significant (p-value = 0.19 and 0.50, respectively) when the foliage retention data for Soapgrass Mountain and Toad Creek were excluded from the MANOVA, indicating that canopy differences at the five lower elevation sites were similar but different than at the higher elevation sites.

[2] Including sites Cascade Head, Woods Creek, and Klickitat Mountain, Moose Mountain, and Falls Creek. Soapgrass Mountain and Toad Creek were excluded because almost all SNC values from those sites were zeros.

[3] Including sites Cascade Head, Woods Creek, and Klickitat Mountain, Moose Mountain, Falls Creek, Soapgrass Mountain, and Toad Creek.

Table 4
Results of MANOVA by individual sites with *N. gaeumannii*. Because site is a crucial factor involved in most interactions, the MANOVA was re-run by site to clarify the effects from other factors. Tree age was another key factor in SNC severity index analysis and involved in many interactions. Canopy position contributed to foliage retention when considering the site effect.

		SNC Severity Index			Foliage retention		
		F-value	p-value		F-value	p-value	
CH[1]	Tree age	26.0	**0.007**	**	0.8	0.413	
	Year	6.0	0.070	.	0.4	0.567	
	Tree age × Year	0.8	0.413		2.0	0.229	
	Canopy	20.9	**0.017**	*	4.1	0.137	
	Tree age × Canopy	5.3	0.105		2.2	0.256	
	Year × Canopy	5.5	0.100	.	6.3	0.084	
	Tree age × Year × Canopy	4.9	0.115		0.8	0.519	
KT[1]	Tree age	35.6	**0.009**	**	0.4	0.596	
	Year	45.9	**0.007**	**	0.0	0.938	
	Tree age × Year	44.1	**0.007**	**	2.0	0.252	
	Canopy	0.0	0.988		338.3	**0.003**	**
	Tree age × Canopy	0.1	0.948		46.4	**0.021**	*
	Year × Canopy	0.2	0.864		1.8	0.361	
	Tree age × Year × Canopy	0.3	0.783		7.4	0.120	
WC[1]	Tree age	136.7	**< 0.001**	***	23.9	**0.008**	**
	Year	17.5	**0.014**	*	0.4	0.549	
	Tree age × Year	17.3	**0.014**	*	0.4	0.566	
	Canopy	14.6	**0.028**	*	9.3	**0.052**	.*
	Tree age × Canopy	15.0	**0.027**	*	0.9	0.498	
	Year × Canopy	3.7	0.154		0.0	0.996	
	Tree age × Year × Canopy	3.8	0.151		0.7	0.577	

		SNC Severity Index			Foliage retention		
		F-value	p-value		F-value	p-value	
MM[1]	Tree age	17.12	**0.014**	**	1.8	0.251	
	Year	284.6	**< 0.001**	***	0.9	0.392	
	Tree age × Year	258.5	**< 0.001**	***	12.9	**0.023**	*
	Canopy	4.8	0.117		257.3	**< 0.001**	***
	Tree age × Canopy	3.9	0.148		5.3	0.105	
	Year × Canopy	1.4	0.379		1.5	0.349	
	Tree age × Year × Canopy	0.9	0.490		1.3	0.396	
FC[1]	Tree age	98.0	**0.001**	***	0.0	0.942	
	Year	0.4	0.565		4.4	0.105	
	Tree age × Year	0.4	0.585		2.0	0.227	
	Canopy	4.2	0.134		4.6	0.122	
	Tree age × Canopy	4.5	0.127		4.9	0.114	
	Year × Canopy	42.8	**0.006**	**	0.3	0.766	
	Tree age × Year × Canopy	34.4	**0.009**	**	0.8	0.528	
SG[1]	Tree age	–	–		0.2	0.700	
	Year	–	–		1.4	0.310	
	Tree age × Year	–	–		0.2	0.651	
	Canopy	–	–		1.5	0.358	
	Tree age × Canopy	–	–		0.0	0.980	
	Year × Canopy	–	–		0.2	0.869	
	Tree age × Year × Canopy	–	–		1.1	0.443	
TC[1]	Tree age	–	–		8.3	**0.045**	*
	Year	–	–		0.0	0.968	
	Tree age × × Year	–	–		1.1	0.361	
	Canopy	–	–		14.6	**0.029**	*
	Tree age × Canopy	–	–		13.4	**0.032**	*
	Year × Canopy	–	–		0.0	0.972	
	Tree age × Year × Canopy	–	–		0.4	0.687	

[1] The abbreviation of study sites is Cascade Head (CH), Woods Creek (WC), and Klickitat Mountain (KT), Moose Mountain (MM), Falls Creek (FC), Soapgrass Mountain (SG), and Toad Creek (TC).

mature trees was observed in 3–5-year-old needles except for Cascade Head, followed by a decline with increasing needle age. Also, there was more variation in SNC incidence among old trees than in the adjacent young trees, which implies the young trees were more evenly infected by *N. gaeumannii* than were old trees.

Graphical exploration also showed that in young trees, *N. gaeumannii* was present on almost all needles older than two years in all three canopy positions. In mature trees, the percentage of needles with *N. gaeumannii* present was greater in the middle and lower canopy than in the upper canopy, At Soapgrass Mountain and Toad Creek, most needles except for lower and mid-canopy needles in young trees at Soapgrass did not have any pseudothecia present (Fig. 2). SNC incidence pattern was unique for mature trees at most sites: 3–5-year-old needles had the greatest SNC incidence (Fig. 2). These were the needle cohorts that emerged in 2011–2014.

3.2. SNC severity index

The SNC severity index on two-year-old needles varied by site, tree age, canopy position, and year (Fig. 3). The SNC severity index was nearly 0% for young trees at Soapgrass Mountain and Toad Creek and for old trees at all sites except Cascade Head and Klickitat Mountain. The MANOVA excluded the data for Soapgrass Mountain and Toad Creek due to lack of variation. Differences in SNC severity between
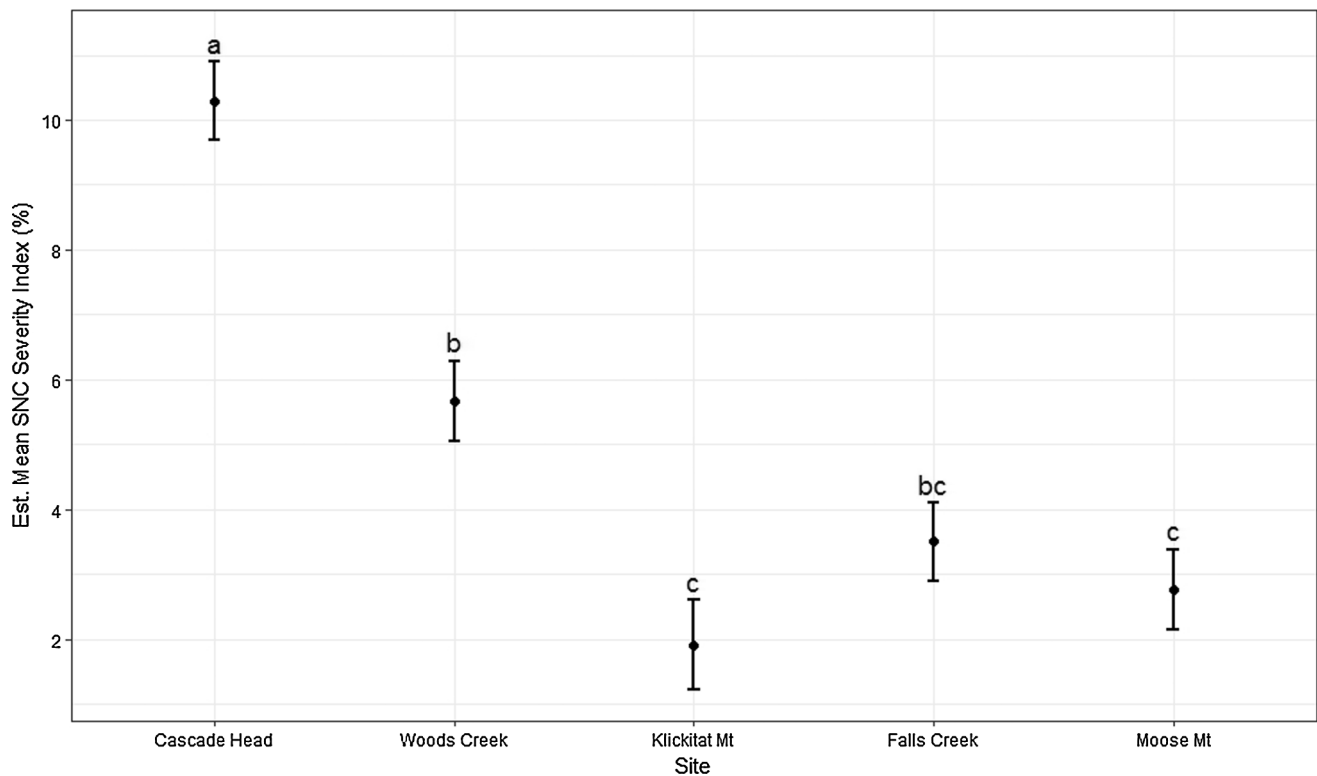
Fig. 4. Least square means of SNC severity index by site. Only five sites were present in MANOVA and mean comparison. Soapgrass Mountain and Toad Creek, the most continental sites, were excluded from the analysis because most all values were zeros. The error bar represents mean ± 1standard error. Letters represent groups. The least square means of SNC severity index between any two groups is statistically different if the letters are different.

sites, tree ages, canopy positions, and years were all significant (p < 0.05, Table 3). SNC severity was greater in young trees than in mature trees (p < 0.001). Several interactions involving tree age were noted but were of minor importance because their F-values were an order of magnitude less than that for tree age (Snedecor and Cochran, 1967). Several interactions involving site, year, and/or canopy position were also statistically significant (p < 0.05, Table 3). Based on the mean separation test on site with Bonferroni adjustment, the SNC severity index was different in Cascade Head than in the other four sites (Fig. 4). Consequently, MANOVA was performed on the SNC severity index by site to test for the main effects of tree age, canopy, and year, and their interactions (Table 4).

Differences in SNC severity index between canopy positions were statistically significant at Cascade Head (p = 0.017) and Woods Creek (p = 0.029) (Table 4). In young and old trees at Cascade Head, the SNC severity index was significantly greater in the upper canopy than in the lower and middle canopies in 2016 and 2017 (Fig. 3). At all sites excluding Cascade Head, SNC severity index values for young trees were greater than for old trees. For young trees at Woods Creek, the SNC severity index was significantly lower in the upper canopy in 2016 than in the lower and middle canopies but was uniformly low in all three canopy layers in 2017. For young trees at Woods Creek, Klickitat Mountain, and Moose Mountain, the mean SNC severity index was greater in 2016 than in 2017 (Fig. 3).

3.3. Foliage retention

Mean foliage retention for the first four years of age classes differed among sites (p < 0.001) and canopy positions (p < 0.001), and included several two- and three-factor interactions (Fig. 5, Table 3). When foliage retention data for Soapgrass Mountain and Toad Creek were excluded from the MANOVA, the tree age × canopy and site × canopy interactions were not statistically significant (p = 0.19

and 0.50, respectively), indicating that foliage retention at the high elevation sites differed from the other areas examined (Table 3). Because the F-values for the interaction terms with canopy were about an order of magnitude less than those for the constituent main effects and not statistically significant when data for the two high-elevation sites were excluded, the interactions were considered as either not important or important only for Soapgrass Mountain and Toad Creek.

Post-MANOVA, we proceeded to examine the differences in foliage retention between the main effects for site and canopy based on the Bonferroni mean separation test. We also considered the importance of the significant interactions and tested for the effects of age, canopy, and year and their interactions on foliage retention based on MANOVA for individual sites focusing on the two high-elevation sites. Based on the mean separation test on site with Bonferroni adjustment, the seven sites were partitioned into two distinct groups (Fig. 6). Foliage retention was significantly less in young and mature trees at Cascade Head and Klickitat Mountain than at the five inland sites (Figs. 5 and 6). Furthermore, the mean foliage retention in the upper canopy was significantly less than that in the lower and middle canopies (Fig. 6). However, in the analysis of individual sites, canopy and age differences in foliage retention were not statistically significant at Soapgrass Mountain (Table 4). In contrast, there was evidence that mean foliage retention differed in young and old trees at Woods Creek and Toad Creek as well as a significant main effect for canopy and an age × canopy interaction at Toad Creek (Table 4). At Toad Creek, foliar retention was least in the upper canopy of young Douglas-fir whereas no canopy differences were evident in mature trees (Fig. 5).

3.4. Foliage total nitrogen

Mean total nitrogen concentration differed among years, canopy positions, and sites, but was not different between older and younger trees (Figs. 7 and 8, Table 3). In addition, there was a significant
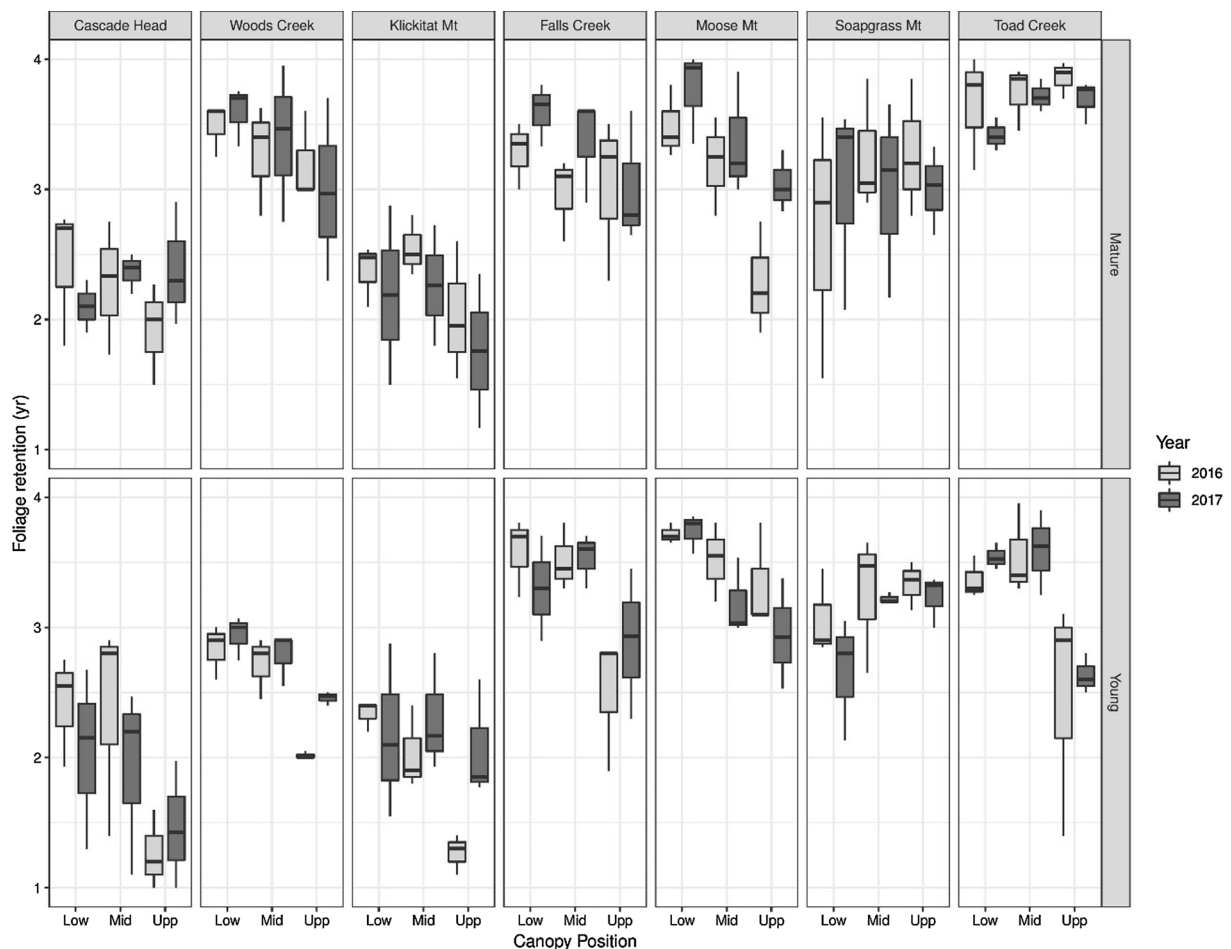
Fig. 5. Foliage retention (in year) for mature and young trees at three canopy positions across seven sites in western Oregon in 2016–2017. Foliage retention was determined by evaluating 1–4 year-old foliage on 4 year-old, or older lateral twigs. The whiskers represented the range of mean values.

site × year interaction that we did not consider important because its F-value was an order of magnitude less than the F-value for year (Snedecor and Cochran, 1967). Mean total nitrogen concentration was significantly greater in 2016 than in 2017 and was greatest in the upper canopy and least in the lower canopy (Fig. 8). Based on the mean separation test on site with Bonferroni adjustment, mean foliage total nitrogen concentration was different at Cascade Head and Klickitat Mountain than at most other sites, and was greater in the upper canopy than in the middle and lower canopy (Fig. 8).

3.5. Leaf wetness data

Leaf surfaces were often wet in all canopy positions in all sites during May and June and mostly dry in July and August at Falls Creek, Moose Mountain, and Soapgrass Mountain (Fig. 9). There were no obvious patterns in leaf wetness among canopy positions. July 2017 was drier than 2016, but May, June, and August did not show strong differences in leaf wetness between years. Leaf wetness did not differ between sites or tree age classes during May-August except at Cascade Head in July and August. However, young trees at Cascade Head had higher leaf wetness than most other sites in nearly all months. Unfortunately, we did not have leaf wetness data from the other two coastal sites so the sample was insufficient for comparisons between coastal and inland sites.

4. Discussion

Swiss needle cast disease severity (incidence of needles with

pseudothecia × percentage of stomates occluded by pseudothecia, for two-year-old needles) was less in old trees than in young trees except for the two high-elevation Cascade Range sites where evidence of *N. gaeumannii* infection was negligible in both old and young trees. Our measurements of leaf nitrogen and leaf wetness were not different between young and older trees except at Cascade Head, and therefore did not explain the differences in disease severity between mature and young trees. However, we found that incidence of *N. gaeumannii*, which is the percentage of infected needles with pseudothecia present, peaked in second year foliage for young trees and 3–5 year foliage in older trees, except at Cascade Head. At Cascade Head, although disease severity was different for mature trees and young trees, incidence of *N. gaeumannii* both peaked in second year foliage for mature and young trees.

Young trees had more stomates occluded by pseudothecia on two-year-old needles than older trees. This may help explain why disease is more severe in young trees. In addition, it appears that foliage in young stands is more fully colonized than older stands because pseudothecia density is correlated with the biomass of the fungus in the needle (Manter et al., 2003), and pseudothecia density was always greater in young trees. This is significant because if a tree has over 3.2 years of foliage retention on average, tree growth will be normal even if the fungus is present within needles (Maguire et al., 2011). If needle chlorosis and casting occur sooner in young trees, due to earlier peak infection incidence and severity, then the chance for foliage retention to drop below three years is much greater in young than older trees.

We hypothesized that foliar nitrogen was positively associated with SNC disease severity. Our hypothesis was not supported by our data,
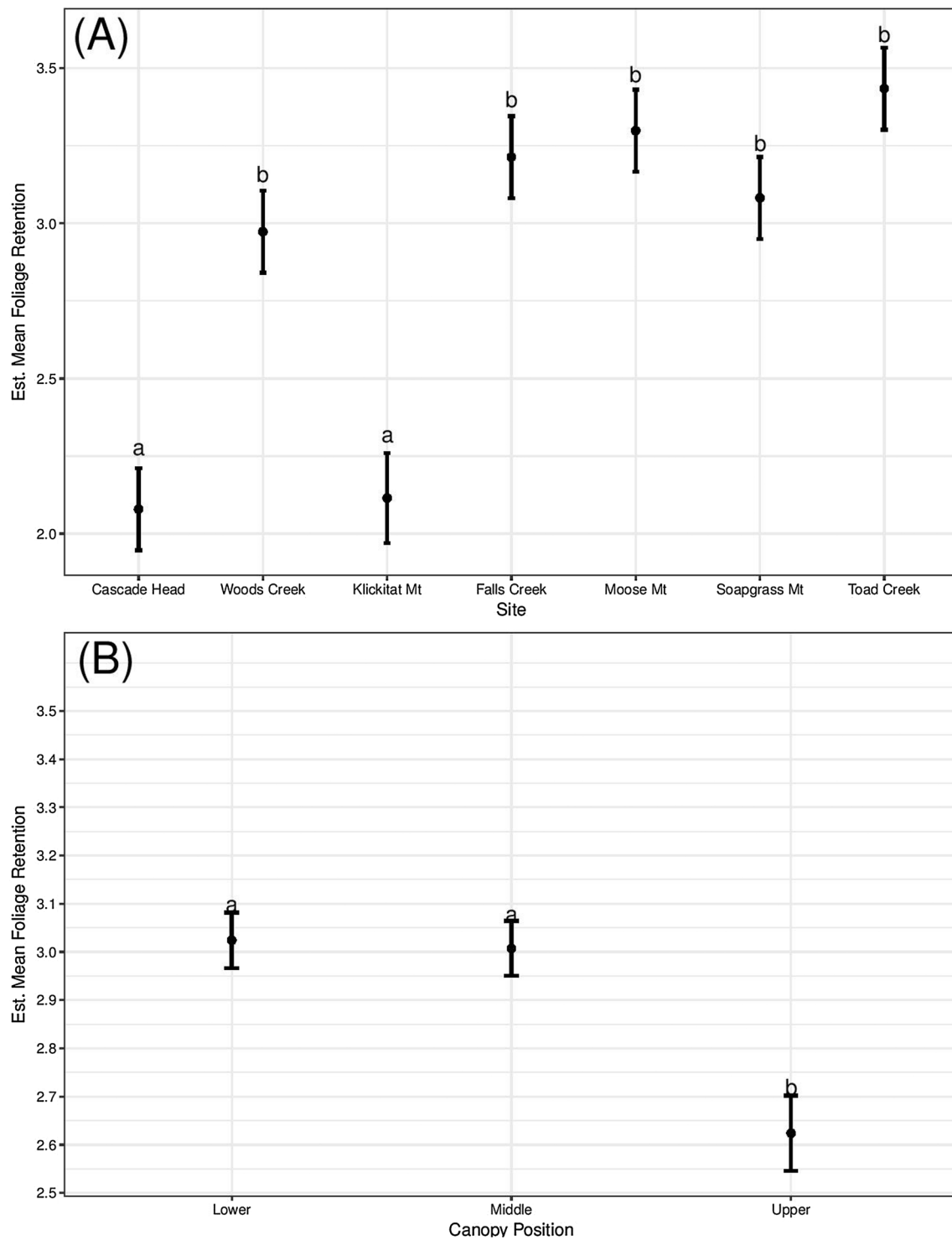
Fig. 6. Least square means of foliage retention in western Oregon A) by site and B) by canopy position. All seven sites were present in MANOVA and mean comparison. The error bar represents mean ± 1standard error. Letters represents groups. The least square means of foliage retention between any two groups is statically different if the letters are different.

which indicated no difference in foliar nitrogen in the samples of young and old trees at individual sites (Fig. 7). El-Hajj et al., (2004) noted that *N. gaeumannii* might acquire nitrogen and carbon from apoplastic spaces within Douglas-fir needles and disease severity could be influenced by fertilization. However, Mulvey et al., (2013) did not demonstrate any change in disease severity after fertilization with nitrogen. Perakis et al., (2006) showed a correlation between increased soil nitrogen and disease occurrence at the landscape scale, following a

pattern of increasing disease east to west in the Oregon Coast Range. Perakis et al., (2006) suggested that greater nitrogen could be associated with increased foliage disease. It may be that nitrogen is important in the epidemic that is occurring along the coast, but that it does not differ enough between young and mature trees to influence differences in disease expression at the tree scale.

Leaf wetness did not explain differences in disease severity between young and mature Douglas-fir trees in this study because young and old
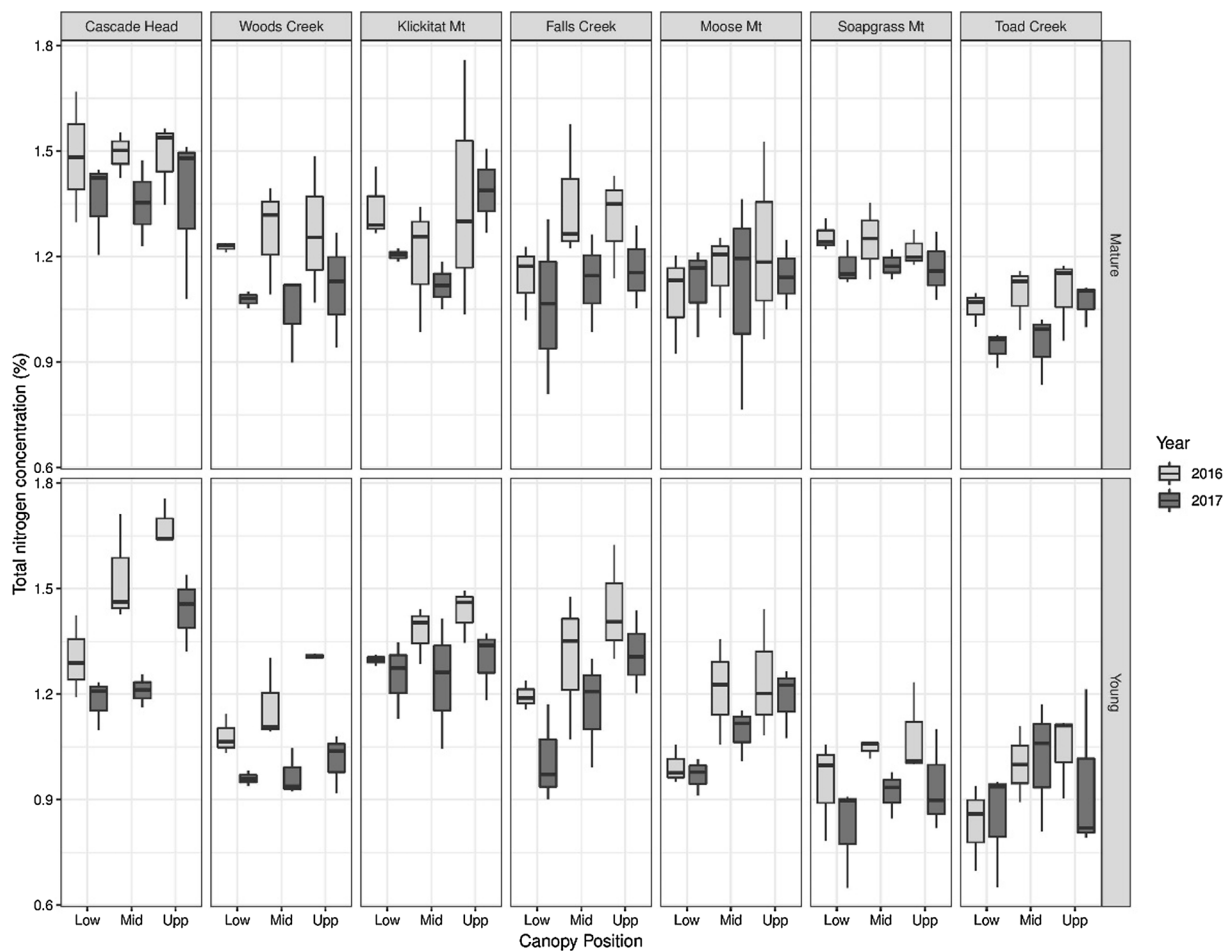
Fig. 7. Total foliage nitrogen concentration for mature and young trees at three canopy positions across seven sites in western Oregon in 2016–2017. Only one-year-old needles were used for foliage nitrogen measurement. The whiskers represented the range of mean values.

stands were consistently wet most of the time and did not differ (Fig. 9). However, vertical and within crown canopy complexity may influence thermal properties of trees and stands, which could influence leaf temperature and fungal growth rates. Hansen et al., (2000) noted that in forest plantations disease severity was greatest in the upper crown, and on southern aspects, which are both more likely to have warmer temperatures in winter, a key period of fungal development (Manter et al., 2005). The thermal dynamics of young canopies and older canopies of Douglas-fir is not well documented, and we can only speculate if differences could account for differences in disease.

Incidence and severity of *N. gaeumannii* were different between adjacent mature and young trees, here we speculate the factors we did not measure which could explain this. One of possibility could be pseudothecia develop sooner on young trees and need more time to mature on old trees. There are only few studies that address differences between needles of old and young trees. In conifers, older trees have needles that are morphologically different from needles of young trees (Apple et al., 2002; Day et al., 2001; England and Attiwill, 2006). These differences may contribute to old Douglas-fir trees being more resistant or tolerant to *N. gaeumannii* infection or development within the leaf. In addition, there are also age-related differences in defensive chemicals (Erwin et al., 2001). Secondary chemical compounds are important in plant defense against pathogens (Espinosa-Garcia and Langenheim, 1991; Cook and Hain, 1986) and could play a role in the observed differences in disease severity. Further, old trees that have been exposed to *N. gaeumannii* for much longer than young trees may have lived so long due to their tolerance to the fungus.

Hansen et al. (2000) found that SNC disease severity was greatest in

the upper canopy of young trees in plantations. We found similar trends at Cascade Head, Klickitat Mountain, and Falls Creek, but disease severity was so low at other sites that we could show no patterns relative to disease severity at different canopy positions of young trees. In older trees we found some evidence that SNC severity was most pronounced in the middle and upper crown layers, but the disease severity was so low in old trees in most areas that we were unable to detect consistent patterns. In our study, *N. gaeumannii* was also rare at two high elevation sites. This is consistent with Manter et al. (2005) who found that warm winter temperatures were positively associated with SNC, and Ritóková et al. (2016) who showed that SNC severity decreased with increasing elevation in the western Cascades.

Our study is the first to directly compare mature and young trees for *N. gaeumannii* caused disease severity. Mildrexler et al. (2019) compared private lands versus public lands in the Oregon Coast Range using aerial detection data, and found that private lands with young forests tended to have more visible disease symptoms than public lands which have more older stands. It appears that mature and older trees are not as likely to express disease impacts to *N. gaeumannii* as young plantation trees in western Oregon. Although *N. gaeumannii* is still present in older tree crowns, disease severity was always lower than young trees. The conclusions of our study should be confirmed by a much larger sample size from throughout the epidemic area because of the implications for landscape management.

The current SNC epidemic area is the region where foliage retention averages < 3 years and visible symptoms of disease such as needle chlorosis, sparse crowns, and reduced growth occur (Ritóková et al., 2016). The weather conditions within the epidemic area of SNC near
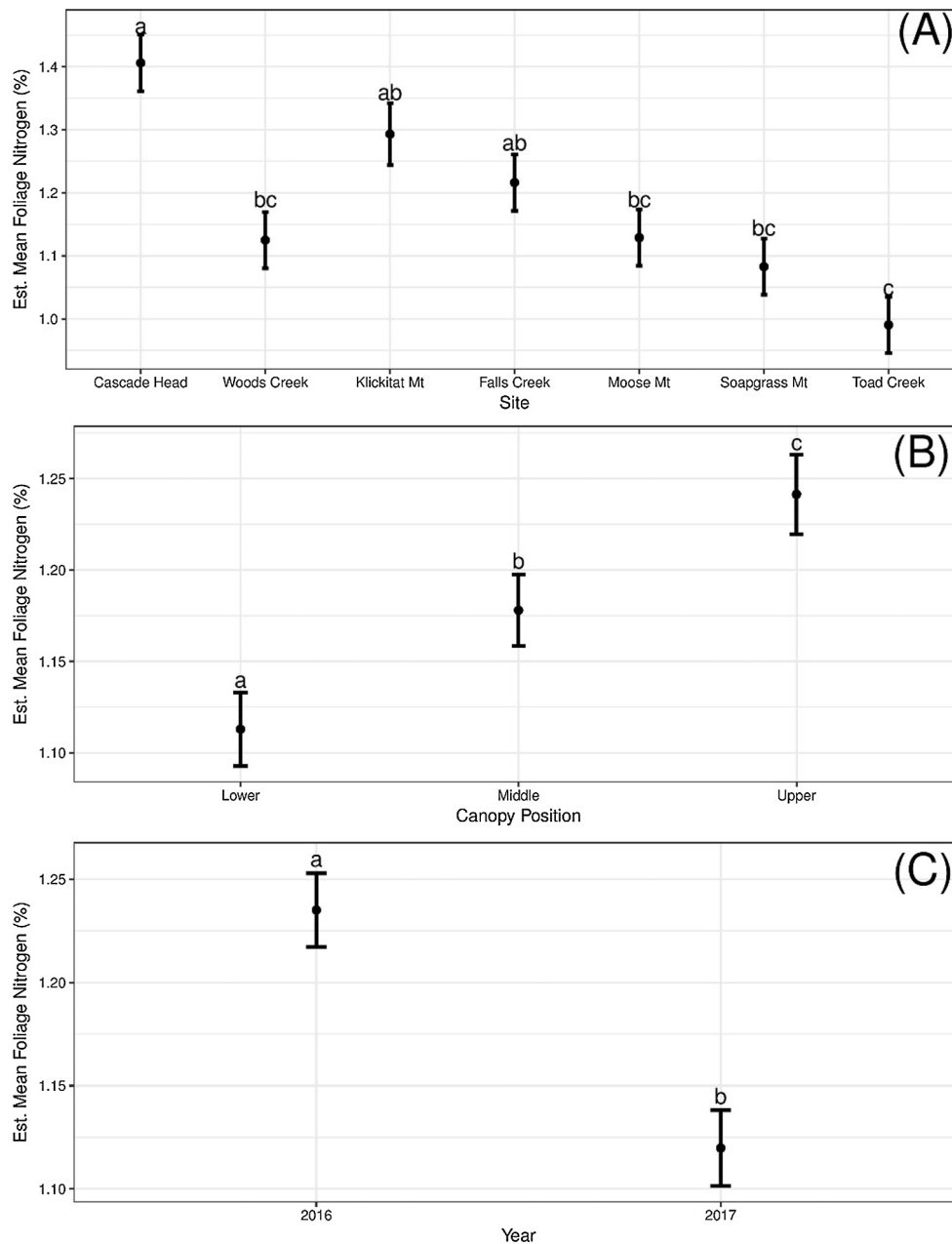
Fig. 8. Least square means of foliage total nitrogen concentration for seven study sites in western Oregon (A) by site, (B) by canopy considering site and year effects, and (C) by year considering canopy and site effects. All seven sites were included in MANOVA and mean comparisons. The error bar represents mean ± 1standard error. Letters represents groups. The least square means of foliage nitrogen concentration between any two groups is statically different if the letters are different.

the coast are distinct from the Cascade Mountains sites, and this influences the geographical distribution of the epidemic (Rosso and Hansen, 2003, Shaw et al. 2011; Ritóková et al., 2016). The three Oregon Coast Range sites used in our study are within the epidemic area, while the four Cascade Mountain sites are outside the epidemic area, and the trees were generally healthy, yet at two lower elevations sites the disease was abundant in the young stands. If we only focused on stands in the epidemic area of the Oregon Coast Range, we may have seen different patterns. For example, on the Oregon coast, Tillamook area is considered as one of the regions in which forests are most severely infected with SNC historically (Hansen et al., 2000), and in this region even mature Douglas-fir forests (~80-year-old) are often infected (Black et al. 2010).

The epidemiology of *N. gaeumannii* has focused on winter temperature and leaf wetness during spore dispersal (May to August) (Rosso and Hansen, 2003; Manter et al., 2005). Variability in climate

will influence infection success, and short-term climate trends are associated with disease intensification (Mildrexler et al., 2019). Land surface temperature trended cooler, and water balance increased from 2003 to 2012 during June and July. Consequently, Swiss needle cast aerial survey area went from a low of 71,465 ha in 2004 to 210,184 ha in 2012 (Ritóková et al., 2016). Lee et al., (2013; 2016; 2017) have noted that the exact climate factors associated with impacts by *N. gaeumannii* likely vary with geographic location. Given that our seven stands had distinct climate conditions, it is significant that patterns of infection between mature and young trees remained consistent.

In conclusion, we found that disease severity is higher in young plantation trees than in mature forest trees and that this may be a result of emergence of pseudothecia in stomates of younger needles in young trees. Although we do not know why disease severity and timing of stomatal occlusion would be different, our data suggest that leaf nitrogen and leaf wetness differences are not the reason. Therefore, future
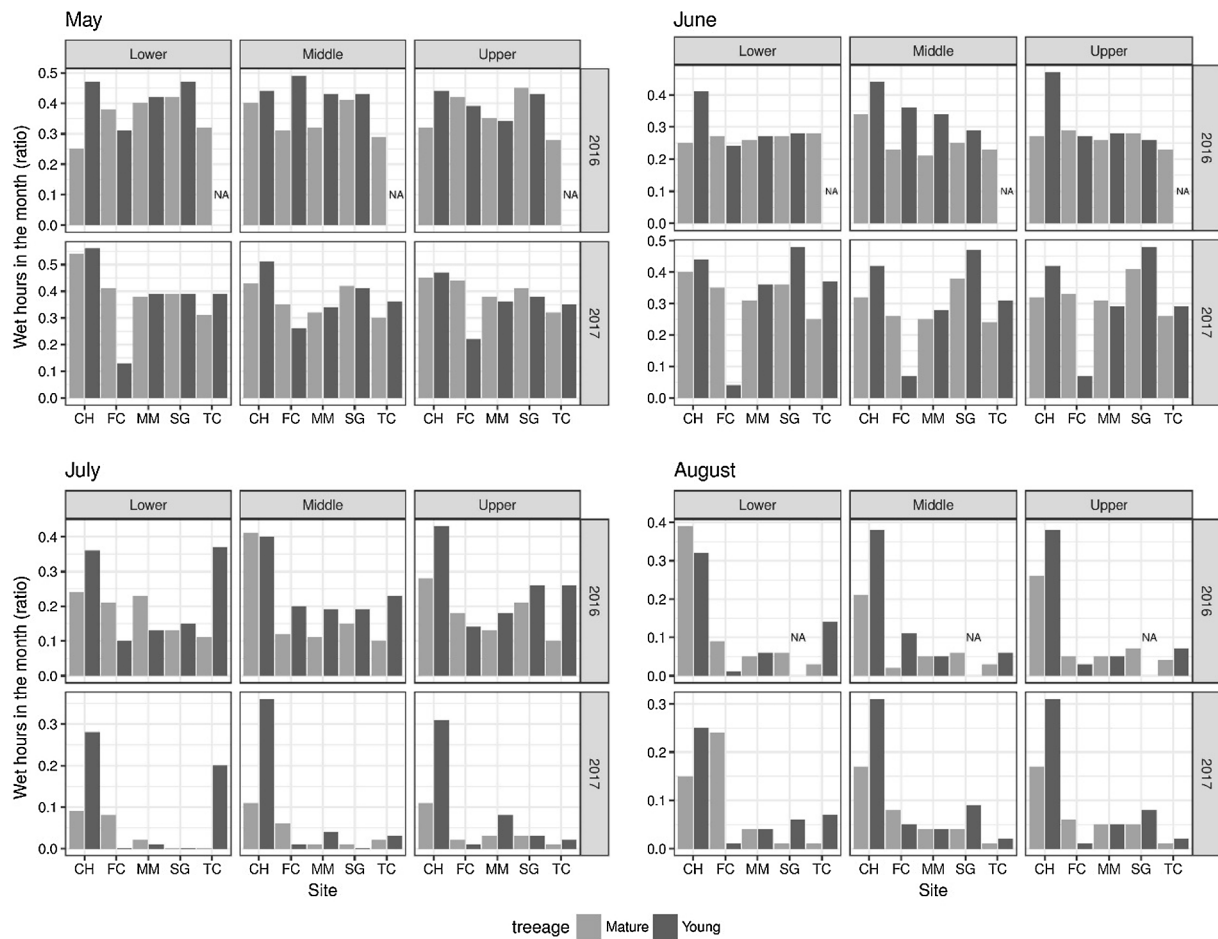
Fig. 9. Wet hour ratio per month for May, June, July and August for one mature and one young tree at each site at Cascade Head (CH), Falls Creek (FC), Moose Mountain (MM), Soapgrass Mountain (SG), and Toad Creek (TC). We set up the wet/dry threshold as 280 mV based on the manual description as well as sensor performance on site and counted it as a wet hour if the raw number > 280 mV. The leaf wetness duration was presented by counting the ratio of total wet hours per month/total hours per month. Due to technical issues of sensors, May 2016 and June 2016 in Toad Creek young plot, and August 2016 in Soapgrass Mountain young plot were missed in the figure and marked as "NA".

research to understand epidemiology of *N. gaeumannii* would investigate why there is higher pseudothecia density in two-year-old needles of younger stands, and to determine the drivers of leaf colonization by the fungus. Possibly including dynamics inside the needle, needle temperature during winter, and other factors that potentially influence pseudothecia development.

Appendix A. . Summary of SNC incidence (in %) of needles with pseudothecia for all needle age classes in 2016, across seven study sites in western Oregon for mature and young trees in the upper, middle and lower crowns. The number in front of ± is average of three trees and the number followed is standard error.

2016			yr1	yr2	yr3	yr4	yr5	yr6	yr7	yr8	yr9	yr10
CH[1]	Mature	Upper	10.0 ± 4.2	88.7 ± 5.8	67.2 ± 27.0	80.0 ± 2.0	63.7 ± 30.3	86.0 ± NA	-	-	-	-
		Middle	4.7 ± 4.7	98.0 ± 0.0	96.0 ± 3.1	85.2 ± 7.8	96.1 ± 1.9	–	–	–	–	–
		Lower	1.3 ± 1.3	88.7 ± 1.3	96.0 ± 4.0	69.3 ± 2.7	90.2 ± 3.1	81.8 ± NA	–	–	–	–
	Young	Upper	95.3 ± 2.4	99.3 ± 0.7	–	–	–	–	–	–	–	–
		Middle	68.7 ± 13.8	100.0 ± 0.0	100.0 ± 0.0	100.0 ± 0.0	100.0 ± NA	–	–	–	–	–
		Lower	8.0 ± 5.0	100.0 ± 0.0	100.0 ± 0.0	100.0 ± 0.0	100.0 ± 0.0	100.0 ± NA	–	–	–	–
KT[1]	Mature	Upper	2.7 ± 1.8	34.7 ± 21.7	60.7 ± 21.5	65.8 ± 13.7	12.0 ± NA	–	–	–	–	–
		Middle	0.0 ± 0.0	24.7 ± 8.7	74.7 ± 7.7	27.6 ± 10.1	17.6 ± 10.0	34.1 ± 17.9	10.9 ± 0.9	7.7 ± NA	–	–

		Lower	0.7 ± 0.7	20.0 ± 7.2	74.0 ± 3.1	29.4 ± 6.9	17.0 ± 7.0	12.5 ± 6.5	0.0 ± NA	–	–	–
	Young	Upper	14.0 ± 7.2	96.7 ± 2.4	–	–	–	–	–	–	–	–
		Middle	15.3 ± 4.8	96.0 ± 4.0	100.0 ± NA	100.0 ± NA	–	–	–	–	–	–
WC[1]	Mature	Lower	2.0 ± 2.0	96.0 ± 3.1	92.7 ± 5.5	89.3 ± 9.7	99.0 ± 1.0	–	–	–	–	–
		Upper	0.0 ± 0.0	0.7 ± 0.7	6.0 ± 5.0	22.0 ± 10.6	5.3 ± 2.9	–	–	–	–	–
		Middle	0.0 ± 0.0	1.3 ± 1.3	29.3 ± 5.8	26.7 ± 6.4	7.0 ± 1.5	6.0 ± 2.0	4.3 ± NA	0.0 ± NA	4.0 ± NA	0.0 ± NA
		Lower	0.0 ± 0.0	4.7 ± 1.8	55.3 ± 6.4	52.7 ± 1.3	12.0 ± 3.1	14.7 ± 4.4	12.0 ± 6.1	2.0 ± 2.0	0.0 ± NA	–
	Young	Upper	0.7 ± 0.7	85.3 ± 7.7	–	–	–	–	–	–	–	–
		Middle	0.0 ± 0.0	99.3 ± 0.7	99.3 ± 0.7	61.0 ± 19.0	–	–	–	–	–	–
		Lower	0.7 ± 0.7	100.0 ± 0.0	100.0 ± 0.0	96.0 ± 4.0	–	–	–	–	–	–

2016			yr1	yr2	yr3	yr4	yr5	yr6	yr7	yr8	yr9	yr10
MM[1]	Mature	Upper	0.7 ± 0.7	17.3 ± 12.5	27.3 ± 17.1	28.0 ± 26.0	63.2 ± NA	-	-	-	-	-
		Middle	5.3 ± 3.5	25.3 ± 19.5	66.7 ± 30.4	63.3 ± 23.7	55.0 ± 30.7	50.0 ± 42.0	20.0 ± NA	10.0 ± NA	38.5 ± NA	–
		Lower	8.7 ± 4.8	24.7 ± 5.5	70.7 ± 23.4	58.0 ± 19.4	44.0 ± 16.0	29.0 ± 15.0	12.0 ± NA	20.0 ± NA		–
	Young	Upper	20.0 ± 2.0	92.7 ± 3.7	100.0 ± 0.0	91.0 ± 9.0	–	–	–	–	–	–
		Middle	17.3 ± 1.8	98.7 ± 1.3	100.0 ± 0.0	97.3 ± 2.7	95.3 ± 4.7	–	–	–	–	–
FC[1]	Mature	Lower	24.0 ± 4.0	99.3 ± 0.7	100.0 ± 0.0	100.0 ± 0.0	100.0 ± 0.0	86.4 ± 13.6	100.0 ± NA	–	–	–
		Upper	4.7 ± 1.8	4.0 ± 1.2	40.0 ± 26.4	42.5 ± 12.8	27.0 ± 5.0	18.4 ± NA	–	–	–	–
		Middle	2.0 ± 1.2	6.7 ± 3.7	78.7 ± 12.7	48.0 ± 12.5	59.5 ± 4.6	40.0 ± 4.0	–	–	–	–
		Lower	8.7 ± 5.9	12.7 ± 5.3	69.3 ± 5.5	64.7 ± 12.0	73.3 ± 12.8	51.5 ± 18.6	40.2 ± 4.5	48.9 ± 23.9	–	–
	Young	Upper	12.0 ± 7.2	98.0 ± 1.2	97.4 ± 2.6	–	–	–	–	–	–	–
		Middle	19.3 ± 3.3	100.0 ± 0.0	98.7 ± 1.3	100.0 ± 0.0	99.3 ± 0.7	97.8 ± NA	–	–	–	–
SG[1]	Mature	Lower	38.0 ± 7.6	98.7 ± 1.3	100.0 ± 0.0	100.0 ± 0.0	100.0 ± 0.0	100.0 ± NA	–	–	–	–
		Upper	0.0 ± 0.0	2.0 ± 1.2	0.0 ± 0.0	0.7 ± 0.7	0.0 ± 0.0	0.0 ± 0.00	0.0 ± NA	0.0 ± NA		–
		Middle	0.0 ± 0.0	0.0 ± 0.0	0.7 ± 0.7	0.0 ± 0.0	0.7 ± 0.7	0.0 ± 0.00	0.0 ± 0.0	2.9 ± 2.9	0.0 ± NA	–
		Lower	1.3 ± 1.3	0.0 ± 0.0	0.0 ± 0.0	0.0 ± 0.0	0.0 ± 0.00	0.0 ± 0.00	0.0 ± 0.0	0.0 ± 0.0	0.0 ± 0.0	0.0 ± 0.0
	Young	Upper	0.0 ± 0.0	0.0 ± 0.0	2.7 ± 2.7	2.7 ± 0.7	2.0 ± 2.0	0.0 ± NA	–	–	–	–
		Middle	0.0 ± 0.0	0.7 ± 0.7	8.7 ± 1.3	8.7 ± 1.8	12.7 ± 10.7	4.7 ± 4.7	4.0 ± 4.0	0.0 ± NA	–	–
TC[1]	Mature	Lower	0.0 ± 0.0	4.0 ± 2.3	46.7 ± 23.3	39.3 ± 15.7	34.7 ± 9.3	34.0 ± 30.0	28.7 ± 24.8	13.8 ± 10.3	90.0 ± NA	–
		Upper	0.0 ± 0.0	0.0 ± 0.0	0.0 ± 0.0	0.0 ± 0.0	0.0 ± 0.0	0.0 ± 0.0	0.0 ± 0.0	0.0 ± NA	0.0 ± NA	
		Middle	0.0 ± 0.0	0.0 ± 0.0	0.0 ± 0.0	0.0 ± 0.0	0.0 ± 0.0	0.0 ± 0.0	0.0 ± 0.0	0.0 ± 0.0	0.0 ± 0.0	0.0 ± 0.0
		Lower	0.0 ± 0.0	0.0 ± 0.0	0.7 ± 0.7	0.0 ± 0.0	0.0 ± 0.0	0.0 ± 0.0	0.0 ± 0.0	0.0 ± 0.0	0.0 ± 0.0	0.0 ± 0.0
	Young	Upper	0.7 ± 0.7	2.7 ± 1.8	2.0 ± 2.0	2.0 ± 2.0	–	–	–	–	–	–
		Middle	3.3 ± 2.4	3.3 ± 2.4	2.0 ± 1.2	2.7 ± 1.8	1.0 ± 1.0	6.0 ± NA	2.0 ± NA	2.9 ± NA	–	–
		Lower	8.0 ± 2.0	1.3 ± 0.7	2.0 ± 1.2	2.0 ± 1.2	1.3 ± 1.3	0.7 ± 0.7	0.0 ± 0.0	–	–	–

1The abbreviation of study sites is Cascade Head (CH), Woods Creek (WC), and Klickitat Mountain (KT), Moose Mountain (MM), Falls Creek (FC), Soapgrass Mountain (SG), and Toad Creek (TC).

2NA means there was only one sample so it lacked of standard error.

3"-" means sample wasn't present.

Appendix B. . Summary of SNC incidence (in %) of needles with pseudothecia for all needle age classes in 2017, across seven study sites in western Oregon for mature and young trees in upper, middle and lower crowns. The number in front of ± is average of three trees and the number followed is standard error.

2017			yr1	yr2	yr3	yr4	yr5	yr6	yr7	yr8	yr9	yr10
CH[1]	Mature	Upper	40.7 ± 15.3	96.7 ± 3.3	80.7 ± 15.5	100.0 ± NA	100.0 ± NA	100.0 ± NA	-	-	-	-
		Middle	35.3 ± 10.1	99.3 ± 0.7	98.7 ± 0.7	98.7 ± 1.3	100.0 ± NA	–	–	–	–	–
		Lower	12.7 ± 3.5	97.3 ± 2.7	100.0 ± 0.0	100.0 ± 0.0	100.0 ± NA	–	–	–	–	–
	Young	Upper	100.0 ± 0.0	100.0 ± 0.0	100.0 ± 0.0	–	–	–	–	–	–	–
		Middle	80.7 ± 11.1	100.0 ± 0.0	100.0 ± 0.0	100.0 ± 0.0	100.0 ± 000	100.0 ± NA	–	–	–	–
KT[1]	Mature	Lower	45.3 ± 14.3	100.0 ± 0.0	100.0 ± 0.0	100.0 ± 0.0	100.0 ± 0.0	100.0 ± NA	–	–	–	–
		Upper	0.0 ± 0.0	12.0 ± 0.0	28.9 ± 8.9	41.7 ± 41.7	–	–	–	–	–	–
		Middle	2.0 ± 2.0	20.0 ± 20.0	44.0 ± 16.0	44.0 ± 12.0	27.0 ± 17.0	0.0 ± NA	7.1 ± NA	6.8 ± NA	–	–
		Lower	3.0 ± 1.0	3.0 ± 1.0	28.0 ± 12.0	57.0 ± 1.0	28.7 ± 4.7	29.0 ± 21.0	10.0 ± NA	6.3 ± NA	–	–
	Young	Upper	8.7 ± 1.3	91.3 ± 4.8	99.3 ± 0.7	100.0 ± NA	–	–	–	–	–	–
		Middle	6.7 ± 3.3	85.3 ± 3.5	98.0 ± 1.2	97.4 ± 2.6	97.2 ± 2.8	100.0 ± NA	–	–	–	–
WC[1]	Mature	Lower	13.3 ± 3.7	80.7 ± 11.6	95.3 ± 4.7	100.0 ± 0.0	95.9 ± 1.4	–	–	–	–	–
		Upper	0.0 ± 0.0	0.7 ± 0.7	1.3 ± 0.7	4.7 ± 2.7	20.0 ± 8.1	0.0 ± 0.0	–	–	–	–
		Middle	0.0 ± 0.0	1.3 ± 1.3	6.7 ± 3.7	32.0 ± 0.0	23.3 ± 4.7	6.8 ± 0.8	7.4 ± 4.6	10.0 ± NA	–	–
		Lower	1.3 ± 0.7	2.0 ± 1.2	17.3 ± 4.1	30.7 ± 4.7	40.0 ± 3.1	10.0 ± 5.3	15.3 ± 4.4	11.5 ± 3.5	1.6 ± 1.6	–
	Young	Upper	0.7 ± 0.7	30.0 ± 16.0	80.0 ± 13.6	–	–	–	–	–	–	–
		Middle	2.0 ± 1.2	50.7 ± 10.9	94.0 ± 5.0	94.0 ± 6.0	–	–	–	–	–	–
		Lower	2.0 ± 2.0	52.7 ± 15.8	99.3 ± 0.7	98.7 ± 0.7	57.9 ± NA	–	–	–	–	–

2017			yr1	yr2	yr3	yr4	yr5	yr6	yr7	yr8	yr9	yr10
MM[1]	Mature	Upper	0.0 ± 0.0	3.3 ± 2.4	16.0 ± 11.4	31.4 ± 13.7	29.4 ± NA	-	-	-	-	-
		Middle	0.7 ± 0.7	0.7 ± 0.7	34.7 ± 17.5	51.9 ± 23.2	26.8 ± 4.8	18.0 ± NA	2.0 ± NA	11.8 ± NA	6.5 ± NA	–
		Lower	0.7 ± 0.7	1.3 ± 1.3	52.7 ± 25.8	56.0 ± 28.7	53.3 ± 27.5	33.0 ± 27.0	25.0 ± 23.0	0.0 ± NA	6.8 ± NA	–
	Young	Upper	0.0 ± 0.0	60.0 ± 23.2	89.9 ± 8.1	83.5 ± 8.5	–	–	–	–	–	–
		Middle	1.3 ± 1.3	67.3 ± 18.0	99.3 ± 0.7	96.0 ± 4.0	100.0 ± NA	–	–	–	–	–
		Lower	3.3 ± 0.7	78.7 ± 14.9	100.0 ± 0.0	100.0 ± 0.0	100.0 ± 0.0	100.0 ± 0.0	–	–	–	–
FC[1]	Mature	Upper	0.0 ± 0.0	2.0 ± 1.2	33.3 ± 11.8	40.0 ± 15.6	60.0 ± NA	38.0 ± NA	40.4 ± NA	–	–	–
		Middle	0.0 ± 0.0	3.3 ± 2.4	34.7 ± 18.0	68.7 ± 22.5	55.3 ± 4.4	57.7 ± 14.3	50.2 ± 11.8	–	–	–
		Lower	0.0 ± 0.0	2.0 ± 1.2	52.7 ± 10.0	88.7 ± 5.7	73.0 ± 10.6	74.0 ± 12.2	39.9 ± 11.9	–	–	–
	Young	Upper	36.0 ± 30.1	97.3 ± 1.8	98.7 ± 1.3	96.0 ± NA	100.0 ± NA	–	–	–	–	–
		Middle	22.0 ± 17.1	99.3 ± 0.7	100.0 ± 0.0	100.0 ± 0.0	100.0 ± 0.0	100.0 ± 0.0	–	–	–	–
		Lower	32.0 ± 25.1	95.3 ± 2.9	100.0 ± 0.0	100.0 ± 0.0	100.0 ± 0.0	100.0 ± NA	–	–	–	–
SG[1]	Mature	Upper	0.0 ± 0.0	0.0 ± 0.0	0.0 ± 0.0	0.0 ± 0.0	4.2 ± 3.0	2.4 ± 0.4	0.0 ± NA	–	–	–
		Middle	0.0 ± 0.0	0.0 ± 0.0	0.7 ± 0.7	0.7 ± 0.7	0.0 ± 0.0	0.0 ± 0.0	0.0 ± 0.0	0.0 ± NA	0.0 ± NA	0.0 ± NA
		Lower	0.0 ± 0.0	0.0 ± 0.0	0.0 ± 0.0	0.0 ± 0.0	0.7 ± 0.7	0.0 ± 0.0	0.0 ± 0.0	0.0 ± 0.0	0.0 ± 0.0	0.0 ± 0.0
	Young	Upper	0.0 ± 0.0	0.0 ± 0.0	1.3 ± 1.3	2.7 ± 1.8	7.0 ± 3.0	4.0 ± NA	3.3 ± NA	–	–	–
		Middle	0.7 ± 0.7	0.0 ± 0.0	19.3 ± 10.4	18.7 ± 11.8	13.3 ± 4.7	10.0 ± 3.1	4.0 ± 4.0	4.0 ± 4.0	–	–
		Lower	1.3 ± 1.3	4.0 ± 3.1	31.3 ± 14.3	43.3 ± 25.4	40.7 ± 21.9	44.4 ± 21.6	58.0 ± 42.0	75.0 ± NA	19.2 ± NA	–
TC[1]	Mature	Upper	0.0 ± 0.0	0.0 ± 0.0	0.0 ± 0.0	0.0 ± 0.0	0.0 ± 0.0	0.0 ± 0.0	0.0 ± 0.0	0.0 ± 0.0	0.0 ± NA	–
		Middle	0.0 ± 0.0	0.0 ± 0.0	0.0 ± 0.0	0.0 ± 0.0	0.0 ± 0.0	0.0 ± 0.0	0.0 ± 0.0	0.0 ± 0.0	0.0 ± 0.0	0.0 ± 0.0
		Lower	0.0 ± 0.0	0.0 ± 0.0	0.7 ± 0.7	0.0 ± 0.0	0.0 ± 0.0	0.0 ± 0.0	0.7 ± 0.7	0.0 ± 0.0	0.0 ± 0.0	0.0 ± 0.0
	Young	Upper	0.0 ± 0.0	0.0 ± 0.0	0.0 ± 0.0	–	–	–	–	–	–	–
		Middle	0.0 ± 0.0	0.7 ± 0.7	0.7 ± 0.7	0.7 ± 0.7	2.0 ± 1.2	0.0 ± 0.0	–	–	–	–
		Lower	0.0 ± 0.0	0.7 ± 0.7	1.3 ± 1.3	0.7 ± 0.7	2.7 ± 0.7	0.0 ± 0.0	0.0 ± 0.0	0.0 ± NA	–	–

1 The abbreviation of study sites is Cascade Head (CH), Woods Creek (WC), and Klickitat Mountain (KT), Moose Mountain (MM), Falls Creek (FC), Soapgrass Mountain (SG), and Toad Creek (TC).

2 NA means there was only one sample so it lacked of standard error.

3 "-" means sample wasn't present.

Appendix C. . Results of preliminary MANOV test for the main effects tree age, site, year and canopy position alone and their interaction on SNC incidence in study areas in western Oregon. Only one- and two-year-old needles were used for statistical analysis because three- and older needles had limited data for testing covariance.

		F-value	p-value	
Needle age = 1	(Intercept)	191.6	< 0.001	***
	Tree age	81.4	< 0.001	***
	Site	55.3	< 0.001	***
	Tree age × Site	18.8	< 0.001	***
	Year	1.1	0.307	
	Tree age × Year	0.2	0.654	
	Site × Year	6.7	0.002	**
	Tree age × Site × Year	1.1	0.375	
	Canopy	8.3	0.003	**
	Tree age × Canopy	3.6	0.048	*
	Site × Canopy	4.3	0.001	***
	Tree age × Site × Canopy	3.1	0.008	**
	Year × Canopy	0.0	0.977	
	Tree age × Year × Canopy	2.4	0.120	
	Site × Year × Canopy	0.7	0.722	
	Tree age × Site × Year × Canopy	1.4	0.220	
NeedleAge = 2	(Intercept)	1320.0	< 0.001	***
	Tree age	403.5	< 0.001	***
	Site	47.6	< 0.001	***
	Tree age × Site	24.1	< 0.001	***
	Year	23.7	< 0.001	***
	Tree age × Year	7.9	0.011	*
	Site × Year	6.3	0.002	**
	Tree age × Site × Year	4.1	0.015	*
	Canopy	5.2	0.017	*
	Tree age × Canopy	0.7	0.494	
	Site × Canopy	1.4	0.234	
	Tree age × Site × Canopy	1.6	0.161	
	Year × Canopy	0.8	0.460	
	Tree age × Year × Canopy	1.8	0.193	
	Site × Year × Canopy	0.7	0.666	
	Tree age × Site × Year × Canopy	0.7	0.678	

Appendix D. . Results of MANOVA by individual sites testing significance of SNC incidence. Because eligible needle age classes were different in each site, the MANOVA was re-run by site and by needle age to clarify the effects from other factors. The MANOVA results for SNC incidence varied by needle age class and site. Tree age was a crucial factor in SNC incidence analysis across most of study sites. SNC incidence for one- and two-year-old needles differed by canopy position at Cascade Head, and possibly two-year-old needles at Woods Creek but not the other sites.

		Needle age = 1 yr			Needle age = 2 yr			Needle age = 3 yr			Needle age = 4 yr		Needle age = 5 yr	
		F-value	p-value		F-value	p-value		F-value	p-value		F-value	p-value	F-value	p-value
CH[1]	(Intercept)	105.6	**0.001**	***	7432.2	**< 0.001**	***	286.8	**0.003**	**	–	–	–	–
	Tree age	36.0	**0.004**	**	5.1	**0.086**	.	0.8	0.457		–	–	–	–
	Year	16.9	**0.015**	*	60.3	**0.001**	**	0.1	0.826		–	–	–	–
	Tree age × Year	0.4	**0.577**		52.0	**0.002**	**	0.1	0.826		–	–	–	–
	Canopy	42.4	**0.006**	**	18.0	**0.021**	*	1.6	0.491		–	–	–	–
	Tree age × Canopy	14.3	**0.029**	*	20.7	**0.018**	*	1.6	0.491		–	–	–	–
	Year × Canopy	0.6	**0.608**		132.6	**0.001**	**	0.1	0.896		–	–	–	–
	Tree age × Year × Canopy	5.2	**0.106**		126.4	**0.001**	**	0.1	0.896		–	–	–	–
KT	(Intercept)	10.6	**0.047**	*	234.8	**0.001**	***	–	–		–	–	–	–
	Tree age	6.2	**0.089**	.	130.1	**0.001**	**	–	–		–	–	–	–
	Year	0.0	0.976		30.3	**0.012**	*	–	–		–	–	–	–
	Tree age × Year	0.1	0.831		8.1	**0.065**	.	–	–		–	–	–	–
	Canopy	0.3	0.750		0.7	0.585		–	–		–	–	–	–
	Tree age × Canopy	0.5	0.653		0.3	0.773		–	–		–	–	–	–
	Year × Canopy	7.7	0.116		2.5	0.282		–	–		–	–	–	–
	Tree age × Year × Canopy	5.9	0.146		0.1	0.887		–	–		–	–	–	–

		Needle age = 1 yr			Needle age = 2 yr			Needle age = 3 yr			Needle age = 4 yr		Needle age = 5 yr	
		F-value	p-value		F-value	p-value		F-value	p-value		F-value	p-value	F-value	p-value
WC	(Intercept)	5.5	**0.079**	.	75.2	**0.001**	***	–	–		–	–	–	–
	Tree age	2.2	0.210		67.9	**0.001**	**	–	–		–	–	–	–
	Year	2.5	0.193		20.2	**0.011**	*	–	–		–	–	–	–
	Tree age × Year	0.5	0.539		18.8	**0.012**	*	–	–		–	–	–	–
	Canopy	0.6	0.624		9.2	**0.053**	.	–	–		–	–	–	–
	Tree age × Canopy	0.4	0.713		4.8	0.116		–	–		–	–	–	–
	Year × Canopy	1.2	0.414		2.5	0.234		–	–		–	–	–	–
	Tree age × Year × Canopy	7.2	**0.072**	.	2.3	0.244		–	–		–	–	–	–
MM	(Intercept)	86.9	**0.001**	***	76.5	**0.001**	***	51.0	**0.002**	**	–	–	–	–
	Tree age	32.3	**0.005**	**	42.4	**0.003**	**	7.2	**0.055**	.	–	–	–	–
	Year	64.9	**0.001**	**	6.7	**0.061**	.	12.9	**0.023**	*	–	–	–	–
	Tree age × Year	24.9	**0.008**	**	0.2	0.710		6.4	**0.065**	.	–	–	–	–
	Canopy	3.9	0.148		1.6	0.333		5.1	0.108		–	–	–	–
	Tree age × Canopy	0.8	0.541		0.4	0.677		4.7	0.119		–	–	–	–
	Year × Canopy	0.9	0.496		0.1	0.884		0.3	0.735		–	–	–	–
	Tree age × Year × Canopy	3.4	0.170		1.0	0.469		1.5	0.346		–	–	–	–
FC	(Intercept)	55.7	**0.002**	**	3566.3	**< 0.001**	***	163.8	**< 0.001**	***	–	–	–	–
	Tree age	37.9	**0.004**	**	2894.9	**< 0.001**	***	16.4	**0.015**	*	–	–	–	–
	Year	0.0	0.917		4.6	**0.098**	.	16.0	**0.016**	*	–	–	–	–
	Tree age × Year	0.6	0.495		1.4	0.304		18.6	**0.013**	*	–	–	–	–
	Canopy	11.9	**0.037**	*	4.1	0.139		2.4	0.242		–	–	–	–
	Tree age × Canopy	4.6	0.123		2.7	0.216		1.7	0.319		–	–	–	–
	Year × Canopy	0.3	0.751		2.0	0.279		14.1	**0.030**	*	–	–	–	–
	Tree age × Year × Canopy	0.1	0.917		0.6	0.608		17.0	**0.023**	*	–	–	–	–

				Needle age = 2 yr			Needle age = 3 yr			Needle age = 4 yr			Needle age = 5 yr		
		F-value	p-value	F-value	p-value		F-value	p-value		F-value	p-value		F-value	p-value	
SG	(Intercept)	3.6	0.132	36.6	**0.004**	**	6.1	**0.069**	.	8.7	**0.042**	*	12.6	**0.038**	*
	Tree age	0.1	0.725	14.3	**0.019**	*	5.8	**0.073**	.	8.3	**0.045**	*	9.3	**0.055**	.
	Year	0.1	0.725	0.2	0.651		0.2	0.713		0.8	0.409		1.1	0.373	
	Tree age × Year	3.6	0.132	0.1	0.819		0.2	0.713		0.8	0.409		0.3	0.629	
	Canopy	1.7	0.319	2.9	0.199		3.5	0.166		2.5	0.227		6.2	0.138	
	Tree age × Canopy	0.4	0.686	8.5	**0.058**	.	2.8	0.204		2.6	0.223		3.5	0.221	
	Year × Canopy	0.4	0.686	0.4	0.716		1.5	0.347		0.2	0.798		10.1	**0.090**	.
	Tree age × Year × Canopy	1.7	0.319	1.6	0.342		1.5	0.347		0.1	0.874		22.3	**0.043**	*
TC	(Intercept)	15.4	**0.017**	13.0	**0.023**	*	–	–		–	–		–	–	
	Tree age	15.4	**0.017**	13.0	**0.023**	*	–	–		–	–		–	–	
	Year	15.4	**0.017**	3.0	0.158		–	–		–	–		–	–	
	Tree age × Year	15.4	**0.017**	3.0	0.158		–	–		–	–		–	–	

Canopy	2.9	0.199	0.2	0.835	–	–	–	–	–	–
Tree age × Canopy	2.9	0.199	0.2	0.835	–	–	–	–	–	–
Year × Canopy	2.9	0.199	1.5	0.354	–	–	–	–	–	–
Tree age × Year × Canopy	2.9	0.199	1.5	0.354	–	–	–	–	–	–

[1]The abbreviation of study sites is Cascade Head (CH), Woods Creek (WC), and Klickitat Mountain (KT), Moose Mountain (MM), Falls Creek (FC), Soapgrass Mountain (SG), and Toad Creek (TC).

[2]"-" means result wasn't present because of the limited data points.

References

Apple, M., Tiekotter, K., Snow, M., Young, J., Soeldner, A., Phillips, D., Tingey, D., Bond, B.J., 2002. Needle anatomy changes with increasing tree age in Douglas-fir. Tree Physiol. 22, 129–136.

Beedlow, P.A., Lee, E.H., Tingey, D.T., Waschmann, R.S., Burdick, C.A., 2013. The importance of seasonal temperature and moisture patterns on growth of Douglas-fir in western Oregon, USA. Agri. Forest Meteorol. 169, 174–185.

Black, B.A., Shaw, D.C., Stone, J.K., 2010. Impacts of Swiss needle cast on overstory Douglas-fir forests of the western Oregon Coast Range. Forest Ecol. Manage. 259, 1673–1680.

Capitano, B., 1999. The infection and colonization of Douglas-fir by *Phaeocryptopus gaeumannii*. M.Sc. thesis. Department of Botany and Plant Pathology. Oregon State University, Corvallis, Oregon.

Cook, S.P., Hain, F.P., 1986. Defensive mechanisms of loblolly and shortleaf pine against attack by southern pine beetle, *Dendroctonus frontalis* Zimmermann, and its fungal associate, *Ceratocystis minor* (Hedgecock) Hunt. J. Chem. Ecol. 12 (6), 1397–1406.

Day, M.E., Greenwood, M.S., White, A.S., 2001. Age-related changes in foliar morphology and physiology in red spruce and their influence on declining photosynthetic rates and productivity with tree age. Tree Physiol. 21 (16), 1195–1204.

El-Hajj, Z., Kavanagh, K., Rose, C., Kanaan-Atallah, Z., 2004. Nitrogen and carbon dynamics of a foliar biotrophic fungal parasite in fertilized Douglas-fir. New Phytolog. 163 (1), 139–147.

England, J.R., Attiwill, P.M., 2006. Changes in leaf morphology and anatomy with tree age and height in the broadleaved evergreen species. *Eucalyptus regnans* F. Muell. Trees 20, 79–90.

Erwin, E.A., Turner, M.G., Lindroth, R.L., Romme, W.H., 2001. Secondary plant compounds in seedling and mature aspen (*Populus tremuloides*) in Yellowstone National Park Wyoming. American Midland Naturalist 145 (2), 299–308.

Espinosa-Garcia, F.J., Langenheim, J.H., 1991. Effect of some leaf essential oil phenotypes in coastal redwood on the growth of several fungi with endophytic stages. Biochem. Syst. Ecol. 19 (8), 629–642.

Ewers, F.W., Schmid, R., 1981. Longevity of needle fascicles of *Pinus longaeva* (Bristlecone pine) and other North American pines. Oecologia 51, 107–115.

Fox, J., Weisberg, S., 2011. An R companion to applied regression (accessed 19 July 2018). Second Ed. Sage, Thousand Oaks CA. http://socserv.socsci.mcmaster.ca/jfox/Books/Companion.

Hansen, E.M., Stone, J.K., Capitano, B.R., Rosso, P., Sutton, W., Kanaskie, A., McWilliams, M.G., 2000. Incidence and impact of Swiss needle cast in forest plantations of Douglas-fir in coastal Oregon. Plant Dis. 84, 773–779.

Lee, E.H., Beedlow, P.A., Waschmann, R.S., Burdick, C.A., Shaw, D.C., 2013. Tree-ring analysis of the fungal disease Swiss needle cast in western Oregon coastal forests. Can. J. For. Res. 43, 677–690.

Lee, E.H., Beedlow, P.A., Waschmann, R.S., Tingey, D.T., Wickham, C., Cline, S., Bollman, M., Carlile, C., 2016. Douglas-fir displays a range of growth responses to temperature, water, and Swiss needle cast in western Oregon USA. Agri. Forest Meteorol. 221 (1), 176–188.

Lee, E.H., Beedlow, P.A., Waschmann, R.S., Tingey, D.T., Wickham, C., Cline, S., Bollman, M., Carlile, C., 2017. Regional patterns of increasing Swiss needle cast impacts on Douglas-fir growth with warming temperatures. Ecol. Evol. 7 (24), 11176–11196.

Lenth, R., 2018. emmeans: estimated marginal means, aka least-squares means (accessed 19 July 2018). R package version 1 (1), 3. https://CRAN.R-project.org/package=emmeans.

Maguire, D.A., Kanaskie, A., Voelker, W., Johnson, R., Johnson, G., 2002. Growth of young Douglas-fir plantations across a gradient in Swiss Needle Cast severity. West. J. Appl. Forestry 17 (2), 86–95.

Maguire, D.A., Mainwaring, D.B., Kanaskie, A., 2011. Ten-year growth and mortality in young Douglas-fir stands experiencing a range in Swiss needle cast severity. Can. J. For. Res. 41, 2064–2076.

Manter, D.K., Bond, B.J., Kavanagh, K.L., Rosso, P.H., Filip, G.M., 2000. Pseudothecia of Swiss Needle Cast Fungus, *Phaeocryptopus gaeumannii*, physically block stomata of Douglas-fir, reducing CO_2. New Phytolog. 3, 481–491.

Manter, D.K., Winton, L.M., Filip, G.M., Stone, J.K., 2003. Assessment of Swiss needle cast disease: temporal and spatial investigations of fungal colonization and symptom severity. J. Phytopathol. 151, 344–351.

Manter, D.K., Reeser, P.W., Stone, J.K., 2005. A climate-based model for predicting geographic variation in Swiss needle cast severity in the Oregon coast range. Phytopathology 95, 1256–1265.

Mildrexler, D.J., Shaw, D.C., Cohen, W.B., 2019. Short-term climate trends and the Swiss needle cast epidemic in Oregon's public and private coastal forestlands. For. Ecol. Manage. 432, 501–513.

Michaels, E., Chastagner, G.A., 1984. Seasonal availability of *Phaeocryptopus gaeumannii* ascospores and conditions that influence their release. Plant Dis. 68 (11), 942–944.

Mulvey, R.L., Shaw, D.C., Maguire, D.A., 2013. Fertilization impacts on Swiss needle cast disease severity in western Oregon. For. Ecol. Manage. 287, 147–158.

Perakis, S.S., Maguire, D.A., Bullen, T.D., Cromack, K., Waring, R.H., Boyle, J.R., 2006. Coupled nitrogen and calcium cycles in forests of the Oregon coast range. Ecosystems 9 (1), 63–74.

Pinheiro, J., Bates, D., DebRoy, S., Sarkar, D., R Core Team, 2017. nlme: Linear and Nonlinear Mixed Effects Models. R package version 3.1-131. (accessed 19 July 2018). < https://cran.r-project.org/web/packages/nlme/index.html > .

Core Team, R., 2017. R: A language and environment for statistical computing (accessed 19 July 2018). R Foundation for Statistical Computing, Vienna, Austria. https://www.R-project.org/.

Reich, P.B., Koike, T., Gower, S.T., Schoettle, A.W., 1995. Causes and consequences of variation in conifer leaf life-span. In: Smith, W.K., Hinckley, T.M. (Eds.), Ecophysiology of Coniferous Forests. Academic Press, New York, USA, pp. 225–254.

Ritóková, G., Shaw, D.C., Filip, G., Kanaskie, A., Browning, J., Norlander, D., 2016. Swiss needle cast in western Oregon Douglas-Fir plantations: 20-year monitoring results. Forests 7, 155.

Rosso, P.H., Hansen, E.M., 2003. Predicting Swiss needle cast disease distribution and severity in young Douglas-Fir plantations in coastal Oregon. Phytopathology 93, 790–798.

Shaw, D.C., Filip, G.M., Kanaskie, A., Maguire, D.A., Littke, W.A., 2011. Managing an epidemic of Swiss Needle Cast in the Douglas-Fir region of Oregon: The role of the Swiss Needle Cast Cooperative. J. Forest. 109 (2), 109–119.

Shaw, D.C., Woolley, T., Kanaskie, A., 2014. Vertical foliage retention in Douglas-fir across environmental gradients of the western Oregon coast range influenced by Swiss needle cast. Northwest Sci. 88, 23–32.

Snedecor, G.W., Cochran, W.G., 1967. Statistical Methods, sixth ed. The Iowa State University Press, IA, USA.

Videira, S.I.R., Groenewald, J.Z., Nakashima, C., Braun, U., Barreto, R.W., de Wit, P.J.G.M., Crous, P.W., 2017. Mycosphaerellaceae – Chaos or clarity? Stud. Mycol. 87, 257–421.

Wickham, H., 2009. ggplot2: Elegant Graphics for Data Analysis. Springer-Verlag, New York.

Wickham, H., Francois, R., Henry, L., Müller, K., 2017. dplyr: A Grammar of Data Manipulation. R package version (7), 4. (accessed 19 July 2018). https://CRAN.R-project.org/package=dplyr.

Zhao, J., Maguire, D.A., Mainwaring, D.B., Kanaskie, A., 2012. Climatic influences on needle cohort survival mediated by Swiss needle cast in coastal Douglas-fir. Tree 26, 1361–1371.

Increased streamflow in catchments affected by a forest disease epidemic

Kevin D. Bladon [a,*], Sharon Bywater-Reyes [a,b], Jared M. LeBoldus [a,c], Susanna Keriö [c], Catalina Segura [a], Gabriela Ritóková [a], David C. Shaw [a]

[a] Department of Forest Engineering, Resources, and Management, 280 Peavy Hall, 3100 SW Jefferson Way, Oregon State University, Corvallis, OR 97331, USA
[b] Department of Earth and Atmospheric Sciences, University of Northern Colorado, 501 20th St Box 100, Greeley, CO, 80639, USA
[c] Department of Botany and Plant Pathology, 2082 Cordley Hall, 2701 SW Campus Way, Oregon State University, Corvallis, OR 97331, USA

HIGHLIGHTS

- The Swiss needle cast (SNC) epidemic in the Oregon Coast Range affects Douglas-fir.
- We quantified long-term effects (1990–2015) of SNC on catchment hydrology.
- Runoff ratios (RRs) increased in catchments with >10% area infected by SNC.
- No change in RRs in severely infected catchments related to compensatory transpiration or abiotic evaporation.
- This study is the first to link forest disease to long-term streamflow changes.

GRAPHICAL ABSTRACT
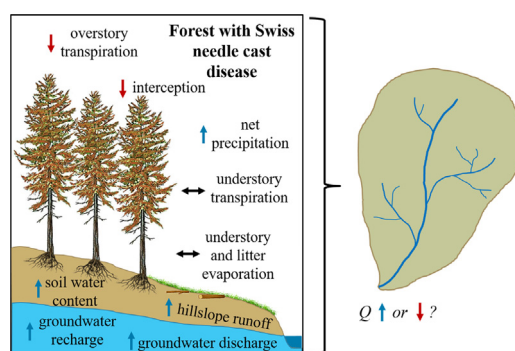
ARTICLE INFO

ABSTRACT

Natural disturbances help maintain healthy forested and aquatic ecosystems. However, biotic and abiotic disturbance regimes are changing rapidly. For example, the Swiss needle cast (SNC) epidemic in the Coast Range of Oregon in the U.S. Pacific Northwest has increased in area from 53,050 to 238,705 ha over the 1996–2015 period. We investigated whether the hydrologic regime (i.e., annual streamflow, runoff ratio, and magnitude and timing of peak flows and low flows) was affected by SNC in 12 catchments in western Oregon. The catchments ranged in size from 183 to 1834 km^2 and area affected by SNC from 0 to 90.5%. To maximize the number of catchments included in the study, we analyzed 20 years of SNC aerial survey data and 15–26 years of stream discharge (Q) and PRISM precipitation (P) and air temperature (T_{air}) data to test for trends in hydrologic variables for each catchment. As expected, we found that runoff ratios (Q/P) increased in five catchments, all with an area impacted by SNC >10%. This was likely due to the effects of SNC on the hydraulic architecture (i.e., needle retention, sapwood area, sapwood permeability) of affected trees, leading to decreased canopy interception and transpiration losses. Interestingly, two catchments with the greatest area affected by SNC showed no changes in hydrologic regime. The lack of hydrologic response could either be due to compensatory transpiration by vegetation unaffected by the disease or sub-canopy abiotic evaporation, which counteracted reductions in transpiration. This study is the first to illustrate that chronic canopy disturbance from a foliage pathogen can influence catchment scale hydrology.

© 2019 Elsevier B.V. All rights reserved.

* Corresponding author at: 280 Peavy Hall, College of Forestry, Oregon State University, Corvallis, OR 97331, USA.
  E-mail address: bladonk@oregonstate.edu (K.D. Bladon).

1. Introduction

Natural disturbances are key for maintaining healthy forested ecosystems, but globally, disturbance regimes are changing rapidly (Allen et al., 2015; Raffa et al., 2008; Seidl et al., 2016; Sommerfeld et al., 2018; Turner, 2010). Recent evidence suggests increases in the occurrence, intensity, and severity of many of the major forest disturbance agents, including droughts (Allen et al., 2010; Dai, 2013), wildfire (Flannigan et al., 2009, 2013), insect outbreaks (Kurz et al., 2008; Logan et al., 2003), and disease (Mildrexler et al., 2019; Woods et al., 2016; Wyka et al., 2017). As such, rapid and widespread declines in tree growth rates and elevated tree mortality have emerged as phenomenon affecting forests in many parts of the world (Allen et al., 2015; Cohen et al., 2016; Seidl et al., 2017; Sommerfeld et al., 2018; van Mantgem et al., 2009). Intensification in disturbance regimes has raised concerns about maintenance of biological diversity and risks to ecosystem services from forests, including provision of natural storage, filtration, and supply of water (Allen et al., 2010; Bladon et al., 2014; Robinne et al., 2018; Thom and Seidl, 2016).

Disturbances affecting forest canopy composition and structure can have extensive impacts on forest hydrology (Adams et al., 2012; Hallema et al., 2017). A principle hydrologic response to a loss of forest canopy cover or leaf area is a decline in canopy interception storage capacity, resulting in more precipitation (i.e., throughfall) reaching the soil surface (Boon, 2012; Varhola et al., 2010). Disturbances that result in partial or complete removal of the forest canopy can also reduce catchment-scale transpiration (Bearup et al., 2014; Maxwell and Condon, 2016). These changes in hydrological processes can lead to increases in soil moisture (Mikkelson et al., 2013) and groundwater recharge (Bent, 2001). Thus, close to a century of hydrology research has illustrated increases in net precipitation after forest disturbance, producing more annual streamflow, as well as elevated peak flows and summer low flows, in the first few years after the disturbance (Bates and Henry, 1928; Bethlahmy, 1974; Bosch and Hewlett, 1982; Brown et al., 2005; Hallema et al., 2018b; Stednick, 1996). Such shifts in annual water yields have important implications for source water quality from forests, increasing delivery of sediment, carbon, and nutrients to streams (Emelko et al., 2011, 2016). Moreover, disturbance effects on water yields can cause both immediate and longer-term effects on aquatic ecosystem health (Hicks et al., 1991; Silins et al., 2014).

Hydrologic responses to disturbances can be highly variable due to catchment differences in forest type, soils, geology, topography, climate, and hydrologic regime (e.g., rain-dominated versus snow-dominated) (Brown et al., 2005). In part, the hydrologic response will also depend on the type of disturbance and the nature of its damaging properties (e.g., frequency, magnitude, and severity) (Mirus et al., 2017; Poff, 1992). Temporally, disturbances may affect ecosystems in a pulse, press, or ramp manner, resulting in disparate effects on hydrologic processes and timescales of recovery (Lake, 2000). Pulse disturbances, which are abrupt or acute, such as a wildfire, landslide, earthquake, or forest harvest, tend to produce the most dramatic hydrologic responses, increasing annual water yields, peak flows, and low flows in the first few years after the disturbance (Ebel and Mirus, 2014; Hallema et al., 2018a; Mirus et al., 2017). Comparatively, press and ramp disturbances, which are stressors that are more gradual, often result in a progressive reduction in leaf area or forest canopy without an immediate soil disturbance (Biederman et al., 2014). The continual or persistent impacts on the forest canopy associated with these forest disturbances may have a less immediate impact on soil water content and result in a muted and difficult to detect streamflow signal (Adams et al., 2012; Mikkelson et al., 2013). As a result, research on the hydrologic effects of press or ramp disturbances, such as bark beetle or forest pathogen outbreaks, have largely been ignored compared to the more dramatic pulse disturbances.

Swiss needle cast (SNC) is a foliar disease specific to Douglas-fir (*Pseudotsuga menziesii*), which is caused by the fungus *Nothophaeocryptopus gaeumannii*. It is the most damaging foliage disease of coastal Douglas-fir in the U.S. Pacific Northwest (Hansen et al., 2000; Shaw et al., 2011). Recent analysis of annual aerial detection surveys in coastal Oregon indicated a substantial increase in area affected—from 53,050 ha in 1996 to 238,705 ha in 2015 (Fig. 1) (Ritóková et al., 2016). SNC is an ideal example of a press disturbance—its impacts are gradual and can be sustained over decades (Hansen et al., 2000; Maguire et al., 2011; Shaw et al., 2011). Trees infected with the SNC pathogen, *N. gaeumannii*, suffer from chronic stomatal occlusion, leading to reduced needle retention, annual growth rates (i.e., less sapwood area), and sapwood permeability (i.e., increased proportion of latewood in functional sapwood) (Johnson et al., 2005; Manter et al., 2000; Manter and Kavanagh, 2003) (Fig. 2). In theory, these shifts in hydraulic architecture of trees affected by SNC should result in a reduction in forest stand transpiration, leading to increased soil moisture and catchment-scale runoff. However, a recent study following another press disturbance—mountain pine beetle—quantified increased abiotic evaporation, which surprisingly counteracted reductions in transpiration, resulting in no streamflow response (Biederman et al., 2014). Thus, the effects of SNC on streamflow response at the larger catchment scale relevant to water resources, remains uncertain.

The limited number of studies on the hydrologic effects of chronic disturbances, such as SNC disease, hinder predictions of streamflow responses. Moreover, the limited spatial scale (e.g., stand, hillslope) of many studies creates challenges for understanding the potential hydrologic response at the catchment scale, which is the primary decision-making unit of forest watershed managers. Here, we evaluated 20 years of SNC, precipitation, and streamflow data from 12 watersheds along the Oregon Coast Range to answer the question: *to what degree does the chronic press disturbance of SNC affect catchment hydrologic regime (i.e., annual streamflow, runoff ratio, and magnitude and timing of peak flows and low flows)?*

2. Materials and methods

2.1. Study area description

The study area consisted of 12 catchments located in the Coast Range ecoregion of western Oregon (Fig. 3). The catchments ranged in size from 183 to 1834 km^2 (Table 1). Across the study area the climate is maritime with mild winter temperatures and prolonged periods of clouds. The mean daily air temperature across the study catchments ranges between 3.3 and 6.1 °C in January and 16.9–19.1 °C in July. Diurnal temperature fluctuations are narrow, ranging from 6 to 10 °C in a day. Mean annual precipitation is mostly rain and ranges from
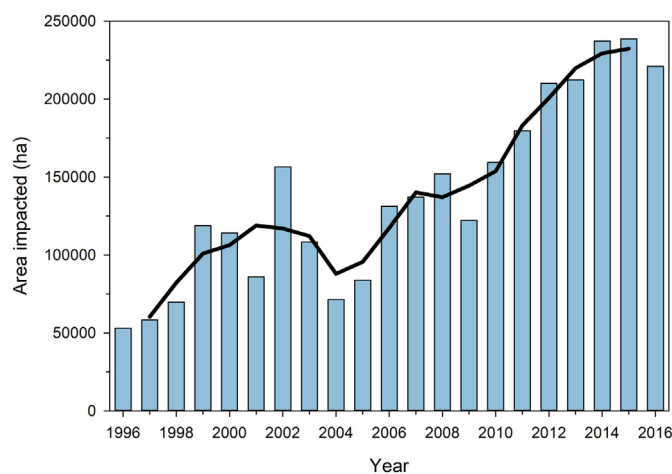

Fig. 1. Annual area (1996–2016) of Douglas-fir forests impacted by Swiss needle cast disease in the Oregon Coast Range as determined from aerial surveys. The solid line represents the rolling three-year average.
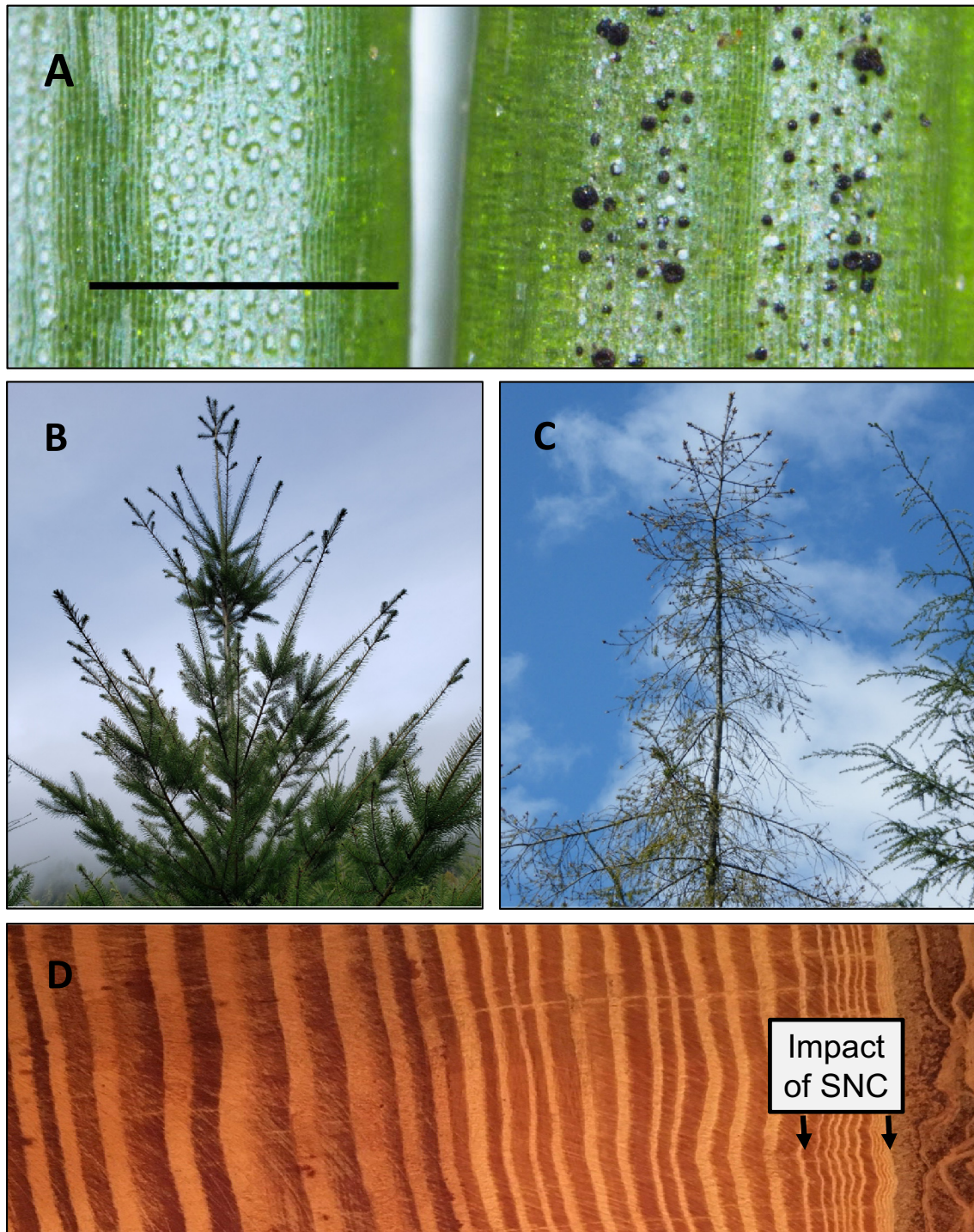
Fig. 2. Symptoms caused by the fungus *Nothophaeocryptopus gaeumannii*, the causal agent of Swiss needle cast. (A) The stomata of a healthy needle on the left and an infected needle on the right with stomatal occlusion due to the pseudothecia (scale bar 0.5 mm). (B) A healthy Douglas-fir will suffer from (C) reduced needle retention due to the occlusion of stomata. The reduced photosynthesis due to occlusion of stomata caused by the infection results in reduced radial growth, which can be observed as thinner annual growth rings. (D) Growth rings from an infected Douglas-fir, with normal growth before the infection and thinner radial growth rings after the infection (indicated with arrows).

~1300–3100 mm across the region, with 75–85% falling between October 1 and March 31 (PRISM Climate Group, 2004).

Two forest types dominate the ecoregion. The Sitka spruce (*Picea sitchensis*) zone is immediately adjacent to the coast, but transitions into the western hemlock (*Tsuga heterophylla*) zone as the maritime influence decreases and elevation increases. In the *Picea sitchensis* zone, soils are typically deep, fine textured, and relatively rich. The major great soil group is Haplohumults (Soil Survey Staff, 2017). The surface soils are high in organic matter, typically acidic, high in total nitrogen, and low in base saturation. In the western hemlock zone, soils are moderately deep with medium acidity. The soils surface horizons are well aggregated and porous with high organic matter content. The majority of the soils in this zone have a sandy loam to clay loam texture. There are a wider variety of great soils groups in this zone compared to the coastal areas, including Dystrochrepts, Haplumbrepts, and Haplohumults. Much of this zone has been logged or burned during the last 150 years and is now dominated by early- to mid-seral Douglas-fir forests, managed as short rotation timber farms.
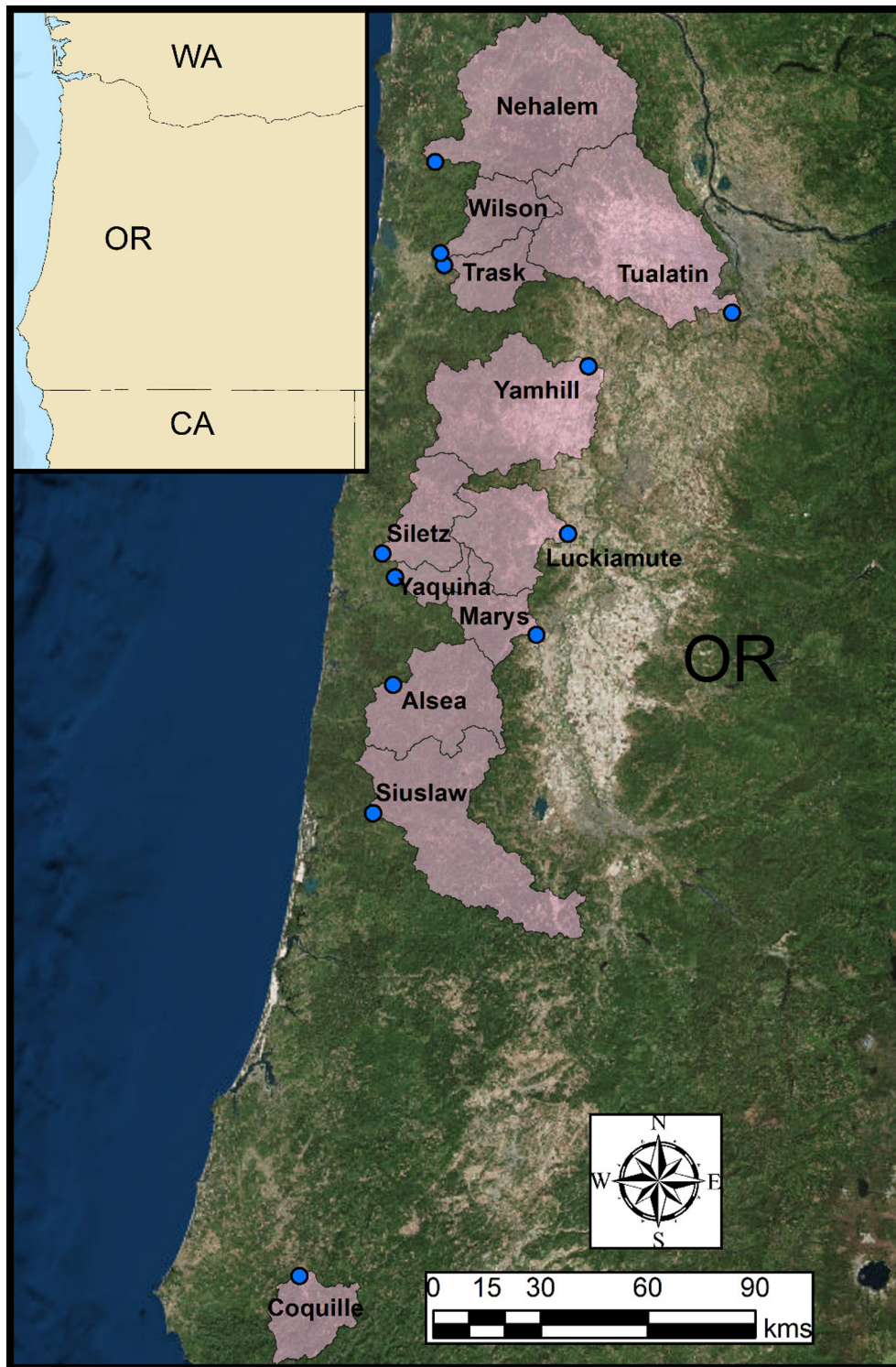
Fig. 3. Study catchments in western Oregon (outlined) impacted by Swiss needle cast with streamflow gauging sites (blue dots at gauges). (For interpretation of the references to colour in this figure legend, the reader is referred to the web version of this article.)

2.2. Swiss needle cast data

The Oregon Department of Forestry and the U.S. Forest Service have conducted annual aerial detection surveys for the presence of visible symptoms (chlorotic foliage) of SNC in the Oregon Coast Range from 1996 to present (USDA Forest Service, 2017). The surveyed area includes the Columbia River in northern Oregon south to the California border. It also extends east from the coastline until obvious symptoms are no longer visible. The area included in the survey in western Oregon is approximately 1.5-million ha. The survey provides a conservative estimate of the impact of the disease, as only those stands with moderate and severe damage were identified. For the purposes of this study, SNC annual survey data from 1996 to 2015 (20 years) were classified in a binary manner—polygons were classified as either "SNC affected" or "SNC unaffected" (Oregon Department of Forestry, 2017). We calculated the percentage of catchment affected by SNC for each year of the study

Table 1
Catchment physiographic characteristics.

USGS site no.	Station name	# Years of data	% SNC[b]	Drainage Area[c] (km²)	Relief[c] (m)	Mean Elevation[c] (m)	Mean Slope[c] (°)
14306030[a]	Yaquina River near Chitwood	26	90.5	183	806	187	17
14305500	Siletz River at Siletz	26	58.4	526	1052	400	18
14302480	Trask R. above Cedar Ck, near Tillamook	19	43.1	374	1054	504	22
14301500	Wilson River near Tillamook	26	26.7	418	1103	509	59
14306500	Alsea River near Tidewater	26	16.5	857	1234	321	19
14301000	Nehalem River near Foss	26	14.5	1744	1111	359	14
14171000	Marys River near Philomath	15	10.8	393	1174	291	12
14194150	South Yamhill River at McMinnville	21	7.2	1358	1058	232	12
14190500	Luckiamute River near Suver	26	4.8	623	958	271	11
14307620	Siuslaw River near Mapleton	19	3.3	1529	1024	292	19
14325000	South Fork Coquille River at Powers	26	1.0	443	1179	653	19
14207500	Tualatin River at West Linn	26	0	1834	1041	195	8

[a] Maintained by Oregon Water Resource Department.
[b] Percent area of SNC calculated in ArcMap 10.2.2 as the total footprint of area affected 1996–2016 from Oregon Department of Forestry Forest Health Aerial Surveys (Oregon Department of Forestry, 2017).
[c] Watershed attributes from StreamStats.

after union of SNC polygons and watershed polygons using the *union* function from the 'raster' package (Hijmans et al., 2016) in R 3.4.0 (R Core Team, 2016). All shapefiles were read into R with the *readOGR* function of the 'rgdal' package (Bivand et al., 2017).

2.3. Hydrometric data

We analyzed streamflow data from 11 U.S. Geological Survey (USGS) and one Oregon Water Resources Department (12 total) gauging sites draining catchments in the Oregon Coast Range (Table 1). Sites were selected based on their record length (minimum 15 yrs. of discharge data), catchment size (>100 km²), and area of the catchment affected by SNC (>1%). For catchments with the minimum 15 years of discharge data, we included as many preceding years as possible (back to 1990) to strengthen time trend analysis, while maximizing the number of catchments to include in the analysis. This resulted in the inclusion of catchments with discharge data spanning 15–26 years. One catchment (Tualatin River, USGS No. 14207500), adjacent to the SNC-affected catchments, was included as an undisturbed reference. We analyzed all hydrometric data according to the water year (October–September). Annual discharge was calculated for each catchment from the mean daily streamflow values, which were imported into R with the 'dataRetrieval' package (Hirsch and De Cicco, 2015). We normalized the volumetric discharge data by drainage area from each catchment. Drainage area and other geospatial attributes (e.g., geology, soils, topography) of catchments were obtained from Gages-II: Geospatial Attributes of Gages for Evaluating Streamflow (Falcone, 2011).

We used the spatial climate dataset from the PRISM Climate Group to determine the annual precipitation (*P*) and annual air temperature (T_{air}) for each catchment (PRISM Climate Group, 2004). As the PRISM climate data were more complete and longer than the discharge records, we used the most comprehensive data range possible for our study catchments, which included 1990–2015. Annual *P* and T_{air} were calculated from extracted (Hijmans et al., 2016) raster values obtained from the *get_prism_monthlys* function of the 'prism' package (Hart et al., 2015). Mean monthly air temperatures were calculated as the mean of monthly minimum and maximum air temperatures estimated for each catchment. We calculated mean annual temperatures as the average of the mean monthly air temperatures.

We estimated annual potential evapotranspiration (PET) using the Thornthwaite equation, with monthly air temperature and the catchment location (i.e., latitude) (Black, 2007). Location (latitude and longitude) was determined with the *calcCentroid* function of 'PBSmapping' package (Schnute et al., 2017). We then calculated the annual runoff ratio for each catchment as the ratio between annual discharge (*Q*) and annual precipitation (*P*).

2.4. Data analysis

We tested for trends over time using the available data record (15–26 years) in each catchment for the following variables: annual discharge, annual minimum discharge, annual maximum discharge, two metrics of flow timing (timing of minimum flow and timing of maximum flow), annual precipitation, annual runoff ratio (*Q/P*), annual ET (mass balance), annual air temperature (T_{air}), and annual PET (Thornthwaite). Because of autocorrelation, which creates inaccurate assessments of the significance of a trend, we used the Yue-Pilon method to remove serial correlation from time series by pre-whitening (Yue et al., 2002). Trends were detected with the *zyp.trend.vector* function of library 'zyp', which computes Sen's slope and performs the rank-based, non-parametric Mann-Kendall (MK) statistical test for significance (Bronaugh and Werner, 2013).

As a more in-depth analysis of factors contributing to detected changes in runoff ratio, we conducted a separate analysis predicting

Table 2
Mean annual precipitation, streamflow, runoff ratio, January air temperature, and July air temperature by catchment for study period.

| USGS site no.	Station name	Mean annual *P* (mm)	Mean annual *Q* (mm)	Mean runoff Ratio (*Q/P*)	Jan. T_{air} (°C)	Jul. T_{air} (°C)
14306030	Yaquina River near Chitwood	1735	1192	0.68	5.6	17.2
14305500	Siletz River at Siletz	2802	2467	0.88	4.6	16.8
14302480	Trask River above Cedar Creek, near Tillamook	2960	2173	0.73	3.3	17.0
14301500	Wilson River near Tillamook	3153	2542	0.81	3.1	16.8
14306500	Alsea River near Tidewater	2063	1415	0.68	5.0	18.2
14301000	Nehalem River near Foss	2325	1360	0.58	3.3	16.7
14171000	Marys River near Philomath	1741	828	0.47	4.3	18.1
14194150	South Yamhill River at McMinnville	1721	1134	0.64	4.5	18.5
14190500	Luckiamute River near Suver	1871	1174	0.62	4.2	18.3
14307620	Siuslaw River near Mapleton	1606	1049	0.65	5.2	18.9
14325000	South Fork Coquille River at Powers	2012	1504	0.73	6.0	18.2
14207500	Tualatin River at West Linn	1287	736	0.55	4.2	18.8
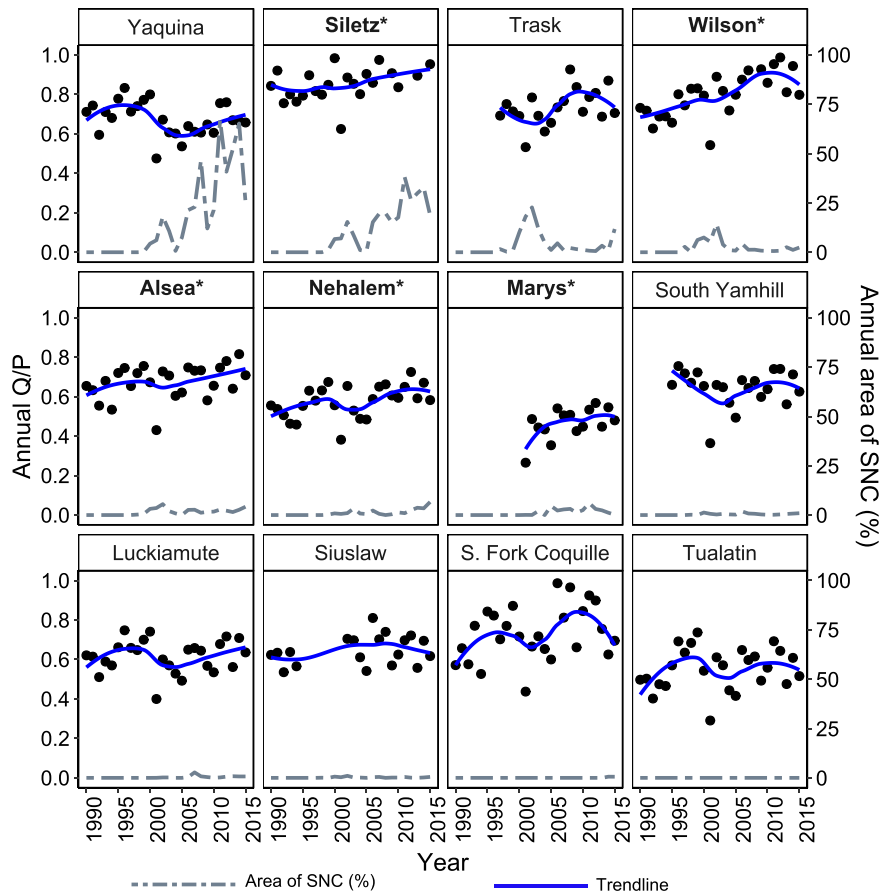
Fig. 4. Annual runoff ratios (Q/P) (dots), smoothed trend (blue line), and SNC coverage (%) (grey dashed line) from 1990 to 2015 for the 12 study catchments. If no SNC polygons were mapped, 0% SNC was assumed. * = Significant changes in Q/P. (For interpretation of the references to colour in this figure legend, the reader is referred to the web version of this article.)

runoff ratio by potential predictors with autoregressive moving average (ARIMA) models. We constructed candidate models predicting runoff ratio (Q/P) by PET, % SNC, or both PET and % SNC and a null model for each site with the exception of the Tualatin River catchment (USGS 14207500), which was not impacted by SNC and served as a reference. For the Tualatin River catchment, we considered a null model and one including PET. Models were developed using the *auto.arima* function of the 'forecast' package, which constructs ARIMA models (Hyndman and Khandakar, 2008). Akaike Information Criterion was used to compare models, where the lowest AIC model, and reduction of AIC of less than four (ΔAIC <4) is preferred (Akaike, 1974; Burnham and Anderson, 2002; Mazerolle, 2017).

2.5. Gradient nearest neighbor vegetation data

To determine potential vegetation structure and composition changes coincident with SNC disturbance, we used annual Gradient Nearest Neighbor (GNN) spatial biomass estimates provided by Landscape Ecology, Modeling, Mapping, & Analysis (LEMMA; USDOI, USGS, 2019). The digital GNN product provides an estimate of vegetation cover and species by combining field data, statistical modeling, remotely-sensed time-series imagery, and small-footprint LiDAR data at 30-m resolution (LEMMA; USDOI and USGS, 2019). Within the model, we used the vegetation class change variable, where classifications were categorical and based on dominant species composition

Table 3
Statistical results from the trend analysis of runoff ratios (Q/P). Catchments with p < .05 are bolded.

USGS site no	Station name	Intercept of Sen's slope	Sen's slope (Q/P per year)	lbound	ubound	Kendall's tau	Kendall's p-value	Least squares trend	% SNC	Years data
14306030	Yaquina River near Chitwood	0.718	−0.0027	−0.0073	0.0025	−0.1467	0.315	−0.0030	90.5	26
14305500	Siletz River at Siletz	0.761	0.0079	0.0038	0.0126	0.5333	<0.001	0.0080	58.4	26
14302480	Trask R. above Cedar Ck, near Tillamook	0.680	0.0071	−0.0012	0.0129	0.2549	0.150	0.0066	43.1	19
14301500	Wilson River near Tillamook	0.676	0.0107	0.0064	0.0151	0.5400	<0.001	0.0103	26.7	26
14306500	Alsea River near Tidewater	0.651	0.0040	−0.0006	0.0076	0.2933	0.042	0.0037	16.5	26
14301000	Nehalem River near Foss	0.521	0.0045	0.0011	0.0086	0.3000	0.038	0.0049	14.5	26
14171000	Marys River near Philomath	0.422	0.0072	−0.0005	0.0167	0.4286	0.037	0.0096	10.8	15
14194150	S. Yamhill River at McMinnville	0.667	−0.0018	−0.0073	0.0036	−0.1368	0.417	−0.0005	7.2	21
14190500	Luckiamute River near Suver	0.616	0.0010	−0.0037	0.0054	0.0467	0.761	0.0008	4.8	26
14307620	Siuslaw River near Mapleton	0.630	0.0020	−0.0045	0.0099	0.1373	0.449	0.0026	3.3	19
14325000	S. Fork Coquille River at Powers	0.654	0.0050	−0.0034	0.0137	0.1267	0.388	0.0060	1	26
14207500	Tualatin River at West Linn	0.520	0.0029	−0.0045	0.0089	0.0733	0.624	0.0024	0	26

Table 4
Comparison of ARIMA models[a] predicting runoff ratio (Q/P) (Table 3). Models with moderate to strong evidence (p < .05) of a probable trend are bolded.

USGS Site No	Station Name	AIC Model 1	AIC Model 2	AIC Model 3	AIC Model 4	% SNC	Best Model
14306030	Yaquina R. near Chitwood	−51.70	−51.70	−49.81	−48.32	90.5	1
14305500	Siletz R. at Siletz	−40.88	−40.88	−53.42	−51.56	58.4	3
14302480	Trask R., near Tillamook	−34.20	−34.20	−34.94	−32.00	43.1	3
14301500	Wilson R. near Tillamook	−39.54	−39.54	−35.13	−37.47	26.7	1
14306500	Alsea R. near Tidewater	−51.04	−51.04	−49.86	−49.81	16.5	1
14301000	Nehalem R. near Foss	−45.40	−45.40	−53.02	−53.72	14.5	4
14171000	Marys R. near Philomath	−22.98	−22.98	−29.77	−29.37	10.8	3
14194150	South Yamhill R. at McMinnville	−37.90	−37.90	−36.19	−34.36	7.2	1
14190500	Luckiamute R. near Suver	−53.06	−53.06	−52.00	−50.58	4.8	1
14307620	Siuslaw R. near Mapleton	−41.34	−41.34	−43.34	−46.78	3.3	4
14325000	South Fork Coquille R. at Powers	−26.06	−26.06	−24.71	−29.03	1	4
14207500	Tualatin R. at West Linn	−40.07	−40.07	NA	NA	0	1

[a] Model 1 = Q/P ~1, Model 2 = Q/P ~PET, Model 3 = Q/P ~% SNC, Model 4 = Q/P ~PET + % SNC.

(e.g., broadleaf, conifer, mixed), canopy cover, quadratic mean diameter of all dominant and codominant trees, and basal area of live trees and Douglas-fir. The dominant class was determined for each watershed polygon per year using zonal statistics in ArcMap 10.5. As a more detailed investigation, we considered separately the spatial average of canopy cover of live trees by watershed polygon per year. Because GNN vegetation structure (class) data are considered more reliable than composition (species) data, we used this analysis to provide insights into potential vegetation changes. Additional research is required to determine vegetation structure and composition changes with the spread of SNC disease.

3. Results

Over the 20-years (1996–2015) of available aerial surveys in the Coast Range of Oregon, Swiss needle cast (SNC) disease increased by approximately 4.2-times (Fig. 1) (Ritóková et al., 2016). However, this response was spatially heterogeneous across the region. We captured that variability in our study catchments, with the area impacted by SNC ranging from 1.0 to 90.5% (Table 2; Fig. 4). The hydrologic variables were also highly variable across study catchments. Mean annual precipitation ranged from 1300 mm (Tualatin River) to 3100 mm (Wilson River; Table 2). Mean annual discharge was generally correlated with precipitation trends (Fig. S1), with the lowest discharge (0.7 m) for Tualatin and highest for Wilson (2.5 m). The mean annual runoff ratios (Q/P) ranged from 0.48 to 0.88 (Table 2).

Trend analysis of the primary climatic variables across the period of record available for each (15–26 years) of the study catchments indicated relatively stable trends. Specifically, there was no evidence for trends in annual precipitation (p = .11–.98; Table S1), air temperature (p = .16–.90; Table S2), or potential evapotranspiration (p = .21–.98; Table S3). Despite no evidence for trends in climatic variables, there was strong evidence (p < .01) for decreasing trends in actual ET in six of the study catchments (Table S4). Interestingly, there was also suggestive evidence (p = .10) for an increasing trend in ET in the Yaquina River catchment, which was the most severely affected by SNC (Table S4).

Table 5
ARIMA model results for five sites with significant Q/P trends (P < .05), showing coefficients for modeling including % SNC as well as % SNC + PET.

USGS site no	Station name	Arima	% SNC	Coefficients PET+% SNC	
				PET	% SNC
14305500	Siletz River at Siletz	(0,0,0)	0.006	−2.00E−04	0.0059
14301500	Wilson River near Tillamook	(0,1,0)	0.013	−8.00E−04	0.0089
14306500	Alsea River near Tidewater	(0,0,0)	0.010	−9.00E−04	0.0086
14301000	Nehalem River near Foss	(0,0,0)	0.010	−0.0012	0.017
14171000	Marys River near Philomath	(0,0,0)	0.013	6.00E−04	0.0153

Time trend analysis also provided moderate to strong evidence that the increase in area disturbed by SNC contributed to increases in runoff ratios (Q/P) in many of the Coast Range catchments in our study. Specifically, there was moderate evidence (.01 ≤ p < .05) for increases in three of the 12 study catchments with percent area impacted by SNC rising to 10.8 to 16.5% of the catchment by the end of the analysis period (Table 3). The runoff ratios in these catchments increased ~10% in Alsea, 13% in Nehalem, 14% in Marys over the analysis period. Comparatively, there was strong evidence (p < .001) that Q/P increased over the period of study in the Wilson River (26.7% SNC) and Siletz River (58.4%) catchments. The increases in Q/P in these more severely affected catchments increased by ~21% in Siletz and 27% in Wilson (Fig. 4).

The five catchments with increased Q/P were some of the more heavily impacted areas, with SNC disturbance covering >10% of the catchment area. All sites with a detectable trend in runoff ratio (p < .05) had preferred ARIMA models (lowest AIC) that included percent SNC, or had preferred models indistinguishable (ΔAIC <4) from ones including percent SNC (Table 4). The ARIMA models suggest positive coefficients for percent SNC, ranging from 0.006 to 0.017 Q/P y^{-1} (Table 5). These models predict an increase in runoff ratio of ~6–17% for a 10% area impacted by SNC. When included, PET had a small, usually negative coefficient, indicating more water loss with increasing PET. Comparatively, in five of the study catchments where there was no evidence for change in Q/P, the area of SNC disturbance was <10% (Tables 2 and 3).

However, increases in runoff ratios with increasing SNC disturbance were not observed in all catchments. Interestingly, there was no evidence for Q/P increases in two of the most heavily impacted catchments—the Yaquina River (91% SNC) or Trask River (43% SNC). For the Yaquina River catchment, in particular, there was suggestive evidence for an *increase* in ET over the analysis period (p < .10), despite presumably lower transpiration for SNC-impacted Douglas-fir in this watershed. General nearest neighbor (GNN) vegetation data suggest a structural or composition change in the forest type for Yaquina during 1990–2001, whereby composition changed from conifer-dominated to broadleaf-dominated, then back to conifer after 2001 (Fig. 5). The forest composition change back to conifer coincided with the first severe peak in SNC incidence in 2001–2002 (Fig. 3). After 2001–2002, and the peaks in the SNC epidemic in 2007–2008 and 2010–2014, GNN data for Yaquina indicated a gradual increase in total basal area of live trees along with decreasing basal area of Douglas-fir (Fig. 6). However, due to problems related to distinguishing Douglas-fir and other conifers based on aerial images, the changes in the basal area of Douglas-fir are speculative. The Luckiamute catchment had a similar trend in vegetation composition, changing from small/medium conifer to open, but then returned to small/medium conifer by the end of the study period (Fig. 5), accompanied by an increase in total basal area of live trees (Fig. 6). In contrast to Yaquina, this catchment had a low SNC footprint (5%) and no detectible changes in hydrologic variables (Tables 2 and 3).
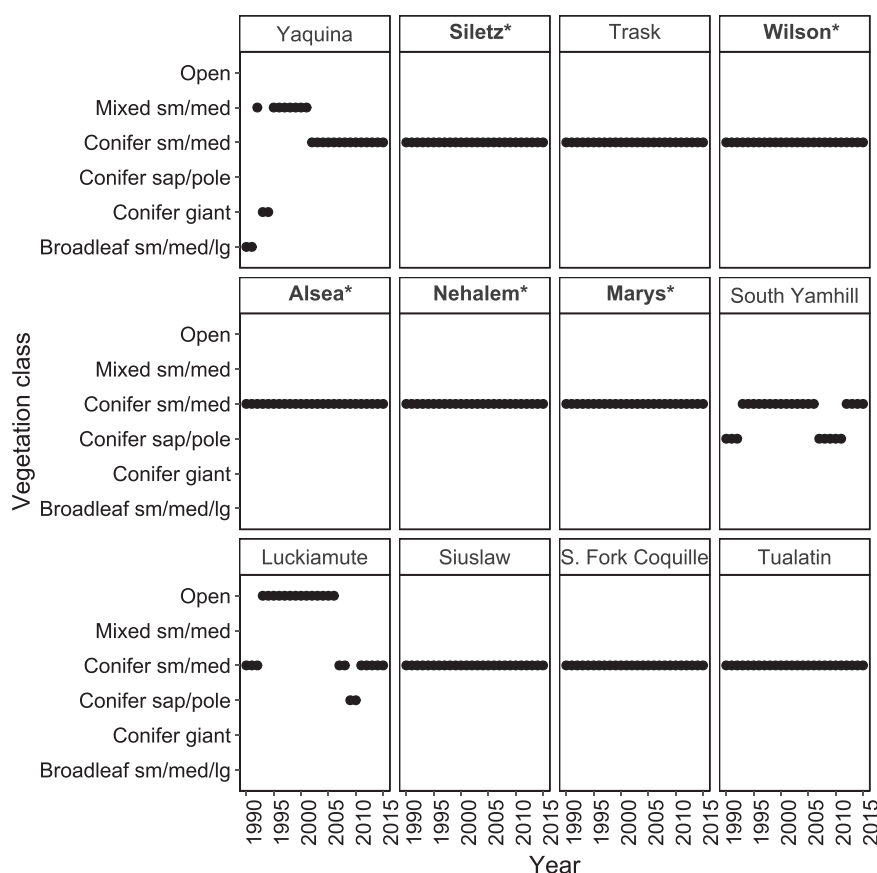
Fig. 5. Gradient Nearest Neighbor (GNN) estimates of vegetation class from 1990 to 2015 based on composition and structure for each study catchment. The Yaquina River catchment, which had the greatest area affected by Swiss needle cast had a change in vegetation class in 2001 to small (sm)/medium (med) conifers. * = Significant changes in Q/P.

For the Trask River catchment, which also had one of the highest areas disturbed by SNC, there was also no discernible trend in the runoff ratio. However, unlike the Yaquina catchment there was not any evidence from the GNN data of a structural change in the forest type. These negative results could be due to a number of factors, including (a) a muted response to the SNC press disturbance, (b) other activities or disturbances in the catchment, or (c) the coarse resolution of the GNN data, which may not have captured a compensatory vegetation response in this catchment.

Statistically, there was no evidence for trends in the timing of annual minimum (Table S6) or maximum (Table S7) streamflow in any of the 12 study catchments. Similarly, there was no evidence for trends in annual minimum (Table S8) or maximum (Table S9) discharge in 11 of the 12 study catchments. The lack of effects of SNC on streamflow timing and peak flows were not surprising in this wet, Mediterranean region where the majority of precipitation falls as rain during the winter, which is out of phase with the period of peak transpiration in this region. However, the lack of effect of SNC on low flows was surprising as the timing of these flows is coincident with the period of peak transpiration and likely peak effects of SNC on affected Douglas-fir. We postulate that the lack of observable effect on low flows is likely due to the coarseness of the available streamflow data, but this requires further investigation to provide more robust evidence to support or refute.

4. Discussion

This study was the first to document a catchment scale hydrologic response to a forest pathogen, *Nothophaeocryptopus gaeumannii*, which causes Swiss needle cast (SNC), the most damaging foliage disease of coastal Douglas-fir in the U.S. Pacific Northwest. Our analysis demonstrates an increase in runoff ratio proportional to the area of

the catchment affected by SNC. In general, we identified a threshold of ~10% SNC beyond which streamflow increased in a manner proportional to the area affected by the disease. The increased streamflow in catchments impacted by SNC is likely a result of the chronic effects of the disease on the hydraulic architecture (i.e., reduced needle retention, sapwood area, and sapwood permeability) of the affected trees (Manter et al., 2000; Manter and Kavanagh, 2003; Shaw et al., 2011). At a catchment scale, these effects would decrease interception and transpiration losses, potentially leading to increased soil water storage, groundwater recharge, and runoff (Fig. 7A) (Nijzink et al., 2016; Phillips et al., 2016). Although, increased streamflow after vegetation removal by a pulse disturbance (e.g., wildfire, forest harvest) has been well established (Bates and Henry, 1928; Bethlahmy, 1974; Bosch and Hewlett, 1982; Brown et al., 2005; Stednick, 1996), this is the first evidence of a similar but more nuanced trend in streamflow caused by a more gradual disturbance—a forest disease.

A second pattern we revealed with our analysis was a lack of streamflow response in the catchments most severely affected by SNC. For instance, the Yaquina River catchment had the greatest area affected by SNC (90.5%), yet we did not observe any changes in runoff ratios. This nuance illustrates the difficulty in predicting the response of streamflow to forest cover change, in part, due to high variability in subsurface storage and differential forest access to available water (McDonnell et al., 2018).

While observations of hydrologic processes were beyond the scope of this project, we posit a couple explanations for the lack of streamflow response, which could be studied further. It is plausible that compensatory transpiration by understory or co-dominant vegetation that wasn't affected by the SNC pathogen may have contributed to the lack of change in streamflow in the heavily impacted catchments (Fig. 7B) (Biederman et al., 2015; Bladon et al., 2006; Reed et al., 2014). In
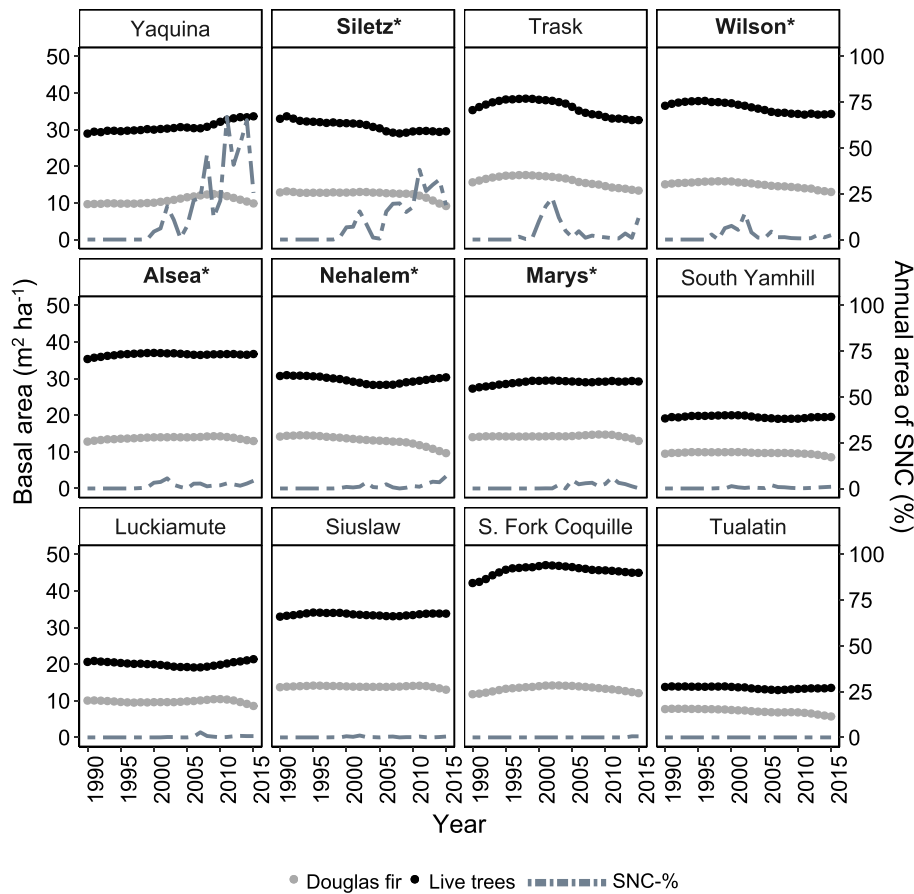
Fig. 6. Annual total basal areas (m² ha⁻¹) for live trees (black dots) and Douglas-fir (grey dots), and SNC coverage (%) (grey dashed line) from 1990 to 2015 for the 12 study catchments. If no SNC polygons were mapped, 0% SNC was assumed. * = Significant changes in Q/P.

catchments severely affected by SNC, like the Yaquina, understory trees (e.g., western hemlock, hardwood species) may increase their transpiration rates and outcompete the weakened Douglas-fir causing increased mortality (Maguire et al., 2011). We also observed evidence for compensatory transpiration and increased growth rates in the spatial biomass data (GNN), where total basal area increased in the Yaquina catchment, despite the high SNC footprint (Fig. 5; Fig. 6). This potential explanation for the lack of streamflow response is also consistent with previous observations that younger trees (unaffected understory trees) tend to have higher rates of evapotranspiration due to several physiological differences from older, overstory trees (e.g., higher sapwood area, higher sapflow per unit sapwood area, higher concentration of leaf area in the upper canopy, less ability to limit transpiration) (Moore et al., 2004; Perry and Jones, 2017).

However, it is also plausible that increased abiotic evaporation may have offset the overall reductions in transpiration by affected Douglas-fir, constraining the expected streamflow increases (Fig. 7B) (Biederman et al., 2014, 2015). Specifically, reduced canopy shading in catchments most severely impacted by SNC could lead to increased incident shortwave radiation, wind speed, and vapor pressure deficit, resulting in increased evaporation and limited water availability (Grant et al., 2013; Kaiser et al., 2013). For forest and water resource managers to make informed decisions in response to SNC, future research should quantify the relative role of vegetation feedbacks or subcanopy vapor loss effects on runoff ratios in catchments chronically impacted by SNC.

The final pattern we observed was no observable changes in ET or runoff in the absence of SNC or under low SNC occurrence (<10% of catchment area) (Fig. 4). Moreover, we did not observe any detectable

trends in precipitation or potential evapotranspiration over the period of study. These were important contextual observations for the first two major findings from this research, suggesting that the changes in runoff ratio we observed were predominantly a result of the SNC epidemic in the Oregon Coast Range and not due to climatic factors. However, it is important to note that there may be slight changes in catchment storage and runoff in catchments with low SNC occurrence, which are difficult to quantify, but could persist for long periods. As such combining observations from long-term gages with robust hydrologic models could provide valuable additional hydrologic forecasting (Penn et al., 2016).

Given that forest diseases, such as SNC, are likely to continue to increase globally (Seidl et al., 2017), the effects on water supply may become more pronounced with impacts to water quantity and aquatic ecosystem health. For example, pulse disturbances, such as timber harvest and wildfire, have been associated with changes in streamflow and suspended sediment (Bywater-Reyes et al., 2018; Wondzell and King, 2003), nutrient concentrations and yields (Rust et al., 2018; Vitousek and Melillo, 1979), with cascading impacts on fish populations (Silins et al., 2014). Similarly, chronic defoliation due to SNC could influence riparian shade, increasing stream temperature and overall aquatic ecosystem health (Kaylor and Warren, 2017; McCullough et al., 2009; Wondzell et al., 2019). In addition to stream impacts, press disturbances like SNC can affect soil moisture, soil temperature, and below-ground carbon allocation (Allen and Kitajima, 2013; Shi et al., 2019). As pressures on water supply and forest health continue to grow (Cohen et al., 2016; Vörösmarty et al., 2010), the corollary effects of foliar diseases in forests on merit further study.
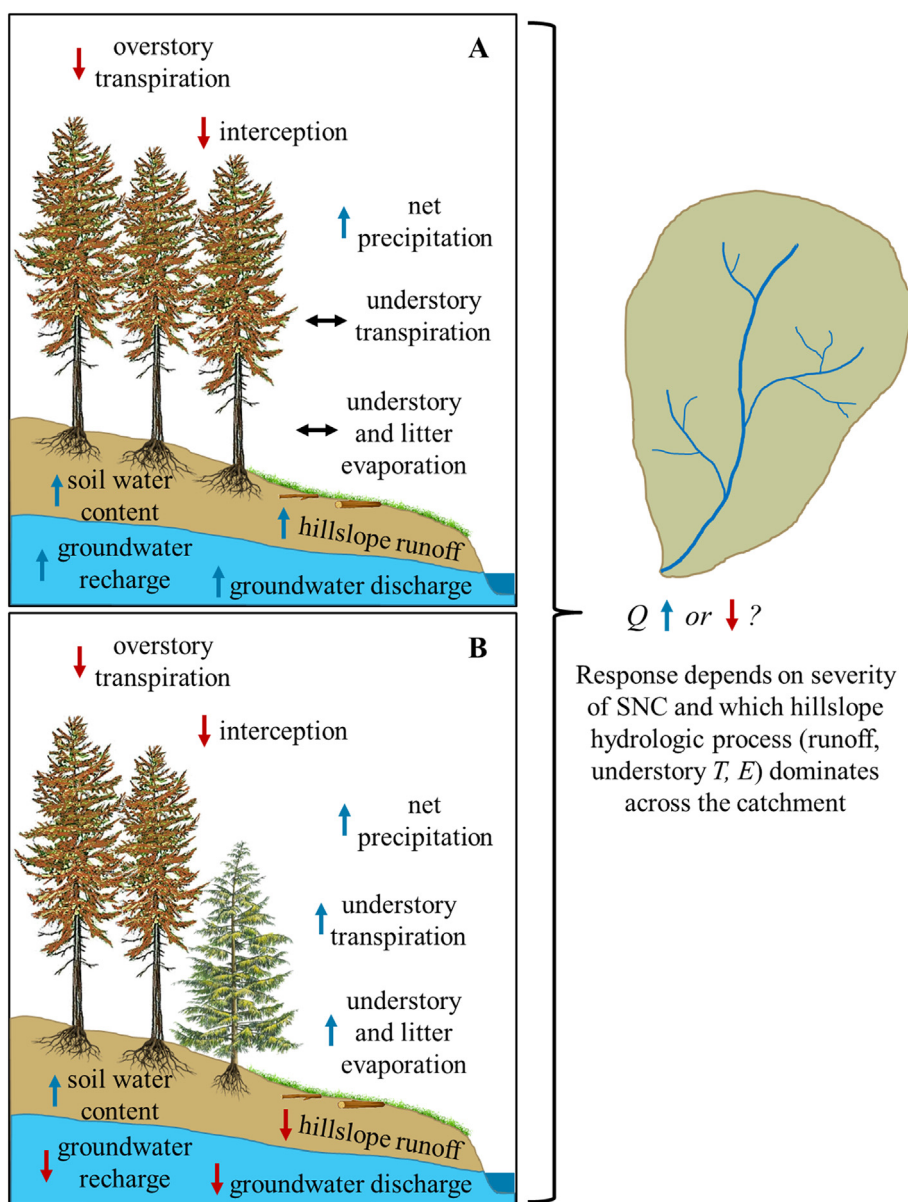
Fig. 7. Conceptual models of the effects of Swiss needle cast disease on hillslope hydrologic processes, resulting in differential streamflow responses at the catchment-scale. (A) Douglas-fir dominated stands affected by a moderate severity Swiss needle cast outbreak may experience increased hillslope runoff and groundwater discharge to streams, resulting in increased runoff ratios. (B) Mixed conifer-Douglas-fir stands severely impacted by Swiss needle cast disease may experience a compensatory growth response and elevated transpiration from understory tree species (e.g., hemlock) and/or elevated evaporation rates from the understory and litter layer, resulting in decreased runoff ratios.

5. Conclusions

We combined 20 years of SNC severity data and streamflow records from 12 catchments to demonstrate that a chronic, press disturbance can affect runoff ratios. In general, streamflow increased as the proportion of the catchment affected by SNC increased. The results also suggested that mixed species stands may be buffered against both the impact of the SNC disease and the changes in streamflow that it can cause. Faced with the increasing occurrence of forest disturbance and extreme weather phenomena driven by global climate change (Allen et al., 2010, 2015; Seidl et al., 2017), it may become increasingly important to switch the emphasis of forest management towards maximizing ecosystem resilience. Thus, forest management should favor genetically diverse mixed species stands, since they appear to be more resilient to SNC and other forest pathogens (Ennos, 2015; Mildrexler et al., 2019). Additionally, given the observed effect of SNC on runoff ratios, there may be associated effects on water quality (sediment, turbidity,

temperature, nutrients) with important implications for aquatic ecosystem health and downstream community drinking water supply that should be investigated in future research.

Supplementary data to this article can be found online at https://doi.org/10.1016/j.scitotenv.2019.07.127.

References

Adams, H.D., Luce, C.H., Breshears, D.D., Allen, C.D., Weiler, M., Hale, V.C., Smith, A.M.S., Huxman, T.E., 2012. Ecohydrological consequences of drought- and infestation-triggered tree die-off: insights and hypotheses. Ecohydrology 5, 145–159. https://doi.org/10.1002/eco.233.

Akaike, H., 1974. A new look at the statistical model identification. IEEE Trans. Autom. Control 19, 716–723. https://doi.org/10.1109/TAC.1974.1100705.

Allen, M.F., Kitajima, K., 2013. In situ high-frequency observations of mycorrhizas. New Phytol. 200, 222–228. https://doi.org/10.1111/nph.12363.

Allen, C.D., Macalady, A.K., Chenchouni, H., Bachelet, D., McDowell, N., Vennetier, M., Kitzberger, T., Rigling, A., Breshears, D.D., Hogg, E.H., Gonzalez, P., Fensham, R., Zhang, Z., Castro, J., Demidova, N., Lim, J.-H., Allard, G., Running, S.W., Semerci, A., Cobb, N., 2010. A global overview of drought and heat-induced tree mortality reveals emerging climate change risks for forests. For. Ecol. Manag. 259, 660–684. https://doi.org/10.1016/j.foreco.2009.09.001.

Allen, C.D., Breshears, D.D., McDowell, N.G., 2015. On underestimation of global vulnerability to tree mortality and forest die-off from hotter drought in the Anthropocene. Ecosphere 6, art129. https://doi.org/10.1890/ES15-00203.1.

Bates, C.G., Henry, A.J., 1928. Forest and Stream-flow Experiment at Wagon Wheel Gap, Colorado: Final Report, on Completion of the Second Phase of the Experiment. U.S. Government Printing Office.

Bearup, L.A., Maxwell, R.M., Clow, D.W., McCray, J.E., 2014. Hydrological effects of forest transpiration loss in bark beetle-impacted watersheds. Nat. Clim. Chang. 4, 481–486. https://doi.org/10.1038/nclimate2198.

Bent, G.C., 2001. Effects of forest-management activities on runoff components and ground-water recharge to Quabbin Reservoir, central Massachusetts. For. Ecol. Manag. 143, 115–129. https://doi.org/10.1016/S0378-1127(00)00511-9.

Bethlahmy, N., 1974. More streamflow after a bark beetle epidemic. J. Hydrol. 23, 185–189. https://doi.org/10.1016/0022-1694(74)90001-8.

Biederman, J.A., Harpold, A.A., Gochis, D.J., Ewers, B.E., Reed, D.E., Papuga, S.A., Brooks, P.D., 2014. Increased evaporation following widespread tree mortality limits streamflow response. Water Resour. Res. 50, 5395–5409. https://doi.org/10.1002/2013WR014994.

Biederman, J.A., Somor, A.J., Harpold, A.A., Gutmann, E.D., Breshears, D.D., Troch, P.A., Gochis, D.J., Scott, R.L., Meddens, A.J.H., Brooks, P.D., 2015. Recent tree die-off has little effect on streamflow in contrast to expected increases from historical studies. Water Resour. Res. 51, 9775–9789. https://doi.org/10.1002/2015WR017401.

Bivand, R., Keitt, T., Rowlingson, B., Pebesma, E., Sumner, M., Hijmans, R., Rouault, E., Warmerdam, F., Ooms, J., Rundel, C., 2017. rgdal: Bindings for the "Geospatial" Data Abstraction Library.

Black, P.E., 2007. Revisiting the Thornthwaite and Mather water balance. J. Am. Water Resour. Assoc. 43, 1604–1605. https://doi.org/10.1111/j.1752-1688.2007.00132.x.

Bladon, K.D., Silins, U., Landhäusser, S.M., Lieffers, V.J., 2006. Differential transpiration by three boreal tree species in response to increased evaporative demand after variable retention harvesting. Agric. For. Meteorol. 138, 104–119. https://doi.org/10.1016/j.agrformet.2006.03.015.

Bladon, K.D., Emelko, M.B., Silins, U., Stone, M., 2014. Wildfire and the future of water supply. Environmental Science & Technology 48, 8936–8943. https://doi.org/10.1021/es500130g.

Boon, S., 2012. Snow accumulation following forest disturbance. Ecohydrology 5, 279–285. https://doi.org/10.1002/eco.212.

Bosch, J.M., Hewlett, J.D., 1982. A review of catchment experiments to determine the effect of vegetation changes on water yield and evapotranspiration. J. Hydrol. 55, 3–23. https://doi.org/10.1016/0022-1694(82)90117-2.

Bronaugh, D., Werner, A., 2013. zyp: Zhang + Yue-Pilon Trends Package. Pacific Climate Impacts Consortium.

Brown, A.E., Zhang, L., McMahon, T.A., Western, A.W., Vertessy, R.A., 2005. A review of paired catchment studies for determining changes in water yield resulting from alterations in vegetation. J. Hydrol. 310, 28–61. https://doi.org/10.1016/j.jhydrol.2004.12.010.

Burnham, K.P., Anderson, D.R., 2002. Model Selection and Multimodel Inference: A Practical Information-theoretic Approach. 2nd ed. Springer-Verlag, New York.

Bywater-Reyes, S., Bladon, K.D., Segura, C., 2018. Relative influence of landscape variables and discharge on suspended sediment yields in temperate mountain catchments. Water Resour. Res. 54, 5126–5142. https://doi.org/10.1029/2017WR021728.

Cohen, W.B., Yang, Z., Stehman, S.V., Schroeder, T.A., Bell, D.M., Masek, J.G., Huang, C., Meigs, G.W., 2016. Forest disturbance across the conterminous United States from 1985–2012: the emerging dominance of forest decline. For. Ecol. Manag. 360, 242–252. https://doi.org/10.1016/j.foreco.2015.10.042.

Dai, A., 2013. Increasing drought under global warming in observations and models. Nat. Clim. Chang. 3, 52–58. https://doi.org/10.1038/nclimate1633.

Ebel, B.A., Mirus, B.B., 2014. Disturbance hydrology: challenges and opportunities. Hydrol. Process. 28, 5140–5148. https://doi.org/10.1002/hyp.10256.

Emelko, M.B., Silins, U., Bladon, K.D., Stone, M., 2011. Implications of land disturbance on drinking water treatability in a changing climate: demonstrating the need for "source water supply and protection" strategies. Water Res. 45, 461–472. https://doi.org/10.1016/j.watres.2010.08.051.

Emelko, M.B., Stone, M., Silins, U., Allin, D., Collins, A.L., Williams, C.H.S., Martens, A.M., Bladon, K.D., 2016. Sediment-phosphorus dynamics can shift aquatic ecology and

cause downstream legacy effects after wildfire in large river systems. Glob. Chang. Biol. 22, 1168–1184. https://doi.org/10.1111/gcb.13073.

Ennos, R.A., 2015. Resilience of forests to pathogens: an evolutionary ecology perspective. Forestry 88, 41–52. https://doi.org/10.1093/forestry/cpu048.

Falcone, J.A., 2011. Gages-II: Geospatial Attributes of Gages for Evaluating Streamflow (USGS Unnumbered Series). U.S. Geological Survey, Reston, VA.

Flannigan, M.D., Krawchuk, M.A., Groot, W.J. de, Wotton, B.M., Gowman, L.M., 2009. Implications of changing climate for global wildland fire. Int. J. Wildland Fire 18, 483–507. https://doi.org/10.1071/WF08187.

Flannigan, M., Cantin, A.S., de Groot, W.J., Wotton, M., Newbery, A., Gowman, L.M., 2013. Global wildland fire season severity in the 21st century. For. Ecol. Manag. 294, 54–61. https://doi.org/10.1016/j.foreco.2012.10.022.

Grant, G.E., Tague, C.L., Allen, C.D., 2013. Watering the forest for the trees: an emerging priority for managing water in forest landscapes. Front. Ecol. Environ. 11, 314–321. https://doi.org/10.1890/120209.

Hallema, D.W., Sun, G., Bladon, K.D., Norman, S.P., Caldwell, P.V., Liu, Y., McNulty, S.G., 2017. Regional patterns of postwildfire streamflow response in the Western United States: the importance of scale-specific connectivity. Hydrol. Process. 3, 1–17. https://doi.org/10.1002/hyp.11208.

Hallema, D.W., Robinne, F.-N., Bladon, K.D., 2018a. Reframing the challenge of global wildfire threats to water supplies. Earth's Future 6, 772–776. https://doi.org/10.1029/2018EF000867.

Hallema, D.W., Sun, G., Caldwell, P.V., Norman, S.P., Cohen, E.C., Liu, Y., Bladon, K.D., McNulty, S.G., 2018b. Burned forests impact water supplies. Nat. Commun. 9, 1307. https://doi.org/10.1038/s41467-018-03735-6.

Hansen, E.M., Stone, J.K., Capitano, B.R., Rosso, P., Sutton, W., Winton, L., Kanaskie, A., McWilliams, M.G., 2000. Incidence and impact of Swiss needle cast in forest plantations of Douglas-fir in coastal Oregon. Plant Dis. 84, 773–778. https://doi.org/10.1094/PDIS.2000.84.7.773.

Hart, E., Bell, K., Butler, A., 2015. PRISM: Access Data From the Oregon State PRISM Climate Project.

Hicks, B.J., Beschta, R.L., Harr, R.D., 1991. Long-term changes in streamflow following logging in western Oregon and associated fisheries implications. J. Am. Water Resour. Assoc. 27, 217–226. https://doi.org/10.1111/j.1752-1688.1991.tb03126.x.

Hijmans, R.J., van Etten, J., Sumner, M., Cheng, J., Bevan, A., Bivand, R., Busetto, L., Canty, M., Forrest, D., Ghosh, A., Golicher, D., Gray, J., Greenberg, J., Hiemstra, P., Geosciences, I. for M.A, Karney, C., Mattiuzzi, M., Mosher, S., Nowosad, J., Pebesma, E., Lamigueiro, O.P., Racine, E.B., Rowlingson, B., Shortridge, A., Venables, B., Wueest, R., 2016. Raster: Geographic Data Analysis and Modeling.

Hirsch, R.M., De Cicco, L.A., 2015. User Guide to Exploration and Graphics for River Trends (Egret) and Data Retrieval: R Packages for Hydrologic Data (USGS Numbered Series No. 4-A10), Techniques and Methods. U.S. Geological Survey, Reston, VA.

Hyndman, R.J., Khandakar, Y., 2008. Automatic time series forecasting: the forecast package for R. J. Stat. Softw. 27, 1–22. https://doi.org/10.18637/jss.v027.i03.

Johnson, G.R., Grotta, A.T., Gartner, B.L., Downes, G., 2005. Impact of the foliar pathogen Swiss needle cast on wood quality of Douglas-fir. Can. J. For. Res. 35, 331–339. https://doi.org/10.1139/X04-170.

Kaiser, K.E., McGlynn, B.L., Emanuel, R.E., 2013. Ecohydrology of an outbreak: mountain pine beetle impacts trees in drier landscape positions first. Ecohydrology 6, 444–454. https://doi.org/10.1002/eco.1286.

Kaylor, M.J., Warren, D.R., 2017. Linking riparian shade and the legacies of forest management to fish and vertebrate biomass in forested streams. Ecosphere 8, e01845. https://doi.org/10.1002/ecs2.1845.

Kurz, W.A., Dymond, C.C., Stinson, G., Rampley, G.J., Neilson, E.T., Carroll, A.L., Ebata, T., Safranyik, L., 2008. Mountain pine beetle and forest carbon feedback to climate change. Nature 452, 987–990. https://doi.org/10.1038/nature06777.

Lake, P.S., 2000. Disturbance, patchiness, and diversity in streams. J. N. Am. Benthol. Soc. 19, 573–592. https://doi.org/10.2307/1468118.

Logan, J.A., Régnière, J., Powell, J.A., 2003. Assessing the impacts of global warming on forest pest dynamics. Front. Ecol. Environ. 1, 130–137. https://doi.org/10.1890/1540-9295(2003)001[0130:ATIOGW]2.0.CO;2.

Maguire, D.A., Mainwaring, D.B., Kanaskie, A., 2011. Ten-year growth and mortality in young Douglas-fir stands experiencing a range in Swiss needle cast severity. Can. J. For. Res. 41, 2064–2076. https://doi.org/10.1139/x11-114.

Manter, D.K., Kavanagh, K.L., 2003. Stomatal regulation in Douglas fir following a fungal-mediated chronic reduction in leaf area. Trees 17, 485–491. https://doi.org/10.1007/s00468-003-0262-2.

Manter, D.K., Bond, B.J., Kavanagh, K.L., Rosso, P.H., Filip, G.M., 2000. Pseudothecia of Swiss needle cast fungus, Phaeocryptopus gaeumannii, physically block stomata of Douglas fir, reducing CO2 assimilation. New Phytol. 148, 481–491. https://doi.org/10.1046/j.1469-8137.2000.00779.x.

van Mantgem, P.J., Stephenson, N.L., Byrne, J.C., Daniels, L.D., Franklin, J.F., Fulé, P.Z., Harmon, M.E., Larson, A.J., Smith, J.M., Taylor, A.H., Veblen, T.T., 2009. Widespread increase of tree mortality rates in the western United States. Science 323, 521–524. https://doi.org/10.1126/science.1165000.

Maxwell, R.M., Condon, L.E., 2016. Connections between groundwater flow and transpiration partitioning. Science 353, 377–380. https://doi.org/10.1126/science.aaf7891.

Mazerolle, M.J., 2017. AICcmodavg: Model Selection and Multimodel Inference Based on (Q)AIC(c).

McCullough, D.A., Bartholow, J.M., Jager, H.I., Beschta, R.L., Cheslak, E.F., Deas, M.L., Ebersole, J.L., Foott, J.S., Johnson, S.L., Marine, K.R., Mesa, M.G., Petersen, J.H., Souchon, Y., Tiffan, K.F., Wurtsbaugh, W.A., 2009. Research in thermal biology: burning questions for coldwater stream fishes. Rev. Fish. Sci. 17, 90–115. https://doi.org/10.1080/10641260802590152.

McDonnell, J.J., Evaristo, J., Bladon, K.D., Buttle, J., Creed, I.F., Dymond, S.F., Grant, G., Iroume, A., Jackson, C.R., Jones, J.A., Maness, T., McGuire, K.J., Scott, D.F., Segura, C.,

Sidle, R.C., Tague, C., 2018. Water sustainability and watershed storage. Nature Sustainability 1, 378. https://doi.org/10.1038/s41893-018-0099-8.

Mikkelson, K.M., Maxwell, R.M., Ferguson, I., Stednick, J.D., McCray, J.E., Sharp, J.O., 2013. Mountain pine beetle infestation impacts: modeling water and energy budgets at the hill-slope scale. Ecohydrology 6, 64–72. https://doi.org/10.1002/eco.278.

Mildrexler, D.J., Shaw, D.C., Cohen, W.B., 2019. Short-term climate trends and the Swiss needle cast epidemic in Oregon's public and private coastal forestlands. For. Ecol. Manag. 432, 501–513. https://doi.org/10.1016/j.foreco.2018.09.025.

Mirus, B.B., Ebel, B.A., Mohr, C.H., Zegre, N., 2017. Disturbance hydrology: preparing for an increasingly disturbed future. Water Resour. Res. 53, 10007–10016. https://doi.org/10.1002/2017WR021084.

Moore, G.W., Bond, B.J., Jones, J.A., Phillips, N., Meinzer, F.C., 2004. Structural and compositional controls on transpiration in 40- and 450-year-old riparian forests in western Oregon, USA. Tree Physiol. 24, 481–491. https://doi.org/10.1093/treephys/24.5.481.

Nijzink, R., Hutton, C., Pechlivanidis, I., Capell, R., Arheimer, B., Freer, J., Han, D., Wagener, T., McGuire, K., Savenije, H., Hrachowitz, M., 2016. The evolution of root-zone moisture capacities after deforestation: a step towards hydrological predictions under change? Hydrol. Earth Syst. Sci. 20, 4775–4799. https://doi.org/10.5194/hess-20-4775-2016.

Oregon Department of Forestry, 2017. Swiss Needle Cast Aerial Survey Data. Forest Health Program, Private Forests Division, Salem, OR.

Penn, C.A., Bearup, L.A., Maxwell, R.M., Clow, D.W., 2016. Numerical experiments to explain multiscale hydrological responses to mountain pine beetle tree mortality in a headwater watershed. Water Resour. Res. 52, 3143–3161. https://doi.org/10.1002/2015WR018300.

Perry, T.D., Jones, J.A., 2017. Summer streamflow deficits from regenerating Douglas-fir forest in the Pacific northwest, USA. Ecohydrology 10, e1790. https://doi.org/10.1002/eco.1790.

Phillips, R.P., Ibáñez, I., D'Orangeville, L., Hanson, P.J., Ryan, M.G., McDowell, N.G., 2016. A belowground perspective on the drought sensitivity of forests: towards improved understanding and simulation. Forest Ecology and Management, Special Section: Drought and US Forests: Impacts and Potential Management Responses. vol. 380, pp. 309–320. https://doi.org/10.1016/j.foreco.2016.08.043.

Poff, N.L., 1992. Why disturbances can be predictable: a perspective on the definition of disturbance in streams. J. N. Am. Benthol. Soc. 11, 86–92. https://doi.org/10.2307/1467885.

PRISM Climate Group, 2004. PRISM gridded climate data. Oregon State University, Corvallis, OR.

R Core Team, 2016. R: The R Project for Statistical Computing. R Foundation for Statistical Computing, Vienna, Austria.

Raffa, K.F., Aukema, B.H., Bentz, B.J., Carroll, A.L., Hicke, J.A., Turner, M.G., Romme, W.H., 2008. Cross-scale drivers of natural disturbances prone to anthropogenic amplification: the dynamics of bark beetle eruptions. BioScience 58, 501–517. https://doi.org/10.1641/B580607.

Reed, D.E., Ewers, B.E., Pendall, E., 2014. Impact of mountain pine beetle induced mortality on forest carbon and water fluxes. Environ. Res. Lett. 9, 105004. https://doi.org/10.1088/1748-9326/9/10/105004.

Ritókóvá, G., Shaw, D.C., Filip, G., Kanaskie, A., Browning, J., Norlander, D., 2016. Swiss needle cast in western Oregon Douglas-fir plantations: 20-year monitoring results. Forests 7, 155. https://doi.org/10.3390/f7080155.

Robinne, F.-N., Bladon, K.D., Miller, C., Parisien, M.-A., Mathieu, J., Flannigan, M.D., 2018. A spatial evaluation of global wildfire-water risks to human and natural systems. Sci. Total Environ. 610–611, 1193–1206. https://doi.org/10.1016/j.scitotenv.2017.08.112.

Rust, A.J., Hogue, T.S., Saxe, S., McCray, J., 2018. Post-fire water-quality response in the western United States. Int. J. Wildland Fire 27, 203–216. https://doi.org/10.1071/WF17115.

Schnute, J.T., Boers, N., Haigh, R., Couture-Beil, A., Chabot, D., Grandin, C., Johnson, A., Wessel, P., Antonio, F., Lewin-Koh, N.J., Bivand, R., 2017. PBSmapping: Mapping Fisheries Data and Spatial Analysis Tools.

Seidl, R., Spies, T.A., Peterson, D.L., Stephens, S.L., Hicke, J.A., 2016. Searching for resilience: addressing the impacts of changing disturbance regimes on forest ecosystem services. J. Appl. Ecol. 53, 120–129. https://doi.org/10.1111/1365-2664.12511.

Seidl, R., Thom, D., Kautz, M., Martin-Benito, D., Peltoniemi, M., Vacchiano, G., Wild, J., Ascoli, D., Petr, M., Honkaniemi, J., Lexer, M.J., Trotsiuk, V., Mairota, P., Svoboda, M., Fabrika, M., Nagel, T.A., Reyer, C.P.O., 2017. Forest disturbances under climate change. Nat. Clim. Chang. 7, 395–402. https://doi.org/10.1038/nclimate3303.

Shaw, D.C., Filip, G.M., Kanaskie, A., Maguire, D.A., Littke, W.A., 2011. Managing an epidemic of Swiss needle cast in the Douglas-fir region of Oregon: the role of the Swiss needle cast cooperative. J. For. 109, 109–119. https://doi.org/10.1093/jof/109.2.109.

Shi, M., Fisher, J.B., Phillips, R.P., Brzostek, E.R., 2019. Neglecting plant–microbe symbioses leads to underestimation of modeled climate impacts. Biogeosciences 16, 457–465. https://doi.org/10.5194/bg-16-457-2019.

Silins, U., Bladon, K.D., Kelly, E.N., Esch, E., Spence, J.R., Stone, M., Emelko, M.B., Boon, S., Wagner, M.J., Williams, C.H.S., Tichkowsky, I., 2014. Five-year legacy of wildfire and salvage logging impacts on nutrient runoff and aquatic plant, invertebrate, and fish productivity. Ecohydrology 7, 1508–1523. https://doi.org/10.1002/eco.1474.

Soil Survey Staff, 2017. Web Soil Survey. Natural Resources Conservation Service, United States Department of Agriculture.

Sommerfeld, A., Senf, C., Buma, B., D'Amato, A.W., Després, T., Díaz-Hormazábal, I., Fraver, S., Frelich, L.E., Gutiérrez, Á.G., Hart, S.J., Harvey, B.J., He, H.S., Hlásny, T., Holz, A., Kitzberger, T., Kulakowski, D., Lindenmayer, D., Mori, A.S., Müller, J., Paritsis, J., Perry, G.L.W., Stephens, S.L., Svoboda, M., Turner, M.G., Veblen, T.T., Seidl, R., 2018. Patterns and drivers of recent disturbances across the temperate forest biome. Nat. Commun. 9, 4355. https://doi.org/10.1038/s41467-018-06788-9.

Stednick, J.D., 1996. Monitoring the effects of timber harvest on annual water yield. J. Hydrol. 176, 79–95. https://doi.org/10.1016/0022-1694(95)02780-7.

Thom, D., Seidl, R., 2016. Natural disturbance impacts on ecosystem services and biodiversity in temperate and boreal forests. Biol. Rev. 91, 760–781. https://doi.org/10.1111/brv.12193.

Turner, M.G., 2010. Disturbance and landscape dynamics in a changing world. Ecology 91, 2833–2849. https://doi.org/10.1890/10-0097.1.

USDA Forest Service, 2017. Aerial Detection Surveys (ADS). United States Department of Agriculture, Pacific Northwest Region Forest Service, Portland, OR.

USDOI, USGS, 2019. Landscape ecology, modeling, mapping & analysis (LEMMA) project links - ScienceBase-catalog [WWW document]. URL https://www.sciencebase.gov/catalog/item/4fcf72c2e4b0c7fe80e814dd, Accessed date: 21 February 2019.

Varhola, A., Coops, N.C., Weiler, M., Moore, R.D., 2010. Forest canopy effects on snow accumulation and ablation: an integrative review of empirical results. J. Hydrol. 392, 219–233. https://doi.org/10.1016/j.jhydrol.2010.08.009.

Vitousek, P., Melillo, J., 1979. Nitrate losses from disturbed forests - patterns and mechanisms. For. Sci. 25, 605–619.

Vörösmarty, C.J., McIntyre, P.B., Gessner, M.O., Dudgeon, D., Prusevich, A., Green, P., Glidden, S., Bunn, S.E., Sullivan, C.A., Liermann, C.R., Davies, P.M., 2010. Global threats to human water security and river biodiversity. Nature 467, 555–561. https://doi.org/10.1038/nature09440.

Wondzell, S.M., King, J.G., 2003. Postfire erosional processes in the Pacific Northwest and Rocky Mountain regions. For. Ecol. Manag. 178, 75–87. https://doi.org/10.1016/S0378-1127(03)00054-9.

Wondzell, S.M., Diabat, M., Haggerty, R., 2019. What matters most: are future stream temperatures more sensitive to changing air temperatures, discharge, or riparian vegetation? J. Am. Water Resour. Assoc. 55, 116–132. https://doi.org/10.1111/1752-1688.12707.

Woods, A.J., Martín-García, J., Bulman, L., Vasconcelos, M.W., Boberg, J., La Porta, N., Peredo, H., Vergara, G., Ahumada, R., Brown, A., Diez, J.J., 2016. Dothistroma needle blight, weather and possible climatic triggers for the disease's recent emergence. For. Pathol. 46, 443–452. https://doi.org/10.1111/efp.12248.

Wyka, S.A., Smith, C., Munck, I.A., Rock, B.N., Ziniti, B.L., Broders, K., 2017. Emergence of white pine needle damage in the northeastern United States is associated with changes in pathogen pressure in response to climate change. Glob. Chang. Biol. 23, 394–405. https://doi.org/10.1111/gcb.13359.

Yue, S., Pilon, P., Phinney, B., Cavadias, G., 2002. The influence of autocorrelation on the ability to detect trend in hydrological series. Hydrol. Process. 16, 1807–1829. https://doi.org/10.1002/hyp.1095.